UC Merced

UC Merced Electronic Theses and Dissertations

Title

Role of Heart Rate, Temperature, and Autonomic Nervous System Regulation in the Cardiac Action Potential and Calcium Handling Dynamics in an Intact Goldfish Heart

Permalink

https://escholarship.org/uc/item/60v4751g

Author

Bazmi, Maedeh

Publication Date

2022

Copyright Information

Peer reviewed|Thesis/dissertation

UNIVERSITY OF CALIFORNIA, MERCED

Role of Heart Rate, Temperature, and Autonomic Nervous System Regulation in the Cardiac Action Potential and Calcium Handling Dynamics in an Intact Goldfish Heart

A dissertation submitted in partial satisfaction of the requirements for the degree of
Doctor of Philosophy

in

Quantitative and Systems Biology

by

Maedeh Bazmi

Committee in Charge:

Dr. Maria-Elena Zoghbi, Chair
Dr. Ariel Escobar, Research Advisor
Dr. Chih-Wen Ni
Dr. Josefina Ramos-Franco

2022

The Dissertation of Maedeh Bazmi is approved by, and it is acceptable in quality and form for publication on microfilm and electronically:

_____

Dr. Ariel L. Escobar, Advisor   Date

_____

Dr. Maria-Elena Zoghbi, Chair   Date

_____

Dr. Josefina Ramos-Franco   Date

_____

Dr. Chih-Wen, Ni   `   Date

University of California, Merced
2022

To my husband, Dryden,
Remember, dear Dryden, I've loved you always. I always will.

○

To my mother, Zahra,
for making the biggest sacrifice of your life all those years ago; I am here because of
your immeasurable courage to leave your home, your country, and everything familiar to
you, with nothing else in your hands aside from your two children. Your blind hope in our
future gave me the courage to go after what I always felt would be impossible; thank you
mom.

○

To my dearest friend, Shari,
no words can ever truly capture the depth of my gratitude for your boundless love and
support, thank you for showing me the meaning of unconditional.

○

To the female scientists that came before me,
for your innumerable contributions to the STEM field, which paved the way for other
women, like me. My work stands on the shoulders of your hard work, courage, and
sacrifice.

TABLE OF CONTENTS

List of Figures

Chapter 6

Figure 6.1 Time courses of cardiac action potentials and Ca^{2+} transients in goldfish hearts as a function of heart rate

Figure 6.2 Effects of increasing temperature on cardiac action potentials and Ca^{2+} transients from goldfish hearts

List of Tables

Acknowledgments

Curriculum Vitae

MAEDEH BAZMI
mbazmi@ucmerced.edu

BIOGRAPHICAL SKETCH

Current Appointment	Quantitative Systems Biology Ph.D. Candidate
University Address	University of California, Merced
	School of Natural Sciences
	5200 Lake Road Merced, Ca 95343
Phone Number	(209) 228-4400
Email	mbazmi@ucmerced.edu

EDUCATION

2018-2022	PhD in Quantitative Systems Biology
	Emphasis: Cardiac Physiology
	University of California, Merced
	GPA: 4.0
2018	B.S in Biological Sciences
	Emphasis: Physiology
	Granted by the California State University, San
Marcos	
	GPA: 3.7

POSITIONS AND APPOINTMENTS

2018-Present	Ph.D. student in Quantitative Systems Biology
	Area of focus: Cardiac physiology
	Dr. Escobar, advisor
	School of Natural Sciences. University of California, Merced
2017-2018	Undergraduate Student Research Assistant in Neurobiology
	Dr. Norris, advisor
	California State University, San Marcos. San Diego, Ca
2017-2018	Undergraduate Student Research Assistant in Immunology
	Dr. Jameson, advisor
	California State University, San Marcos. San Diego, Ca

FUNDING

2019	Quantitative Systems Biology Summer Fellowship
2020	Quantitative Systems Biology Summer Fellowship
2021	Quantitative Systems Biology Summer Fellowship

TEACHING EXPERIENCE

2021	Teaching assistant for Human Physiology, upper division undergraduate students. University of California, Merced
2020	Teaching assistant for Physiology for Engineers, upper division undergraduate bioengineering students. University of California, Merced
	Teaching assistant for Contemporary Biology Laboratory, undergraduate biology students. University of California, Merced
2019	Teaching assistant for Physiology for Engineers, upper division undergraduate bioengineering students. University of California, Merced
	Teaching assistant for Cell Biology for Engineers, upper division undergraduate bioengineering students. University of California, Merced
	Teaching assistant for Contemporary Biology Laboratory, undergraduate biology students. University of California, Merced
2018	Teaching assistant for Introduction to Molecular Biology, undergraduate biology students. University of California, Merced
	Supplemental Instructor for General Biochemistry, undergraduate students. California State University, San Marcos
2017	Supplemental Instructor for Organic Chemistry I, undergraduate students. California State University, San Marcos
	Supplemental Instructor for Organic Chemistry II, undergraduate students. California State University, San Marcos

2016	Supplemental Instructor for Organic Chemistry II, undergraduate students. California State University, San Marcos
	Teaching assistant for Comparative Animal Physiology, undergraduate students. California State University, San Marcos

RESEARCH TRAINEES
Undergraduate Students

Brian Hoang B.S
Arjun Kholi B.S
Mariana Vasquez B.S
Gabriela Hinojosa B.S

UNIVERSITY SERVICE

| 2016-2018 | Lead Academic Tutor at The Academic Success Center, California State University, San Marcos, San Diego |
| 2016-2018 | Lead Coordinator/Facilitator of Organic Chemistry Workshops for undergraduate students, California State University, San Marcos, San Diego, Ca |

SCIENTIFIC SOCIETIES

| 2018-Present | Biophysical Society |
| 2014-2018 | National Honor's Society |

AWARDS AND DISTINCTIONS

| 2014-2018 | Dean's List California State University, San Marcos, San Diego, Ca |

PRESENTED WORK

| 2020 | Poster Presentation: Biophysical Society Meeting "Excitation-Contraction Coupling in the Goldfish (Carassius auratus) Intact Heart" San Diego, Ca |

PEER REVIEWS PUBLICATIONS

1. **Bazmi, M.,** and Escobar, A. L. (2019). How Ca^{2+} influx is attenuated in the heart during a "fight or flight" response. *Journal of General Physiology*, *151*(6), 722-726.

2. **Bazmi, M.,** and Escobar, A. L. (2020). Excitation–Contraction Coupling in the Goldfish (Carassius auratus) Intact Heart. *Frontiers in Physiology*, *11*, 1103.

3. Millet, J., Aguilar-Sanchez, Y., Kornyeyev, D., **Bazmi, M**., Fainstein, D., Copello, J. A., and Escobar, A. L. (2021). Thermal modulation of epicardial Ca^{2+} dynamics uncovers molecular mechanisms of Ca^{2+} alternans. *Journal of General Physiology*, *153*(2).

4. **Bazmi, M.,** Copello, J. A., & Escobar, A. L. (2020). Thermodynamics of myoplasmic Ca^{2+} alternans reveal the molecular mechanisms involved in its genesis. *Physiological Mini Reviews*, 13(6), 56-69.

5. **Bazmi, M.,** and Escobar, A. L. (2021) Relationship between electrophysiology and Ca^{2+} signaling in goldfish intact hearts. *Interventional Cardiology*, 13(6), 134-142.

6. Medei, E., **Bazmi, M.,** and Escobar, A. L. (2022). The repolarization during phase 1 defines Ca^{2+} transients and contractility in perfused mouse hearts. *Interventional Cardiology*.

7. **Bazmi, M.,** & Escobar, A. L. (2022). Autonomic Regulation of the Goldfish Intact Heart. *Frontiers in Physiology*, 149.

<u>Dissertation Abstract</u>

Role of Heart Rate, Temperature, and Autonomic Nervous System Regulation in the Cardiac Action Potential and Calcium Handling Dynamics in an intact Goldfish Heart

Maedeh Bazmi

Doctorate of Philosophy in Quantitative Systems Biology, with an emphasis in Cardiac Electrophysiology at the University of California, Merced, 2022

In the last decade alone fish hearts have become an increasingly popular model for studying heart function. Although fish hearts contain a single atrium and ventricle and present a fundamentally different cardiovascular system when compared to mammalian models, there are many developmental, structural, and functional commonalities between the two vertebrate classes. The goldfish heart, specifically, has remarkably similar electrical properties to that of humans'. For example, the heart rate, action potential morphology, and Ca^{2+} transient kinetics and dynamics of adult goldfish closely parallel those of humans, even more so than mice. In nearly all vertebrate species, direct input from the autonomic nervous system tightly controls cardiac contractility and excitability. Although there is an abundant amount of research on the autonomic control of cardiac contractility and excitability in numerous mammalian species, the characterization of pathophysiological mechanisms is still difficult to obtain for humans specifically. This is in part due to humans having strikingly dissimilar AP characteristics and electrocardiographic morphology in comparison to commonly used animal models such as mice, rats, and rabbits. Fish, on the other hand, are the largest and most diverse group of vertebrates, and as such, their autonomic nervous system regulation can often deviate from the classical vertebrate models used to study autonomic control of cardiac contractility and excitability. Ventricular APs, electrocardiograms, and Ca^{2+} transients recorded from the goldfish intact heart showed perfusion with either 100 nM isoproterenol (sympathetic agonist) or 5 µM carbamylcholine (parasympathetic agonist), was enough to stimulate the sympathetic branch or parasympathetic branch, respectively. Interestingly, our results indicate stimulation of the goldfish autonomic nervous system by these commonly used agonists resulted in a corresponding change in cardiac dromotropism, chronotropism, ionotropism, and lusitropism in a similar manner observed in humans. The data obtained from our experiments have led us to propose the goldfish heart as an excellent model for performing physiological experiments at the intact-heart level. Moreover, its shared ionic and electrical similarities with larger mammals open a new avenue for goldfish hearts to be used as a model to study human physiology.

Graduate Advisor: Dr. Ariel L. Escobar

List of Abbreviations

Symbol	Definition
Ca^{2+}	Calcium
Na^+	Sodium
K^+	Potassium
Cl^-	Chlorine
ECC	Excitation Contraction Coupling
CICR	Calcium Induced Calcium Released
RyR	Ryanodine Receptor
SERCA	Sarcoendoplasmic reticulum Ca^{2+}-ATPase
PLN	Phospholamban
SR	Sarcoplasmic Reticulum
T-tube	Transverse tubule
AP	Action Potential
APD	Action Potential Duration
APD30	Action Potential Duration at 30% Repolarization
APD50	Action Potential Duration at 50% Repolarization
APD90	Action Potential Duration at 90% Repolarization
ECG	Electrocardiogram
ANS	Autonomic Nervous System
NS	Nervous System
PKA	Protein Kinase A
AC	Adenylyl Cyclase
β-AR	Beta-adrenergic Receptor
cAMP	Cyclic Adenosine Monophosphate
ATP	Adenosine Triphosphate
ICa	Ca^{2+} current
INa	Na^+ current
IK	K^+ current
I_{to}	Transient outward K^+ current
ACh	Acetylcholine
M2	Muscarinic receptor 2
I_{KACh}	ACh-sensitive K^+ current
NCX	Sodium Calcium Exchanger
TP	Time to Peak
RT	Rise Time
FT	Fall Time
HD	Half Duration
HR	Heart Rate
Ry	Ryanodine
Tg	Thapsigargin
PLFFM	Pulsed Local Field Fluorescence Microscopy

<u>Preface</u>

For years scientists have attempted to identify and establish animal models with which pathogenesis of human disease at a cellular and molecular level could be understood, and eventually treated. Throughout the years, the most classical models have become dogs, guinea pigs, and mice; however, each of these vertebrate models present unique limitations rendering them in some way different from the human model. Unfortunately, the only animal model with a heart capable of perfectly replicating the mechanical intricacies that constitute the human heart is another human. Due to the unique limitations of each vertebrate model, our knowledge of the human cardiac physiology remains limited to this day.

In the last decade alone, fish hearts have become an increasingly popular model for studying heart function (Nemtsas et al., 2010; Huttner et al., 2013; Ravens, 2018; van Opbergen et al., 2018b; Zhang et al., 2018). Specifically, the zebrafish (*Danio rerio*) has been the model of choice not only for the possibility of performing transgenesis (Chopra et al., 2010; Huttner et al., 2013; Konantz and Antos, 2014; Serbanovic-Canic et al., 2017), but also for studying cardiac physiology and pathophysiology of larger mammals, including humans (Nemtsas et al., 2010; Ravens, 2018; van Opbergen et al., 2018b). Although fish hearts contain a single atrium and ventricle and present a fundamentally different cardiovascular system when compared to other mammalian models, there are many developmental, structural, and functional commonalities between the two vertebrate species (Bazmi and Escobar, 2020; Mersereau et al. 2015; Sandblom and Axelsson, 2011; Xing et al. 2017). The goldfish, specifically, has remarkably similar electrical properties to humans. For example, the heart rate, AP morphology, and Ca^{2+} transient kinetics and dynamics of adult goldfish closely parallel those of humans, even more so than mice and zebrafish models (Bazmi and Escobar, 2020).

The overarching aim of this thesis is to investigate and outline the basic molecular mechanisms involved in the electrical and contractile properties of the goldfish intact heart and to establish this model as an alternative vertebrate to study larger mammalian cardiac physiology and pathophysiology.

<u>Chapter 1:</u> Goldfish cardiac muscle physiology background and significance
This chapter provides the foreground necessary in understanding the electromechanical function of the mammalian and fish hearts. Detailed explanations of the molecular mechanisms involved in the electrical and contractile properties of the vertebrate heart are discussed in detail, elucidating the imperative roles of intracellular Ca^{2+} and action potentials. Finally, the heart rate, temperature regulation, and autonomic nervous system regulation are discussed in relation to the goldfish heart.

<u>Chapter 2:</u> Experimental approach
The novel tools utilized in addressing the questions in this thesis are explicitly described in detail. The commonly used Ca^{2+} molecular fluorescent probe, Rhod-2AM, was used in conjunction with the innovative Pulsed Local Field Fluorescent Microscopy

technique and classical glass microelectrode recordings of the membrane potential in order to dissect the underlying molecular events at the intact heart level. All experiments presented in this thesis were done at the intact heart level, with conditions resembling physiological conditions.

Chapter 3: Excitation contraction coupling in the goldfish intact heart

The aim of this chapter is to elucidate the basic molecular mechanisms underlying excitation contraction coupling in the goldfish heart. By investigating the transient cytosolic Ca^{2+} concentration and the cardiac AP, the role and contribution of the L-type Ca^{2+} channel in the excitation and contractile properties of the goldfish heart is revealed.

Chapter 4: Intrinsic sympathetic NS activity and effect of AP and intracellular Ca^{2+} dynamics

Different vertebrate models exhibit varying degrees of autonomic nervous system regulation. The aim of this chapter is to investigate the role and the degree to which the sympathetic nervous system regulates electrical and contractile properties of the goldfish intact heart. The innovative Pulsed Local Field Fluorescent Microscopy technique in conjunction with electrocardiogram recordings and action potential recordings were used to establish evidence of the presence of a sympathetic response in the goldfish heart.

Chapter 5: Intrinsic parasympathetic NS activity and effect of AP and intracellular Ca^{2+} dynamics

Different vertebrate models exhibit varying degrees of autonomic nervous system regulation. Some vertebrates may only exhibit one branch of the autonomic nervous system, while other vertebrates may exhibit full dual autonomic control. The aim of this chapter is to investigate the role and the degree to which the parasympathetic nervous system regulates electrical and contractile properties of the goldfish intact heart. The innovative Pulsed Local Field Fluorescent Microscopy technique in conjunction with electrocardiogram recordings and action potential recordings were used to establish the presence of a parasympathetic response in the goldfish heart.

Chapter 6: The effect of increasing the heart rate and temperature on AP morphology and intracellular $[Ca^{2+}]$ dynamics

Fish cannot systemically regulate their body temperature; thus, the temperature of the water has a large influence on the physiological behavior of the animal's cardiac function. The aim of this chapter is to elucidate how a change in temperature and heart rate alter the molecular mechanisms underlying excitation contraction coupling in the goldfish heart. The innovative Pulsed Local Field Fluorescent Microscopy technique in conjunction with electrocardiogram recordings and action potential recordings were used to reflect changes in electrical and contractile properties of the goldfish heart.

Chapter 1: Cardiac Muscle Physiology and Background

The heart is arguably the most popular organ with which humans have been obsessed. For centuries, countless poets, painters, musicians, and philosophers have been captivated by the sheer complexity of this exceptional machine. In the fourth century B.C., Aristotle identified the heart as the most important hot, dry organ in the body; the seat of intelligence, motion and sensation, all other organs simply existed to cool the heart. The first recorded discovery of the circulatory system was made in 157AD by a chief physician to the gladiators in Pergamon, Greece. Following battle, the chief physician, Galen, would observe the still beating hearts of fighters who lay dying with their chest ripped open at the blade of their opponent. Later, Galen would move to Rome where vivisections (from Latin vivus "alive", and sectio "cutting") on monkeys and pigs erroneously led him to conclude arterial blood originated in the heart and venosus blood originated in the liver. Michael Servitus, a Spanish physician who had extensive knowledge on Galen's writings, carried out vivisections on animals to further discover the pulmonary circulation. Unfortunately, Servitus was burned at the stake for his religious beliefs in 1553. Realdo Columbo, born in 1515, continued vivisections on animals not only to confirm the pulmonary circulation, but to also discover the four valves of the heart only permitted blood to flow in one direction: from the right ventricle to the lungs back to the left ventricle, and then to the aorta. William Harvey, born in 1578, proved that blood flows in two separate loops: the pulmonary and systemic circulations.

From the vivisections performed in the 1500s to complex intricate cellular cardiac experiments done in present day, the foundation of our cardiac knowledge is built on the knowledge obtained from sacrificing countless different animals. Although these animals have graciously aided in the furtherment of human cardiac physiology, only one animal model could ever perfectly replicate the complexity that embodies the human heart. The heart is often referred to as a machine, and in these terms, every machine operates differently (with respect to its animal model), to achieve the same goal: provide the body, organs, tissues, and muscles with oxygenated blood and dispose of metabolic waste. Unfortunately, the only animal model with a heart capable of perfectly replicating the mechanical intricacies that constitute the human heart, is another human. Thus, our knowledge of the human cardiac physiology remains limited. For decades scientists have attempted to identify and establish animal models with which pathogenesis of human disease at a cellular and molecular level could be understood and eventually, treated. Throughout the years, the most classical models have become dogs, guinea pigs, and mice; however, a range of factors needs to be taken into consideration in addition to anatomical similarity when in search of an appropriate model. For example, mammalian models such as sheep and rats may present similar physiologies and organ sizes, which are crucial to furtherment of surgical therapeutic interventions. However, the basic electrical events occurring at the cellular level are inherently different to that of humans, which limit identification of the perturbed cellular and molecular pathways leading to

human pathogenesis. Nevertheless, the recent advances in science in conjunction with research conducted on different animal models has provided the field of physiology with a reliable understanding of how a healthy mammalian heart functions.

1.1 Anatomy and Functioning of an Electric Pump

The typical mammalian heart is described as an electrical mechanical (or electromechanical) pump consisting of four chambers: the left and right atria and the left and right ventricles. These chambers work together by coupling electrical and contractile properties to complete the primary function of the heart: propel blood through the circulatory system. Unoxygenated (venous) blood enters through the superior and inferior vena cava and travels to the right atrium. As the pressure of the right atrium becomes larger than the right ventricle, the blood is projected into the right ventricle through the bicuspid valve. A ventricular contraction sends the blood to the lungs for oxygenation through the pulmonary artery. The oxygenated blood then re-enters the heart through the pulmonary vein and into the left atrium. This increases the pressure of the left atrium, the contraction of which sends the blood to the left ventricle. Finally, a ventricular contraction propels the oxygenated blood from the left ventricle to the rest of the circulatory system through the aorta.

Although the main sequence of events through this electrical labyrinth is nearly identical across different mammalian species with four chambered hearts, the specific electrical mechanisms underlying these events can vary greatly among species (**Figure 1.1**). The most dramatic difference can be seen when looking at the cellular electrical events in a human heart in comparison to the most predominant model used to investigate human cardiac diseases and patho-electrophysiological conditions: the mouse heart. Although experiments conducted on mouse hearts have provided invaluable insight into the role of many ion channels in a healthy and diseased state, this model is not without limitations. The drastic difference in the electrical properties of the ion currents magnify just how different a mouse heart is from a human heart. Not only does the mouse model have an intrinsic basal high heart rate, but it also has a large and fast phase 1 repolarization, resulting in a short action potential and a very negative plateau phase potential.

It has not been until recently that fish have also been added to the list in hopes to better understand human cardiac physiology. Although initially counterintuitive, since fish have a two chambered heart rendering them fundamentally different in their morphological structure to that of classical mammalian models, fish hearts have proved rather promising as a model to better understand cardiac pathophysiology. In the last decade alone, fish hearts have become an increasingly popular model for studying heart function (Nemtsas et al., 2010; Huttner et al., 2013; Ravens, 2018; van Opbergen et al., 2018b; Zhang et al., 2018). In developmental studies (Novak et al., 2006; Chi et al., 2010; Chablais and Jazwinska, 2012; Ramachandran et al., 2013; Ding et al., 2017), the zebrafish (Danio rerio) has gained prominence as the vertebrate model of choice not only

for the possibility of performing transgenesis (Chopra et al., 2010; Huttner et al., 2013; Konantz and Antos, 2014; Serbanovic-Canic et al., 2017), but also for studying cardiac physiology and pathophysiology of larger mammals, including humans (Nemtsas et al., 2010; Ravens, 2018; van Opbergen et al., 2018b).

During embryogenesis, the transparent nature of the zebrafish heart lends itself to high throughput testing of the effects of pharmacological agents, where the heart rate and rhythm can be directly observed. Furthermore, the cardiac action potential of the zebrafish ventricle shares a striking resemblance to human ventricular action potentials (**Figure 1.1**). Approximately 71% of human genes are found to have at least one corresponding ortholog in the zebrafish genome; however, based on this information alone, interpretation of results obtained from experiments cannot be based on the assumption that the molecular entities and regulatory pathways are identical in the zebrafish and humans. Indeed, the zebrafish model does present its own unique limitations including a much higher heart rate (Lee et al. 2016) and a shorter AP duration (Lin et al. 2015) when compared to that of goldfish, and a diminished fraction of Ca^{2+} induced Ca^{2+} release (Bovo et al. 2013) from the SR when compared to small rodent models. Furthermore, the small size of the Zebrafish heart makes it difficult to perform perfused intact heart measurements. Although it is possible to cannulate the bulbus arteriosus of the zebrafish heart, it is difficult to effectively change the perfusate fast enough to perform pharmacological experiments. This is due to the low perfusion rate the zebrafish heart needs to maintain good hemodynamic and mechanical conditions. Lastly, the ventricular wall of the zebrafish heart is not thick enough to consistently perform flash photolysis experiments at an intact heart level without undergoing considerable damage.

Despite the frequent use of fish as a cardiovascular model to study human hearts (Nemtsas et al. 2010), our knowledge is still limited. In this thesis, the goldfish (*Carassius auratus*) heart is proposed as an alternative novel experimental model in order to study excitation contraction-coupling. Goldfish belong to the same family as zebrafish (Kon et al. 2020; Málaga-Trillo et al. 2002), and as such present with many physiological similarities. The striking similarities between the goldfish and the zebrafish heart is the reason why the goldfish can also be used as an embryological model (Grivas et al. 2014), be altered via transgenesis using CRISPR/Cas9 (Yin et al. 2018), or be used in electrophysiological and Ca^{2+} signaling experiments (Chen et al. 2005; Leo et al. 2019).
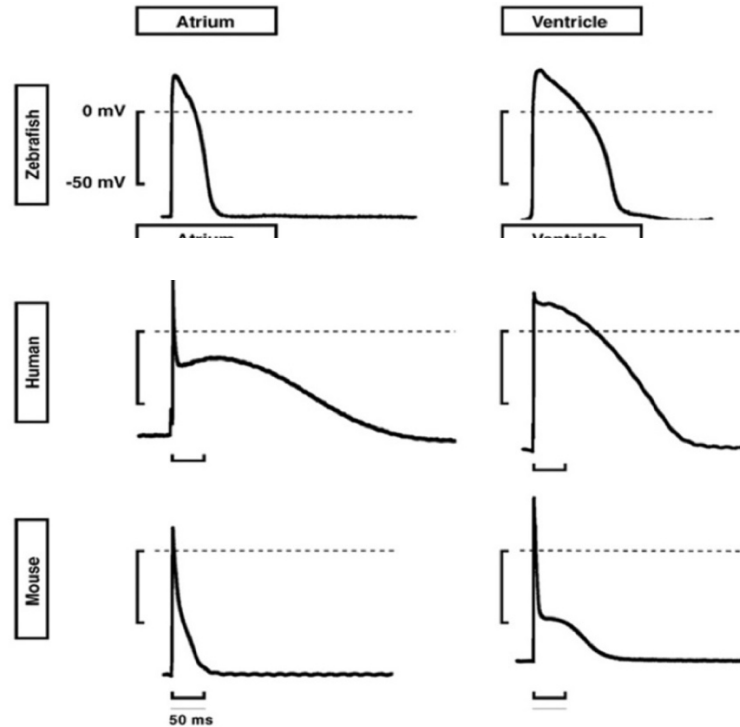
Figure 1.1: Comparison of ventricular action potentials from the zebrafish, human, and mouse model (picture modified from Nemtsas et al., 2010).

The goldfish heart rate, AP morphology, and Ca^{2+} transient kinetics and dynamics of closely parallel those of humans, even more so than mice and Zebrafish models (Bazmi and Escobar, 2020); these reasons the goldfish model seemed a more promising model compared to that of the zebrafish to study larger mammalian cardiac physiology. However, the mechanical properties of the goldfish heart need to be established and discussed prior to investigating electrical properties of the goldfish heart.

Fish heart chambers and blood flow

The goldfish heart has 4 main components constituted by the sinus venosus, atrium, ventricle, and bulbus arteriosus arranged in series contained within a pericardial cavity. These vital structures all work together to deliver unoxygenated blood to the gills, where it is oxygenated, and sent to the systemic circulation (**Figure 1.2**).

The sinus venosus is the most caudal portion of the heart and containing only smooth muscle elements (Yamauchi, 1980). The sinus venosus receives peripheral venous blood from the ducts of Cuveir and the hepatic veins and directs it into the atrial cavity. The single atrium is a sac-like chamber with a size comparable to the ventricle, rich in collagen and elastin whose primary function is to move venosus blood into the ventricle during atrial diastole. The atrio-ventricular region of the heart provides support for the atrioventricular valves, which are comprised of connective tissue and loose collagen fibers. The valve is made up of two leaflets made up of collagen and elastin. The single ventricle is a sac-like muscular chamber, made up of two layers: the outer compact (compacta) and the inner trabeculate (spongiosa), responsible for developing the necessary pressure needed

to propel the blood to the bulbus arteriosus. Finally, the bulbus arteriosus is an atrium-like structure, containing large amounts of elastin, collagen, and smooth muscle cells. Its primary function is to send arterial blood to the gills where it is oxygenated and then sent to the systemic circulation.
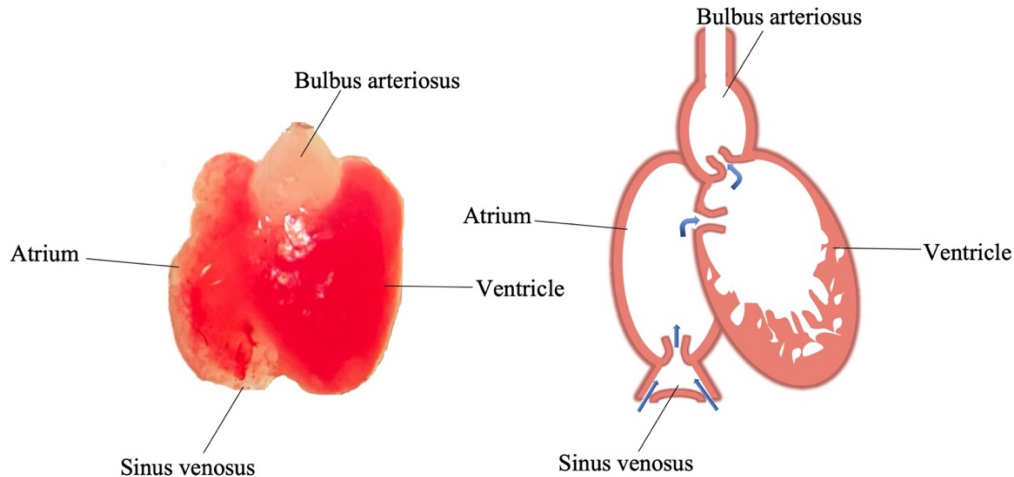
Figure 1.2: The fish heart consists of two chambers (pictured on left) which work together to propel oxygenated blood to the circulatory system. Unoxygenated blood travels through the heart and to the gills to be oxygenated prior to being sent through the rest of the circulatory system.

The heart is an electromechanical pump

The intrinsic electrical activity of the vertebrate heart powers it to successfully propel oxygenated blood through the organism. The electrical activity of the heart can either be measured at a cellular level (referred to as action potentials, APs) or at a whole organ level (referred to as an electrocardiogram, ECG). At a cellular level, the vertebrate heart functions as an electrically driven electromechanical pump by generating an excitatory electrical signal (cardiac AP) which propagates through the heart in a coordinated manner, triggering a cascade of cellular events setting cardiac contraction into motion. The heart can only serve as the leader of propulsion of blood in the body if it can successfully couple electrical excitability to the correct timing of sequential contractions of the atrial and ventricular muscles. Indeed, a faulty or inadequate excitation contraction coupling process has been identified as the basis for numerous pathophysiological conditions.

Electrical Signal propagation

In the vertebrate heart, there is a small cluster of specialized myocardial cells located in the sinoatrial node (SAN) with a unique feature to generate spontaneous APs. This feature enables the cardiomyocytes to set the autonomous rhythm of the heart and are appropriately referred to as "pacemaker cells". The pacemaker region of the fish heart was anatomically identified over 100 years ago; since then, the nodal tissue has been described in several fish species as a "ring-like" structure bordering the sinus venosus

and the atrium. How these cells develop the autonomous rhythm of the heart can best be understood by looking at their electrical properties at a cellular level, and more specifically, their unique AP.

Although the morphology of the fish pacemaker AP is similar to that of other vertebrate species, the ionic bases of these APs are practically unexplored. Thus, the presented information below is heavily based on the knowledge of ionic mechanisms of pacemaker cell function obtained from mammalian and frog models. Pacemaker APs have a slow and gradual diastolic depolarization (phase 4) toward a threshold voltage of the AP upstroke (Phase 0) and a repolarization phase (phase 3) immediately succeeding the upstroke (**Figure 1.3**). The rate (or slope) of the diastolic depolarization in phase 4 is proportionately related to heart rate. For example, a faster rate of diastolic depolarization would result in reaching the AP threshold faster, and thus increase heart rate. The major ion currents active in phase 4 of the nodal AP are: the Na^+-Ca^{2+} exchanger current (I_{NCX}), funny current (I_f), and T-type Ca^{2+} channel current (I_{CaT}). So, it makes sense that altering any of these currents would in turn produce a respective change in the rate of diastolic depolarization and thus, alter heart rate. During phase 0 of the AP, the current generated by the L-type Ca^{2+} channel (I_{CaL}) becomes the major ion current, followed by immediate activation of the rapid and slow components of the delayed rectifier K^+ current (I_{Kr} and I_{Ks}, respectively), which are the major currents active during phase 3 and responsible for the repolarization of the nodal AP. Increases in beating frequency alter ventricular AP duration, Ca^{2+} transient amplitude, and Ca^{2+} transient kinetics in ventricular cardiomyocytes, the molecular mechanisms for which are discussed in great detail in chapter 6 of this thesis. The electrical waves generated by the pacemaker cells are transmitted to neighboring atrial cardiomyocytes, depolarizing them and triggering a wave of excitation throughout the fish heart.
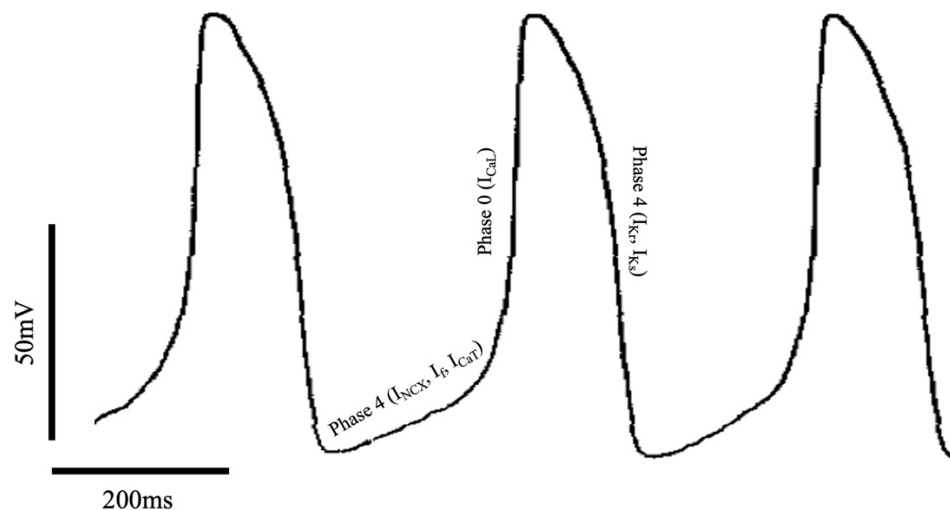
Figure 1.3: Action potential recordings of an enzymatically isolated pacemaker cell of the brown trout with the major ion currents shown in parenthesis. Pacemaker action potentials have a slow and gradual diastolic depolarization (phase 4) toward a threshold voltage of the AP upstroke (Phase 0) and a repolarization phase (phase

3) immediately succeeding the upstroke. During phase 0 of the AP, the current generated by the L-type Ca^{2+} channel (I_{CaL}) becomes the major ion current followed by immediate activation of the rapid and slow components of the delayed rectifier K^+ current (I_{Kr} and I_{Ks}, respectively), the major currents active during phase 3 and responsible for the repolarization of the nodal AP. The major ion currents active in phase 4 of the nodal AP are: the Na^+-Ca^{2+} exchanger current (I_{NCX}), funny current (I_f), and T-type Ca^{2+} channel current (I_{CaT}) (Reprinted by permission from Copyright Clearance Center: Springer Nature, Pflügers Archive European Journal of Physiology, Action potential and membrane currents of single pacemaker cells of the rabbit heart, Toshio Nakayama et al ©1984)

In mammals, the electrical impulse generated by the SAN cells first travels to the right and left atria, before propagating to the Bundle of His, then to the Bundle Branches along the ventricle, before finally reaching the Purkinje Fibers innervating the ventricular walls leading to excitation of the ventricular myocytes. The process of electrical impulse conduction is less elucidated in fish cardiomyocytes; in fact, recognizable morphological conducting tissue has yet to be identified in the fish. However, functional studies have revealed the presence of a conducting system in fish almost identical to mammals; one that can accelerate and decelerate the rate of impulse conduction. Nevertheless, previous studies have identified a general pattern for AP propagation throughout the fish heart.

The AP generated from the sinoatrial pacemaker region of the fish heart travels to the atrium, then to the atrial wall, then to the atrioventricular canal where there is a delay in order to allow for ventricular filling. Preceding this delay, the signal travels from the atrioventricular canal to the apex of the ventricle to the base of the ventricle generating a forward movement of blood, resulting in the ejection of blood. It is important to note, however, the direction at which the ventricle is activated is under debate. Some studies suggest the ventricle is activated from the base of the ventricle, or even in a spiral manner from the base to the apex of the ventricle.

1.2 Molecular Basis underlying the electrical activity of the heart

Excitable muscle cells in the fish heart (cardiomyocytes) are electrically coupled via *gap junctions*. These gap junctions allow for electrical impulses (or APs) to travel among neighboring cardiomyocytes, leading to whole heart contractions. It is important to note, however, the morphology of the AP can vary dramatically depending on which region of the heart is under examination. The cardiac AP present in non-nodal cardiac cells is generated by a transient change in the membrane voltage, powered by the electrochemical gradients of Na^+, K^+, and Ca^{2+} ions across the plasma membrane of a cell. The membrane of a cell acts as a capacitor, and as such, it separates ionic charges. The separation of these charged ions creates a voltage difference across the membrane, generating a voltage. The membrane potential (V_m) is then defined as the voltage difference across the membrane; at an unexcited state, the resting membrane potential (RMP) and the voltage difference are the same. Note, the electrochemical gradient has two components: one electrical (generated by the separation of a negatively charged extracellular space from a positively charged intracellular one) and the other chemical

(generated by an unequal distribution of cations across the intra- and extracellular space), hence *electrochemical*.

The cardiac AP is preceded by the activation of selective ion channels sensitive to voltage changes across the membrane. Once an electrical stimulus reaches these voltage-sensitive ion channels, it causes a structural conformational change such that the open state of the channel becomes more stable than the closed state, increasing the open probability of the channel. This sets up the opportunity for ions to travel across the membrane. However, the opening of selective ion channels alone is not sufficient to allow the movement of ions across the membrane.

The electrochemical gradient provides the driving force necessary for ion entry or exit through selective voltage-gated ion channels. The movement of ions will ensue until each ion reaches its respective equilibrium potential. At an ion's equilibrium potential, the net movement across the membrane for that ion becomes zero, and its respective influx or efflux dramatically decreases. The different ion concentrations for a typical teleost fish are shown below, and from these values the Nernst equilibrium potential for each ion species is determined.

Ion	Intracellular [mM]	Extracellular [mM]	Equilibrium Potential (mV)
Na^+	13	155	$^+55$
K^+	150	4	-81
Ca^{2+}	0.0001	2	$^+108$

Table 1. Intracellular and extracellular ion concentrations

The opening of these specific ion channels generates either an inward current (at voltages more negative than the equilibrium potential) or an outward current (at voltages more positive than the equilibrium potential). The normal voltage range of a typical teleost cardiac AP is between -90mV and $^+$50mV, thus it is safe to assume the Na^+ and Ca^{2+} currents will typically be inward and K^+ currents will typically be outward. Basic principles of the major ion currents involved in electrical excitation is the same between mammals and fish; however, there may be a difference in the molecular basis of the ion currents in fish model. Generally, fish ventricular AP can be divided into 5 phases and is determined by a complex sequence of activation and inactivation of channels carrying Na^+, K^+, and Ca^{2+} across the sarcolemma.

Phases of the ventricular action potential

There are 4 total phases that encompass the fish ventricular AP (**Figure 1.4**). during phase 0, the RMP will depolarize to a threshold level of AP firing when the total density of the inward Na^+ current exceeds the total density of the outward K^+ current. Once a depolarization occurs, a fast upstroke is generated, referred to as phase 0. Although we know the fast upstroke is generated due to an inward Na^+ current (I_{Na}), the specific channel responsible is still under debate. However, there is substantial evidence to suggest I_{Na} in the fish cardiomyocytes is due to activation of $NaV_{1.4}$ conductance.

Although many mammalian models exhibit isoforms of the same Na^+ channel, their $NaV_{1.4}$ is almost exclusive to skeletal muscles and not cardiac muscles.

The change in the voltage induced by I_{Na} increases the open probability of the K^+ channels, causing a rapid repolarization of the membrane potential, referred to as phase 1. This rapid repolarization is due to the activation of the transient outward potassium current (I_{to}), which is due to activation of a K^+ channel conductance and is typical for many mammalian species; however, this phase is small or completely missing in the hearts of many fish. The absence of I_{to} suggests channels generating I_{to} are not expressed in fish hearts, which is arguably the most predominant difference between fish and mammalian cardiac action potentials. Previous studies have shown an increased T-type Ca^{2+} channel current in zebrafish hearts. If this is also true for the goldfish heart, an increased T-type Ca^{2+} channel current and a limited I_{to} could explain why phase 1 is not pronounced in the goldfish heart. However, further research, specific to the goldfish heart, is needed in order to corroborate this hypothesis.

Phase 2 is brought on by a dominant I_{Ca} through the L-type Ca^{2+} channel (LTCC). The large influx of Ca^{2+} through this channel is responsible for the plateau phase of the AP; an absent feature in mice models but present in the goldfish and humans. Nonetheless, the large Ca^{2+} influx through the LTCC activates the ryanodine receptor protein (RYR) located on the membrane of intracellular Ca^{2+} storing organelles (Sarcoplasmic Reticulum, SR). The process of Ca^{2+} influx triggering Ca^{2+} release from the SR is referred to as Ca^{2+} induced Ca^{2+} release (CICR) and is the primary process powering cardiac contractions, greatly affecting the morphology of phase 2 of the AP. The significant increase in the intracellular Ca^{2+} concentration activates a protein that is a bi-directional regulator of cytosolic Ca^{2+}, the NCX.

In the forward mode, this exchanger utilizes the energy stored in the electrochemical gradient of Na^+ to exchange 3 Na^+ ions across the sarcolemma (SL) and into the cytosol for every 1 Ca^{2+} ion it extrudes from the cytosol. The influx of Na^+ through the NCX results in a net influx of positive charge across the SL. This creates an electrogenic effect, shifting the membrane potential towards a more positive (depolarized) value; however, this depolarization does not produce the same spike in the AP morphology as observed in phase 0. This is due to the presence of a different, counter current. This counter current is produced by the rapid and slow component of the delay rectifier potassium current (I_{Kr} and I_{Ks}, respectively), and balances the current from the NCX. This balance is the reason for the presence of a morphologically characteristic plateau in phase 2 of the AP.

Phase 3 is the start of repolarization of the action potential. Stronger I_{Kr} and I_{Ks} currents along with activation of the inward rectifier (I_{K1}) start to repolarize the membrane potential towards the K^+ equilibrium potential.

Finally, in phase 4 there is complete restoration of the negative RMP. Phase 4 is defined as the negative RMP of atrial and ventricular myocytes during diastole. Typically, this is around -70mV to -90mV in unexcited myocytes. The inward rectifier

current (I_{K1}) maintains the RMP but is thought to be less dense in fish cardiomyocytes as their RMP is closer to -70mV and that of humans is closer to -90mV. Also active during this phase of the AP are the currents from the NCX and the N^+/K^+ ATPase.
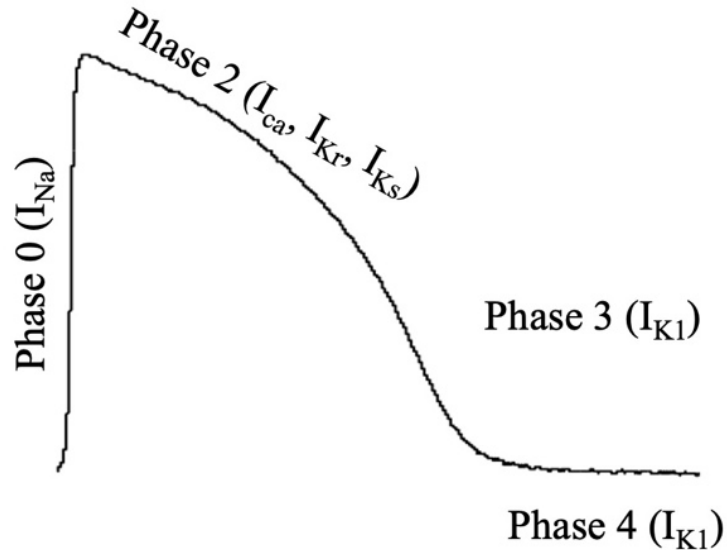
Figure 1.4: Different currents involved during the goldfish ventricular AP. Major ion currents involved in shaping the morphology of the AP are shown in parentheses.

1.3 The propagation of the electric signal changes Ca^{2+} concentrations leading to contractions of the heart

The electrical excitation (or AP) of the sarcolemma (SL) cardiac myocytes increases the concentration of intracellular Ca^{2+} and produces a force essential for cardiac contraction. The process by which electrical excitation is coupled to contraction of the myofilaments via changes in Ca^{2+} concentration is referred to as excitation-contraction coupling (**Figure 1.5**; ECC). During the ECC process, the AP propagates through the heart and increases the open probability of the LTCC; through this channel, there will be an increased I_{Ca} current.
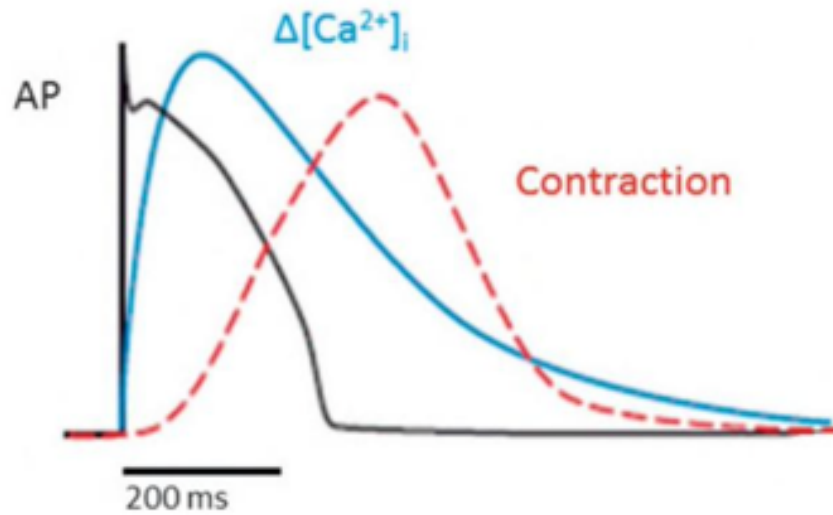
Figure 1.5: Excitation contraction coupling showing the action potential triggering the increase in the intracellular Ca^{2+} concentration resulting in muscular contraction (reprinted by permission from Copyright Clearance Center: Springer Nature, Nature, Cardiac excitation–contraction coupling, Donald M. Bers © 2002).

In mammals, ECC in adults occurs at the T-tubules; however, similar to mammalian neonatal models, fish cardiomyocytes lack the t-tubular system. So where does the ECC process occur in the fish? Although the fish heart does not possess T-tubules, it does have smaller invaginations called caveolae; however, the majority of the Ca^{2+} enters the cytosol across the SL. The process for ECC in fish myocytes is remarkably resembles that of mammals (**Figure 1.6**). ECC starts when there is an influx of Ca^{2+} through the LTCC. The LTCC in fish myocytes are located on the SL of the fish cardiomyocyte. Similar to mammals, an AP increases the open probability of the LTCC resulting in an influx of Ca^{2+} (the Ca^{2+} current (I$_{Ca}$)). However, a I$_{Ca}$ can also be generated by the NCX.

The NCX is a bi-directional regulator of cytosolic Ca^{2+} and, thus, contributes to the Ca^{2+} transient. In the forward mode, the NCX exchanges 3 Na$^+$ ions across the SL and into the cytosol for every 1 Ca^{2+} ion it extrudes from the cytosol; this mode operates almost exclusively during the relaxation phase on the Ca^{2+} transient. However, the directionality of ion transport by the NCX is complex; the electrochemical gradient determining whether the NCX works in the forward or reverse mode is dependent on the Vm, ion concentration, and the net gradient changes during the cardiac cycle. Nevertheless, during the Vm depolarization, the NCX reverses its directionality moving Ca^{2+} in and Na$^+$ out of the cytosol (reverse mode). During the ECC process, the NCX is operating in the reverse mode, and thus contributes significantly to the I$_{Ca}$.

Regardless, both the LTCC and NCX result in an increased cytosolic Ca^{2+} concentration. The influx of Ca^{2+} triggers the release of Ca^{2+} from the sarcoplasmic reticulum (SR) through the ryanodine receptors (RYR), referred to as CICR. The LTCC is co-localized with RYR. This causes a transient rise in the intracellular Ca^{2+}

concentration, setting the stage for myofilament contraction. The free Ca^{2+} in the cytosol binds to a specific part of the cardiac muscle, sarcomeres, initiating contraction. The sarcomere is composed of actin (thin), and myosin (thick) filaments. The interaction of these filaments during a contraction are referred to as cross-bridge formation and is essential for a successful cardiac contraction (systole). The thin filament is associated with the regulatory proteins responsible for initiating and controlling the activation of force generation, referred to as troponin I (TnI), troponin T (TnT), and troponin C (TnC) while the thick filament is composed of myosin.

Troponin C has a binding site for Ca^{2+} (hence the "C" in troponin C), and once Ca^{2+} binds to this site, it induces a conformational change in TnI, removing its inhibitory effect (hence the "I" in TnI), and moving tropomyosin across actin in order to expose the myosin binding sites on the actin filament. The myosin heads interact with ATP molecules during this process to successfully bind and unbind from the actin filaments. Once ATP binds to the myosin head, it can be hydrolyzed into ADP, causing the myosin head to move into a "cocked state" ready to bind to actin. Once myosin binds to actin, the actin filaments slide over the myosin filaments toward the M-line, generating a "power stroke". Following the power stroke, the myosin heads release the APD molecule, and get ready for another ATP molecule to bind.

Relaxation of the muscles occurs when the cytosolic Ca^{2+} decays. Either Ca^{2+} is removed from the cytosol and placed back into the SR via SR Ca^{2+} pumps (SERCA), or Ca^{2+} is transferred back across the SL by the forward mode of the NCX. SERCA replenishes the SR Ca^{2+} content by hydrolyzing 1 molecule of ATP for every 2 Ca^{2+} ions pumped back into the SR. The rate at which Ca^{2+} is pumped back into the SR is highly influenced by a protein called phospholamban (pln). Under normal conditions, pln has a negative inhibitory effect on SERCA, limiting the rate at which it can pump Ca^{2+} back into the SR. Pln, however, is regulated by Protein Kinase A (PKA). Under a "fight or flight" response (or sympathetic response), PKA will phosphorylate pln and remove its inhibitory effect on SERCA, allowing more Ca^{2+} to be pumped back into the SR. The relaxation of the heart (diastole) is then defined as the point in the cardiac cycle in which no force is generated.
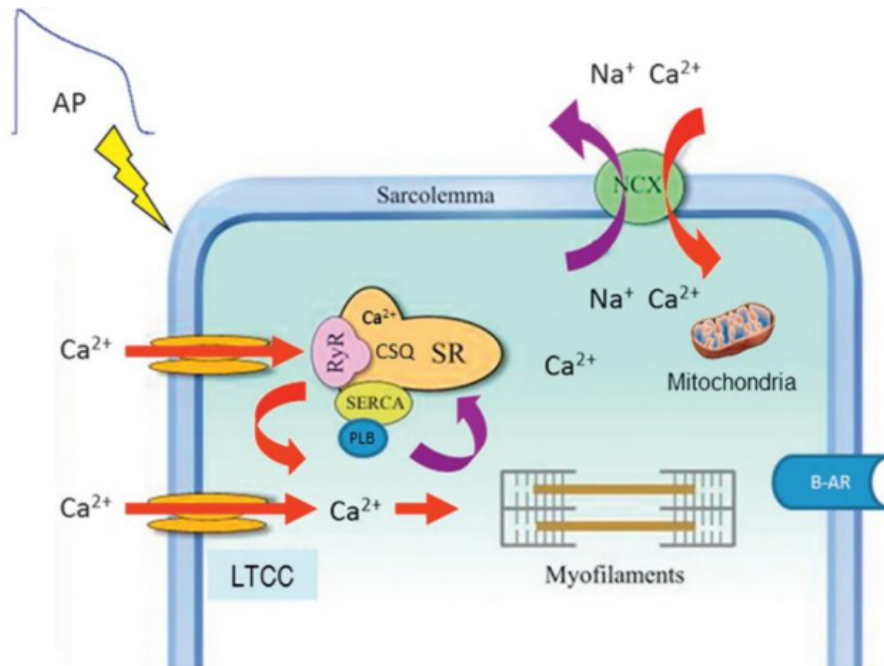
Figure 1.6: ECC starts when an action potential (AP) increases the open probability of the LTCC, located on the SL of the fish cardiomyocyte, resulting in an influx of Ca^{2+} (the Ca^{2+} current (I_{Ca}). The LTCC is co-localized with ryanodine receptor and an influx of Ca^{2+} triggers the release of Ca^{2+} from the sarcoplasmic reticulum (SR) through the RYR2. This causes a transient rise in the intracellular Ca^{2+} concentration. The free Ca^{2+} in the cytosol binds to the sarcomeres on the myofilaments, initiating contraction (reprinted by permission from Copyright Clearance Center: Springer Nature, Nature, Cardiac excitation–contraction coupling, Donald M. Bers © 2002).

1.4 The Autonomic Nervous System (ANS) affects cardiac excitability

In nearly all vertebrate species, direct input from the autonomic nervous system tightly controls cardiac contractility and excitability (Lee and Shideman, 1959; Katz, 1967; Lindemann and Watanabe, 1985; Cohn, 1989; Henning, 1992). Although there is an abundant amount of research on the autonomic control of cardiac contractility and excitability in numerous mammalian species, the characterization of pathophysiological mechanisms is still difficult to obtain for humans specifically. This is in part due to humans having strikingly dissimilar AP characteristics and electrocardiographic morphology in comparison to commonly used animal models such as mice, rats, and rabbits (Bazmi and Escobar, 2020; Nakamura et al. 2002; Tsai et al. 2011). Fish, on the other hand, are the largest and most diverse group of vertebrates, and as such, their autonomic nervous system regulation can often deviate from the classical vertebrate models used to study autonomic control of cardiac contractility and excitability. The most drastic difference in autonomic system regulation can be observed when comparing the hagfish, which have no known autonomic nervous system control, to the teleost, which exhibit fully functional autonomic regulation in cardiac function (Sandblom and Axelsson, 2011). Nevertheless, if a fish species does exhibit autonomic regulation, it is

likely similar in function to mammalian species. In vertebrate species exhibiting full autonomic control, the autonomic nervous system functions through two closely intertwined antagonistic branches: the sympathetic branch and the parasympathetic branch.

The sympathetic nervous system

The sympathetic branch of the nervous system, referred to as the sympathetic nervous system, augments cardiac function, excitability, and contractility through the release of transmitters referred to as catecholamines (**Figure 1.7**; Lee and Shideman, 1959; Evans, 1986; Marks, 2013). The endogenous catecholamines released during a "fight or flight" response bind to and stimulate β-adrenergic receptors, which in turn increase the speed of conduction through the atrioventricular node (referred to as a positive dromotropic effect), increase heart rate (referred to as a positive chronotropic effect), increase contractility (referred to as a positive inotropic effect), and increase the velocity of myocardial relaxation during diastole (referred to as a positive lusitropic effect). Locally released catecholamines, such as norepinephrine (NE), stimulate the β-adrenergic receptors by activating adenylyl cyclase (AC) (Hildebrandt et al. 1983; Brum et al. 1984) and increasing cyclic adenosine monophosphate (cAMP) levels (Osterrieder et al. 1982). Increased cAMP levels activate protein kinase A (PKA) (Krebs, 1972; Hayes and Mayer, 1981) and induce the dissociation of its catalytic subunit. Levels of cAMP, and thus PKA, are finely regulated by cyclic nucleotide phosphodiesterases (PDEs) which degrade cAMP into 5'-AMP. Nevertheless, the catalytic subunit of PKA phosphorylates several key Ca^{2+} handling proteins such as the LTCC (Collins et al. 1981; Osterrieder et al. 1982), the RYR2 (Suko et al. 1993; Valdivia et al. 1995), and pln (Weilenmann et al. 1987). These modifications not only alter the electrical activity of the myocardium, which have positive dromotropic and chronotropic effects, but also Ca^{2+} handling dynamics in the myocardium which lead to positive inotropic and lusitropic effects (Aguilar-Sanchez et al. 2019).

Although the augmentation of cardiac function is critical during a fight or flight response, regulation of this mechanism is arguably even more significant. Without a mechanism regulating the positive inotropic actions induced by catecholamines, excessive Ca^{2+} influx into the cardiomyocyte would lead to Ca^{2+} overload, increasing the probability of spontaneous SR Ca^{2+} release events during diastole. This overload could lead to severe pathological conditions inducing delayed diastolic depolarizations. These delayed diastolic depolarizations could trigger extrasystolic APs, and eventually ventricular tachycardias and arrythmias (Katra and Laurita, 2005; Curran et al., 2010; Ko et al., 2017).

The positive inotropic actions of catecholamines are under negative feedback control *via* Ca^{2+} dependent inactivation (CDI; Tillotson, 1979; Lipp et al., 1987; Lacampagne et al., 1996; Peterson et al., 2000) and voltage dependent inactivation (VDI; Cota et al., 1984; Kass and Sanguinetti, 1984; Lee et al., 1985; Zhang et al., 1994; Ferreira et al., 1997, 2003) of the LTCC ($Ca_V1.2$). Under these negative feedback mechanisms, $Ca_V1.2$ can reduce its own open probability, and limit the amount of Ca^{2+}

influx into the cardiomyocytes; completely avoiding the aforementioned pathologic conditions (Zhang et al., 2014). Although VDI is poorly elucidated in fish ventricular myocytes, CDI is likely to be present. CDI is mediated by the Ca^{2+} sensor protein, calmodulin (CaM; Zühlke et al., 1999; Peterson et al., 2000; Pitt et al., 2001). CaM has an IQ motif located in the cytoplasmic C-terminal tail of the channel's α1 subunit (**Figure 1.7;** Peterson et al., 1999; Qin et al., 1999; Zühlke et al., 1999) and four helix-loop-helix domains (EF-hands) grouped within two lobes with low and high affinity for Ca^{2+} (Chin and Means, 2000) critical for CDI. Under β-adrenergic stimulation, there is an increased sarcolemmal Ca^{2+} influx. The Ca^{2+} bind to CaM and reduce the open probability of $Ca_V1.2$, limiting the influx of Ca^{2+} across the sarcolemma, and counteracting the positive inotropic effects induced by β-adrenergic stimulation.
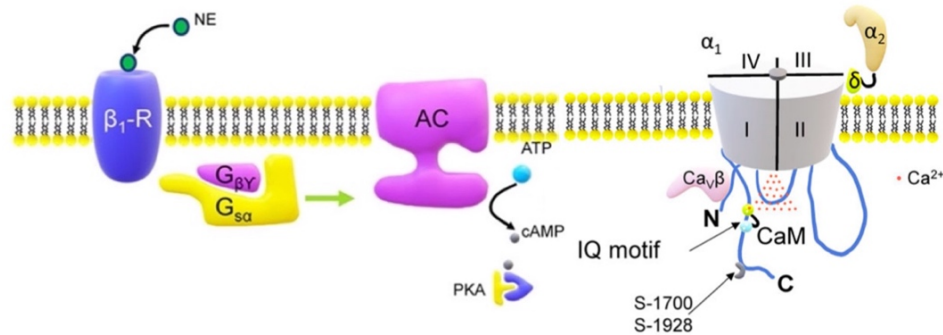
Figure 1.7: The norepinephrine (NE) activation of the G-protein coupled receptor complex leads to PKA phosphorylation of the α1 subunit of the LTCC. When α1 is phosphorylated, there is an increase in the Ca^{2+} current through the LTCC, promoting a local increase in the free Ca^{2+} concentration on the cytosolic face of the channel. This elevation in Ca^{2+} concentration will increase the probability of binding between Ca^{2+} and CaM, promoting CDI. The central molecular components of a $Ca_V1.2$ channel are shown as the pore-forming subunit α1 and the regulatory subunits α2, δ, and CaV β. The interaction of CaV β and the N terminus of α1 are essential in defining the VDI. CaM binding site at the IQ motif located at the C terminaus is the protein locus involved in CDI. The PKA phosphorylation sites (S-1700 and S-1928) are located on the C terminus of the LTCC (Picture modified from Bazmi and Escobar, 2019).

The parasympathetic nervous system

The sympathetic branch of the nervous system is highly antagonized by the parasympathetic branch. Referred to as the parasympathetic nervous system, this branch modulates cardiac contractility and excitability through the local release of the transmitter acetylcholine (ACh) from postganglionic cholinergic intracardiac neurons. The ACh subsequently binds to and stimulates muscarinic (M2) receptors. Activation of M2 receptors stimulates a Gi protein, which inhibits AC (Krebs, 1972). This inhibition leads to significantly lower levels of cAMP, a reduced fraction of activated PKA, and a decreased degree of phosphorylation in the key Ca^{2+} handling proteins (LTCC, RYR2, pln). These modifications result in negative inotropic, chronotropic, dromotropic, and lusitropic effects, all of which are crucial in countering the sympathetic nervous system

and maintaining homeostasis in the vertebrate central nervous system (Aguilar-Sanchez et al. 2019; Watanabe and Lindemann, 1984). Previous literature suggests few fish models exhibit autonomic control in a similar manner to larger mammals; however, it is not clear how autonomically driven AP kinetics impact cardiac contractility in the fish intact heart specifically.

Despite its physiological significance, the molecular and ionic mechanisms involved in the fish cardiac pacemaker are poorly understood. In the mammalian model, adrenergic or cholinergic agonists augment the cardiac pacemaker, inducing an increased or decreased heart rate, respectively. The changes in the mammalian heart rate are mediated by corresponding changes in the two "clock" mechanisms located in the cardiac pacemaker cells. Although the significance of each mechanism in cardiac rhythm is heavily disputed, both clocks appear to contribute to the discharge of pacemaker APs. The first clock mechanism is a "membrane clock" and is produced by a small I_{Na}, various I_K currents (I_{kr}, I_{Ks}, I_{to}), I_{Ca} (I_{CaL}, I_{CaT}), I_{NCX}, and I_f. Proponents of the membrane clock hypothesis regard the inward current produced by I_f as the key operator in promoting diastolic depolarization and arbitrating the effects of the autonomic nervous system on heart rate. The Ca^{2+} clock, on the other hand, is based on spontaneous local release of Ca^{2+} from the SR by RYR2, which generates a small inward current via the NCX and drives the membrane potential to the threshold of I_{Ca} dependent AP. Proponents of the Ca^{2+} clock hypothesis attribute the effects of the autonomic nervous system on heart rate to the rate of Ca^{2+} cycling through the SR, which push the membrane potential to an I_{Ca} dependent AP.

Regardless, both clock mechanisms are dependent on the phosphorylation and dephosphorylation of key Ca^{2+} handling operators (LTCC, RYR2, CaM) in a cAMP dependent manner. As discussed previously, the cAMP can directly influence I_f and alter cardiac rhythm. Interestingly, HCN4 channels responsible for generating the I_f current have only been identified in the goldfish model (Newton et al. 2014; Tessadori et al. 2012); however, their role in modulating cardiac rhythm during a cholinergic or adrenergic response is poorly elucidated. Although this thesis does not identify the role(s) of the I_f specifically; it does aim to show that the goldfish heart exhibits strong ventricular adrenergic and cholinergic responses, something that has not been identified previously in fish ventricular cardiac myocytes (Fritsche and Nilsson, 1990; Laurent et al. 1983; Steele et al. 2009).

Significance

In this thesis, the goldfish heart is proposed as an alternative novel vertebrate model to study larger mammalian cardiac physiology. Electrophysiological properties of the goldfish heart such as the excitation–contraction coupling process along with autonomic nervous system augmentation of cardiac electrical and contractile behavior were investigated to assess and establish the relevance and applicability of this novel fish model. Goldfish were initially chosen as an alternative vertebrate model due to their physiological similarities to the zebrafish model (Málaga-Trillo et al., 2002; Kon et al., 2020). Preliminary research highlighted the similar advantages of the goldfish heart, such as the possibility of being used as an embryological model (Grivas et al., 2014), being altered via transgenesis using CRISPR/Cas9 (Yin et al., 2018), or being used in electrophysiological and Ca^{2+} signaling experiments (Chen et al., 2005; Leo et al., 2019), without the disadvantages presented in the zebrafish heart detailed in the introduction.

The mechanisms involved in mammalian cardiac excitation-contraction coupling process has been studied extensively and is well established. However, the models used to establish the current mechanistic understandings present limitations, which make characterization of pathophysiological mechanisms using these models difficult to obtain and apply to humans specifically. This is in part due to humans having strikingly dissimilar AP characteristics and electrocardiographic morphology in comparison to commonly used animal models such as mice, rats, and rabbits. Thus, the suitability of an alternative vertebrate model relies heavily on its resemblance of AP characteristics, Ca^{2+} handling dynamics, electrocardiographic morphology, and heart rate/temperature dependency in comparison to larger mammalian models. The main mechanisms involved in the excitation-contraction coupling process during the cardiac cycle of a goldfish heart were investigated in this thesis through experiments aimed to (i) evaluate the dependency of the AP and Ca^{2+} transients on heart rate and temperature, (ii) assess the role of L-type Ca^{2+} currents in the excitability of the myocytes, as well as its contribution to Ca^{2+} transients, and (iii) weigh the contribution of SR Ca^{2+} release to Ca^{2+} transients and AP repolarization. These experiments were tackled using a combination of pulsed local field fluorescence microscopy (Mejía-Alvarez et al., 2003; Escobar et al., 2004, 2006; Aguilar-Sanchez et al., 2017), sharp microelectrode intracellular recordings (Ferreiro et al., 2012; López Alarcón et al., 2019; Aguilar-Sanchez et al., 2019), and flash photolysis (Escobar et al., 2012; Ramos-Franco et al., 2016; López Alarcón et al., 2019; Aguilar-Sanchez et al., 2019).

Mammalian autonomic regulation of cardiac excitability and its associated ionic currents have been studied extensively and are well established. Thus, the appositeness of an alternative experimental vertebrate model will heavily rely on its resemblance of autonomic control to larger mammalian models. To explore and establish how the goldfish autonomic nervous system augments cardiac dromotropism (rate of impulse conduction), chronotropism (heart rate), ionotropism (contractility), and lusitropism (myocardial relaxation), experiments in this thesis were designed and performed to (i) assess changes in the cardiac AP, electrocardiogram, and Ca^{2+} transient dynamics under a sympathetic drive, (ii) assess changes in the cardiac AP, electrocardiogram, and Ca^{2+}

transient dynamics under a parasympathetic drive using a combination of pulsed local field fluorescence microscopy and sharp microelectrode intracellular recordings.

Chapter 2: Materials and Methods

2.1 Intact fish and mice hearts were stabilized in a Langendorff perfusion apparatus

The experiments presented in this thesis were completed using the goldfish, zebrafish, and mouse models. Goldfish, zebrafish, and mice were maintained in accordance with the National Institutes of Health Guide for the Care and Use of Laboratory Animals (NIH Publication No. 85–23, Revised 1996) and the Institutional Animal Care and Use Committee guidelines of the University of California Merced (Protocol # 2008–201).

Both fish models used were 1 year old and anesthetized by immersion in ice cold water containing 0.16 mg ml–1 tricaine methanesulfonate for 2–5 min prior to the extraction of the heart. Extraction of an intact heart from any animal model is extremely difficult as even a small cut could significantly damage the cardiac muscles and lower the credibility of the data obtained during the experiment. Indeed, damaged fish cardiac muscle could show signs of ischemia, have increased intracellular Na^+ concentrations, or even a more depolarized membrane. Since the fish hearts are so small (**Figure 2.1**), strict precautions were followed to limit any unnecessary damage to the intact heart. Fish were initially placed in the ice-cold water as the cool temperature of the water reduces the metabolic rate, motility, and function of the fish motor skills. The tricaine methanesulfonate in the ice-cold water blocks skeletal voltage gated Na^+ channels ($NaV_{1.5}$), in order to further prevent movement of the fish. The immobility of the fish is crucial during recovery of the intact heart, as this limits tissue damage to the cardiac muscle. As the zebrafish and goldfish are different in body size, each were submerged in tanks having different volumes with respect to the fish size. The tail of the fish was held with a small curved tweezer to check if each fish were completely anesthetized before decapitation. After decapitating the fish with scissors, the heart was removed rapidly from the animal's chest. The zebrafish or goldfish heart was cannulated onto either a 32-gauge needle or a 27-gauge needle, respectively, on the Langendorff apparatus (**Figure 2.2**). The largest limitation present during the heart extraction is arguably the increased difficulty of retrieving an intact heart with minimal damage from such a small animal model. For the mouse heart on the other hand, the limitation during the extraction process could be the formation of blood clots which cause permanent and irreparable damage to the tissue. Interestingly, neither formation of blood clots nor ischemic myocadiac tissue were observed in the goldfish smaller than 5 inches in length. For this reason, the goldfish hearts were easier to extract and cannulate.

Mouse hearts were obtained from 8-week-old c57BL/6 male mice (Charles River Laboratories). Animals were injected intraperitoneally with sodium heparin 15 minutes prior to cranial dislocation. Sodium heparin acts as a blood thinner, and thus, prevents blood clots from forming in the capillaries and damaging the cardiac tissue. Mice were injected with 15,000 USP units per Kg using 1000USP/mL sodium heparin. These

measurements were based on the mass of the mouse, and since the average mouse weighs roughly 20kg, each mouse was injected with 20 units (or 200uL) of 1000USP/mL sodium heparin. Following the 15-minute waiting period, the mice were euthanized by cranial dislocation. No sedatives were administered to the mice prior to cranial dislocation, as these pharmacological agents have been known to alter cardiac behavior and function. Once the mice were euthanized, the heart was rapidly removed from the animal's chest and cannulated onto a 23-gauge needle on the Langendorff apparatus. Rapid extraction and recovery of the mice heart is crucial during this stage in order to prevent any ischemic damage to the cardiac tissues. Indeed, ischemic damage can greatly depolarize the RMP, increase the intracellular Na^+ concentration, or alter cytosolic Ca^{2+} handling dynamics.

— 1mm
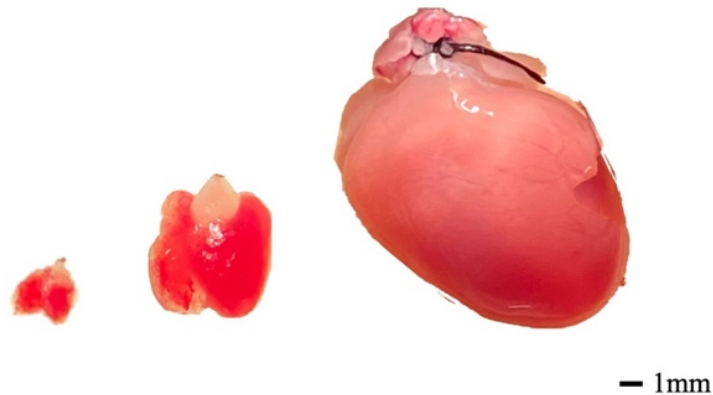
Figure 2.1: Recovered intact zebrafish, goldfish, and mouse heart pictured at 1mm scale, from left to right.

The Langendorff system was developed in 1895 and has arguably become one of the most reliable methods employed to maintain mammalian hearts *ex vivo*. Although this method was initially common for mammalian hearts, today, this method is widely used for vertebrate hearts in general as it unfailingly keeps an intact heart viable for several hours. The importance of experimenting on an intact heart cannot be underestimated; as mentioned before, the heart is an electromechanical organ and separation of the tissue results in separation of electrically, mechanically, and metabolically coupled processes. In the Langendorff system, the heart is allowed to remain intact and is placed in a more physiologic setting compared to that of a system in which the cardiac cells are separated from the heart and studied independently. When the heart remains intact, the syncytium of the heart is maintained and the uncoupling of these critical processes is minimized; however, if the cardiac tissue in the heart is dissociated to allow for cellular research, these critical processes become uncoupled as a result of the harsh enzymatic dissociation process. Thus, an intact organ is critical to allow for reliable assessment of cellular variables such as Ca^{2+} handling dynamics and membrane potential changes.

The Langendorff setup retroperfuses the heart with Tyrode solution (equilibrated with 100% O_2 in all mice experiments) i.e., with Tyrode solution that enters the heart in the opposite direction to that of regular physiological blood flow. As discussed previously, in a normal physiological setting, blood is ejected through either the bulbous

arteriosus (for the fish model), or the aorta (for the mammalian model). However, during retroperfusion, Tyrode solution delivers crucial nutrients to the heart through the coronary arteries; this is how the Langendorff system can maintain a healthy intact heart vital for hours. Since the heart is being constantly retroperfused with Tyrode, adverse metabolic byproducts are washed from the heart and collect in the horizontal chamber. The solution that collects in this horizontal chamber is constantly being removed by a suction vacuum system and discarded (**Figure 2.2**). In order to keep the heart stable during this perfusion process, the heart of each animal was held in position with a non-absorbable surgical suture that was tied around either the bulbous arteriosus (for the fish model), or the aorta (for the mammalian model). If the hearts were not tied into position, the flow of the Tyrode would push the heart off the cannula.
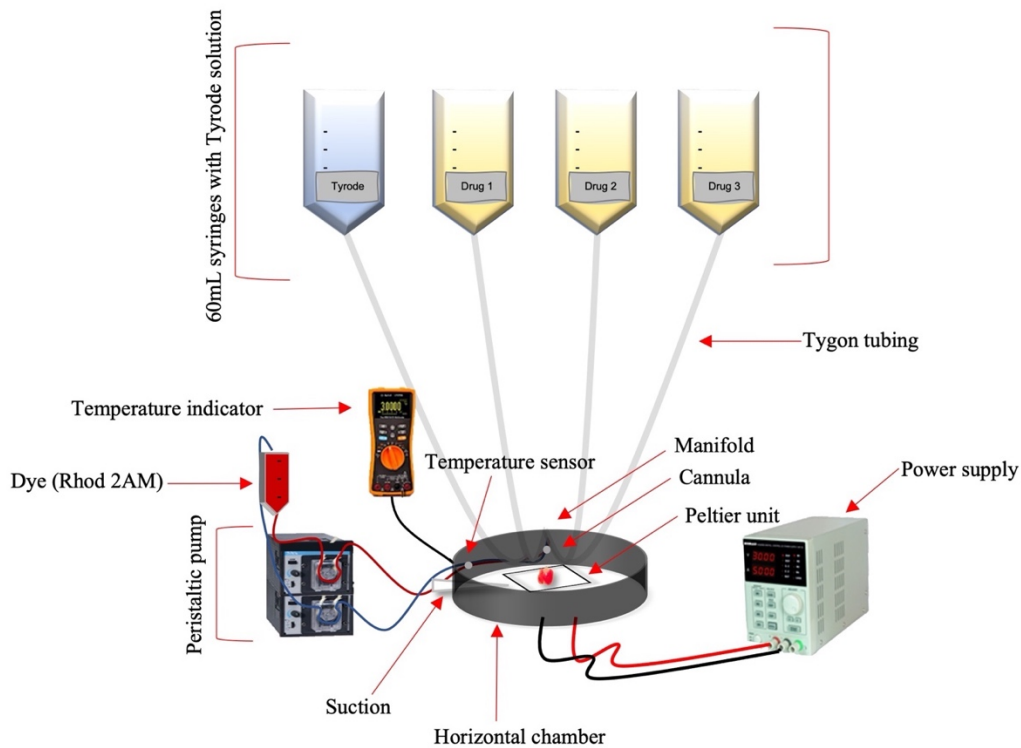
Figure 2.2: The Langendorff perfusion apparatus used to retro perfuse Tyrode solution into fish and mice hearts. The temperature is set by the Peltier unit located under the chamber.

The nutrients in Tyrode solution are crucial for maintaining healthy cardiac tissue during the course of the experiment. Indeed, if the ionic concentrations in the Tyrode are even a little off, it can result in whole heart ischemia, or even premature death of the cardiac tissue. Thus, to ensure the longevity of the cardiac tissue and experiment, the ionic concentrations in the Tyrode solution need to be as close as possible to those found in the endogenous blood serum. **Table 2.1** and **2.2** list the concentrations used to make Tyrode solution for the fish and mouse models, respectively. The acidity of Tyrode

solution was measured by its corresponding pH value and was adjusted to either 7.3 and 7.4 for the fish and mouse models, respectively. It is important to note, unlike blood, Tyrode solution lacks necessary proteins, antibodies, and neurotransmitters; all of which could affect the results obtained and discussed in this thesis. In order to compensate for another compound circulating in the blood, O_2, the Tyrode solution perfused into mice hearts was saturated with 100% O_2, using submerged "air stones" connected to the O_2 supply tank. However, consistent with literature corresponding to fish hearts specifically, the Tyrode solution for the fish model was not oxygenated. Previous literature has argued Tyrode oxygenation (for the fish model specifically) does not alter the cardiac function or longevity; indeed, when we conducted experiments in the fish model with oxygenated Tyrode solution, no significant morphological difference in the AP, Ca^{2+} transients, or ECG of the fish heart were observed. All data presented in this thesis corresponding to the fish model were obtained without oxygenating the Tyrode solution.

Compound	Molecular Weight [g/mol]	Concentration [mM]
NaCl	58.44	150
KCl	74.55	3
$CaCl_2$	147.02	1.8
$MgCl_2$	203.3	1.2
$NaPO_4H_2$	138	0.42
HEPES	238.31	10
Glucose	16	10

Table 2.1. Tyrode solution concentrations used to perfuse the zebrafish and goldfish heart. The acidity of the solution was measured by the pH value and adjusted to 7.3 at 28°C to more accurately replicate the endogenous blood serum.

Compound	Molecular Weight [g/mol]	Concentration [mM]
NaCl	58.44	140
KCl	74.55	5.4
$CaCl_2$	147.02	2
$MgCl_2$	203.3	1
$NaPO_4H_2$	138	0.33
HEPES	238.31	10
Glucose	16	10

Table 2.2. Tyrode solution concentrations used to perfuse the mice. The acidity of the solution was measured by the pH value and adjusted to 7.4 at 37°C to more accurately replicate the endogenous blood serum.

The heart of each vertebrate model was retroperfused with regular Tyrode at room temperature for 10 minutes to ensure the extracted heart was in a stable condition for the experiments. This stabilization period allows for the heart to recover from any minor insult acquired during the extraction process. Unless stated otherwise, the temperature of

the horizontal chamber was controlled by a Peltier unit and adjusted to either 28°C or 37°C the physiological temperature of the fish and mice model, respectively. However, the data presented in this thesis corresponding to the mice model were conducted at 32°C. At 32°C, the activity of certain ATP-binding cassette (ABC) transporters can be minimized, and the removal of exogenous molecules from the cytosol is mostly inhibited. This is particularly advantageous, as the excretion of the fluorescent indicator, Rhod-2AM, is minimized and is maintained in the heart for the duration of the experiment. Furthermore, a few sections of this thesis address the temperature dependency of the membrane potential and the intracellular Ca^{2+} concentrations. The data collected in these experiments were collected with varying temperatures, controlled by the Peltier unit positioned at the bottom of the recording chamber and measured with a linearized semiconductor temperature sensor.

All data presented in this thesis either examine changes in the membrane potential and/or the Ca^{2+} transients of an intact heart. The tools used to measure these changes are extremely delicate and vulnerable to motion of any kind. For example, the membrane potential is measured by a small glass microelectrode (described in section 2.2). This microelectrode is so delicate, that even the smallest motion could cause it to break, rendering it useless. If the microelectrode does not break, it will only reflect the motion artifact in the data, and nothing else. Furthermore, these motion artifacts are also recorded by the highly sensitive optical fibers recording Ca^{2+} transients. Thus, preventing mechanical motion of the heart is crucial for obtaining reliable data. However, as previously discussed, the heart contracts during systole. The small movement of the heart during systole is enough to either break the glass microelectrode or cause the collected data to become unreadable due to the presence of the motion artifacts. In order to combat this problem and prevent systolic mechanical activity, the heart of the fish and mouse model was perfused with blebbistatin (Sigma, St. Louis, MO). Blebbistatin is arguably the most common pharmacological agent used in muscular experiments and works by inhibiting the actin-myosin interaction without altering cardiac electrical activity or Ca^{2+} dynamics. For this reason, 100 μl of blebbistatin was perfused through the fish and mouse heart prior to the start of any experiment.

Pharmacological Agents

The goldfish heart was perfused with fish Tyrode solution containing 4 mM blebbistatin prior to obtaining any electrophysiological recordings to suppress cardiac motion. In order to elicit a sympathetic response, the goldfish heart was perfused with fish Tyrode solution containing 100 nM isoproterenol for 10 minutes before the start of any AP and Ca^{2+} transient recordings. To determine if the sympathetic response to isoproterenol could be reversed, the goldfish heart was perfused with fish Tyrode solution for a prolonged amount of time. Indeed, the effects of isoproterenol could be completely reversed if the goldfish heart were continuously perfused with fish Tyrode solution for 20 minutes. In contrast, to elicit a parasympathetic response the goldfish heart was perfused with fish Tyrode solution containing 5 μM carbamylcholine for 10 minutes prior to the start of any AP and Ca^{2+} transient recording. The effects of carbamylcholine could be completely reversed after continuously perfusing the heart with fish Tyrode solution for

60 minutes. Recordings obtained prior to perfusion with isoproterenol or carbamylcholine were considered as control and recordings obtained following isoproterenol or carbamylcholine perfusion were considered as experimental.

Consistency in the experimental approach for this thesis was ensured and maintained through identical protocol execution, i.e., all hearts were cannulated, stabilized, and retroperfused in an identical manner.

2.2 Electrical measurements using sharp microelectrodes and ECG

The electrical activity of the heart is crucial in defining cardiac function. At a cellular level, electrical activity is measured by the AP and is reflective of the cumulative ionic currents involved in triggering the cascade of cellular events responsible for setting cardiac contraction into motion. As different ionic currents are activated with respect to the phase of the AP, the effects of an administered agonist can be deciphered by addressing the new morphological changes in the phases of the AP.

Sharp glass microelectrodes

All electrical AP recordings presented in this thesis were recorded from the epicardial layer of the ventricle using sharp glass microelectrodes filled with 3 M KCl. Glass microelectrodes were fabricated with a micropipette puller (Sutter Instrument Co., CA) with a resistance of 10–20 MΩ and were connected to a high-input impedance differential amplifier (World Precision Instruments (WPI), Sarasota, FL). A manual mechanical micromanipulator was used in order to gradually position the glass microelectrode onto the surface of the ventricle, located in the horizontal chamber. Once the microelectrode was positioned in the horizontal chamber, the readout obtained from the electrode was adjusted to 0 in reference to an accompanying grounding AgCl electrode pellet (WPI, Sarasota, CA). The ventricular epicardium was impaled with the glass microelectrode in order to obtain membrane recordings. Data were recorded with an acquisition system Digidata 1440A (Molecular Devices, Sunnyvale, CA) using pClamp 10 software.

Whole Heart Electrocardiographic Measurements

An ECG provides profound insight on the status of whole heart electrical activity. Even in a transmural ECG, each wave reflects a corresponding electrical change taking place in different chambers and muscular layers of the heart. The transmural ECGs presented in this thesis were only obtained from the goldfish model. Generally, the goldfish ECG consisted of 3 main components: the QRS complex (ventricular depolarization), J wave (likely due to a voltage gradient due to the presence of a prominent AP notch in the epicardium but not the endocardium), ending with T wave (ventricular repolarization). The transmural ECG recordings were obtained using a miniature ECG device constructed in Dr. Escobar's lab. This device had two reference

Ag-AgCl micropellets; one of which was placed inside the left ventricle through a small hole created by an acupuncture needle, the other was positioned on the surface of the left ventricle (**Figure 2.3**). As mentioned previously, these were transmural ECG recordings and thus lacked a P-wave (atrial depolarization). Signals were amplified by a custom-made DC-coupled instrumentation amplifier and were digitally sampled identically to the AP recordings.
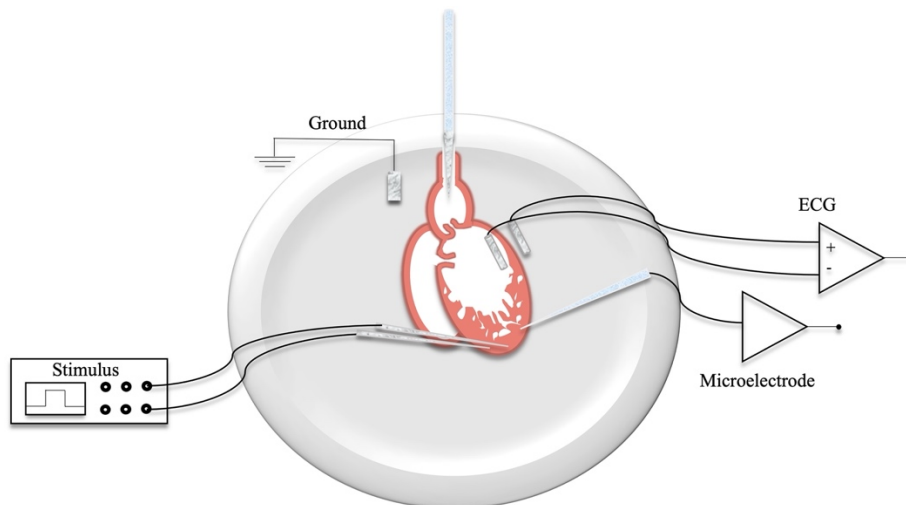
Figure 2.3: Electrophysiological measurements were recorded with sharp glass microelectrodes (cellular) and electrocardiograms (ECG; ventricular). The sharp glass microelectrode impaled the ventricular epicardium to obtain membrane recordings. The transmural ECG contained two reference Ag-AgCl micropellets; one positioned inside the left ventricle through a small hole created by an acupuncture needle, the other positioned on the surface of the left ventricle. The hearts were paced from 1-3Hz with the aid of two acupuncture needles located in the apex of the ventricle.

One important confounding variable in any experimental procedure examining the intact heart is the heart rate. If the heart rate is not consistent throughout the experiment, then changes observed in the duration of the AP or the Ca^{2+} could become unreliable, as they would instead reflect a lowered or increased heart rate, and not the pharmacological agent used. Thus, fish and mice hearts were continuously paced at 1-3Hz with the aid of two acupuncture needles placed in the apex of the ventricle in the presence and absence of the pharmacological agents. The acupuncture needles were connected to wave generator that produced square current pulses at 1ms. However, the hearts were not paced in experiments assessing ANS induced changes in the spontaneous heart rate.

2.3 Detecting intracellular Ca^{2+} signals: Rhod-2AM loading

The use of fluorescent molecular probes has enabled scientists to make astounding advancements in better understanding the molecular events underlying physiological phenomena. In this thesis, the Ca^{2+} indicator dye Rhod-2AM was used to directly assess changes in intracellular Ca^{2+} dynamics and kinetics. Although the AP can reflect changes in the Ca^{2+} handling, the use of specific dyes allows for a more direct and

reliable insight on how the Ca^{2+} dynamics change in the presence of pharmacological agents.

Rhod-2 AM is an acetoxymethyl (AM) ester (Invitrogen, Carlsbad, CA) rhodamine-based dye belonging to a larger group of red fluorescent calcium indicators, rhod-2. The uptake of Rhod-2AM into the cell is facilitated by the AM group. Once inside the cell, cytoplasmic esterases remove the membrane permeant ester group, preventing extrusion of rhod-2 from the cell, resulting in an accumulation of rhod-2 in the cytosol. Rhod-2 has a high affinity BAPTA binding site, which facilitates the binding of Ca^{2+} to rhod-2. Once bound to Ca^{2+} the fluorescence of the rhod-2 increases 100-fold and can be recorded using the pulsed local field fluorescent microscopy technique, described in section 2.4. Pulsed local field fluorescent microscopy excites rhod-2 with a 532nm wavelength light source and if Ca^{2+} is bound, will record the emitted fluorescence of 560-630nm.

Fluorophore loading of Rhod-2AM

Rhod-2AM (50 μg) was dissolved in 20 μl Dimethyl sulfoxide (DMSO) and 20 μl of 20% triblock copolymer surfactant pluronic in 1 ml fish Tyrode solution. The dye solution was then sonicated (FS20 Ultrasonic Cleaner; Fisher Scientific, Pittsburgh, PA) for 35 minutes to minimize formation of precipitates which could potentially injure the cardiac tissue during the perfusion process.

Cannulated hearts of the goldfish, zebrafish, and mice were allowed to stabilize for 15 minutes at 23°C (room temperature) via continuous retro perfusion of Tyrode solution prior to dye perfusion. Once stabilized, the dye was perfused into the goldfish and zebrafish heart with the aid of a NE-1000 Programmable Single Syringe Pump (New Era Pump Systems, Inc., Farmingdale, NY) programmed to 10 μl/min and 30 μl/min for the goldfish and zebrafish hearts, respectively. The dye solution was oxygenated and perfused into the intact mice heart with the aid of two peristaltic pumps (Masterflex, Vernon Hills, IL).

2.4 Pulsed Local Field Fluorescence Microscopy used to excite and record emission from dyes

The Pulsed Local Field Fluorescence Microscopy (PLFFM) technique works in conjunction with fluorescent molecular probes (e.g., Rhod-2AM), to record and "visualize" critical cellular events at a whole organ level. Once these fluorescent probes are electromagnetically excited by a light source, their emitted light can be recorded with PLFFM. In order to excite Rhod-2AM, a green 532 nm solid-state neodymium-doped yttrium aluminum garnet (Nd-YAG) laser (Enlight Technologies, New Jersey, USA) was used.

The Nd-YAG laser excited exogenous fluorescent dyes (e.g., Rhod-2AM) loaded in the tissue. Once excited, these dyes emit light at a different wavelength. The emitted

light at the excited wavelength traveled back through a multimode fiber optic (200 μM diameter, 0.67 NA) placed on the surface of the intact heart and was filtered with a dichroitic mirror; allowing only longer wavelengths to pass. The emitted light was further spectrally filtered by an emission filter, eliminating any wavelengths below 610 nm and reducing any source of light contamination from the excitation light. This filtered emitted light was focused onto an avalanche photodiode (Perkin Elmer, Waltham, MA) with the aid of a microscope objective. The avalanche photodiode converted light photons into a measurable current, which was amplified via a resistive feedback element. The signal was then digitized by an A/D converter (National Instruments) and acquired by a PC.

2.5 Methods of analysis and statistics employed

Specific parameters of the AP and Ca^{2+} transient recordings were defined prior to statistical analysis of the data to determine if an observed morphological change in the AP or Ca^{2+} were statistically significant. These parameters are well-established and are the most commonly used in the field of cardiac electrophysiology. The AP and Ca^{2+} transient traces analyzed in this thesis were averaged from approximately 30 traces; as such, all AP traces shown in this thesis are averaged traces. As noise artifacts are near impossible to avoid, the averaging of the traces aided in the elimination of the noise artifacts present in the data.

It is important to note, there are two main causes of variance in whole heart experiments. The first, is no two hearts are electrically or physiologically completely identical to one another, regardless of the species. The second, is although Ca^{2+} transients and APs are recorded from the same general region of the heart (the midregion of the left ventricle epicardium), it is near impossible to record them from the same precise cellular location from one heart to another. Thus, the data are presented as multiple measurements (n; dot cloud) recorded for different measurements on different hearts (N) with the mean ± standard deviation (SD) or standard error (SE).

Methods of analysis

AP recordings were normalized from 0 to 1 preceding the establishment of the AP parameters. Next, the parameters for the AP trace were defined as the duration of time for the AP to reach 30%, 50%, or 90% repolarization; these parameters were referred to as APD30, APD50, and APD90, respectively (**Figure 2.4**). The repolarization times for the control and treatment group were evaluated and normalized to the control repolarization times for each heart used. After this normalization, the values were compiled from 5 experiments (N=5, or otherwise noted) and statistical significance was tested using a two-sample Kolmogorov–Smirnov test (OriginPro 2020). The difference between the control and treatment groups were considered significant if the p-value were < 0.01.

Preceding the establishment of the Ca^{2+} transient parameter, the intracellular Ca^{2+} transient recordings were normalized between 0 (minimum fluorescence) and 1 (maximum fluorescence). The parameters examining the kinetics of the Ca^{2+} transient (**Figure 2.4**) were defined as the rise time (RT; time for the Ca^{2+} transient to rise from 10% to 90% of its maximum amplitude), half duration (HD; duration of the Ca^{2+} transient at 50% of its maximum amplitude), and fall time (FT; time for the Ca^{2+} transient to fall from 90% to 10% of its maximum amplitude). Time constants τ_{on} and τ_{off} were calculated as $\tau_{on} = RT/2.2$ and $\tau_{off} = FT/2.2$ (Kornyeyev et al., 2012). All kinetic parameters mentioned for the control and treatment groups were evaluated and normalized to the control values for each heart used. After this normalization, the values were compiled from 5 experiments (N=5, or otherwise noted) and statistical significance was tested using a two-sample Kolmogorov–Smirnov test (OriginPro 2020). The difference between the control and treatment groups were considered significant if the p-value were < 0.01.
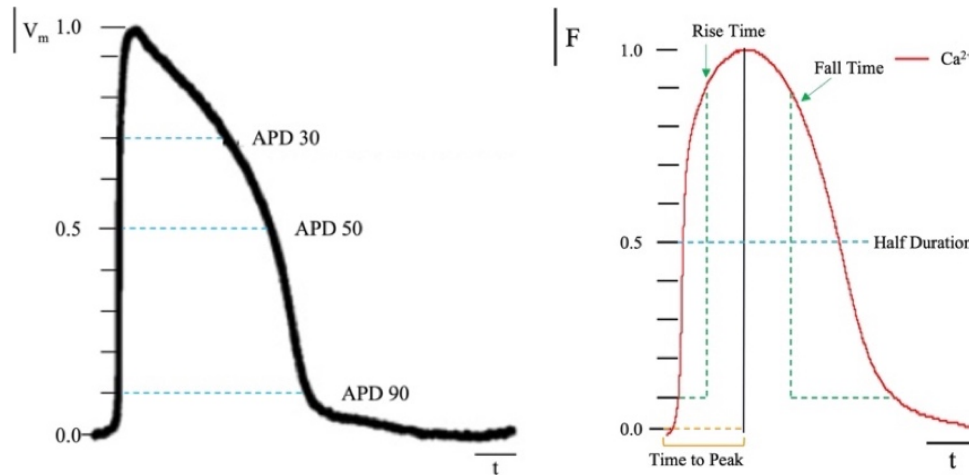
Figure 2.4: The parameters for the AP trace (left) were defined as the duration of time for the AP to reach 30%, 50%, or 90% repolarization; these parameters were referred to as APD30, APD50, and APD90, respectively. The parameters examining the kinetics of the Ca^{2+} transient (right) were defined as the rise time (RT; time for the Ca^{2+} transient to rise from 10% to 90% of its maximum amplitude), half duration (HD; duration of the Ca^{2+} transient at 50% of its maximum amplitude), and fall time (FT; time for the Ca^{2+} transient to fall from 90% to 10% of its maximum amplitude)

Statistics employed: the Kolmogorov–Smirnov test

As mentioned previously, there are two main causes of variance in whole heart experiments. The first, is no two hearts are electrically or physiologically completely identical to one another, regardless of the species. For example, experiments done on goldfish hearts of differing sizes altered the collected data, resulting in a bimodal/trimodal distribution (Figures 4.1b, 4.2b, 4.5b, 4.6, 5.4a). These experiments

were otherwise completely identical, aside from the sizes of the heart which were no more than 1-2mm larger/smaller. The second cause of variance is, although Ca2+ transients and APs are recorded from the same general region of the heart (the midregion of the ventricular epicardium), it is near impossible to record them from the same precise cellular location from one heart to another. For these reasons, the majority of the data presented in chapter chapters 4 and 5 this thesis did not have a normal Gaussian distribution.

To account for the issues presented, the statistical test employed for all the data presented in this thesis was the two-sample Kolmogorov-Smirnov test (KS test). Although not all the data presented in this thesis lacked a normal Gaussian distribution, the KS test was employed for all the data presented in order to maintain statistical consistency. The KS test is a nonparametric statistical procedure in which the continuous distribution of two unrelated (or independent) samples are compared; operating under the null hypothesis that the two samples are drawn from the same distribution. In other words, the KS tests if two arbitrary distributions are the same by comparing two cumulative distribution functions (CDF). The CDF is an integral of the probability density function, evaluated from infinity to a value, x.

However, it is imperative to mention a parametric test, such as a two-sample t-test would have been the ideal and more appropriate statistical analysis tool to use in order to test for significance, especially for data having a normal Gaussian distribution. This is crucial because where the KS tests for significance between the different distributions, a parametric test, such a t-test would test for significance between the means of the groups. Since the KS test did not test for a significant difference in the mean of the control and experimental groups, it is impossible to accurately extract information on whether the changes observed in the means of the experimental group(s) presented in this thesis were significant. Nevertheless, the KS is particularly attractive in that it requires a relatively large number of data points, and it is an exact test; the chi-square goodness of fit test is dependent on an adequate sample size for the approximations to be valid. Arguably, the KS test is the most useful general nonparametric test in that it is sensitive to differences in both the location and the shape of the empirical CDF of two samples.

Chapter 3: Excitation contraction coupling in the goldfish intact heart

3.1 General properties of goldfish excitability and Ca²⁺ transients

Fish hearts have become an interesting model used to study both cardiac physiology and pathophysiology. Specifically, zebrafish hearts have come to be a very popular model due to the possibility of developing transgenic animals. However, zebrafish present some experimental limitations when compared to goldfish. The first one is the size of the animal. Goldfish are three times longer and 2.7 times wider than the zebrafish (**Figures 3.1a, c**). Additionally, the volume of the goldfish is 20 times bigger than the zebrafish. This difference in size makes the dissection of the goldfish much easier. On the other hand, the size of the goldfish heart is also larger. For example, the goldfish ventricle is 3.7 times longer and three times wider than in the zebrafish (**Figures 3.1b, d**). Also, the total volume of the ventricle is 34 times bigger in the goldfish. Furthermore, the most important difference is the size of the bulbus arteriosus. The zebrafish heart needs to be cannulated using a 32 to 34-gauge needle, and the goldfish heart can be cannulated on a 27-gauge needle. The use of a larger needle for cannulation is a huge advantage because it allows for larger fluxes during perfusion and will allow for different drugs to be perfused significantly more quickly.
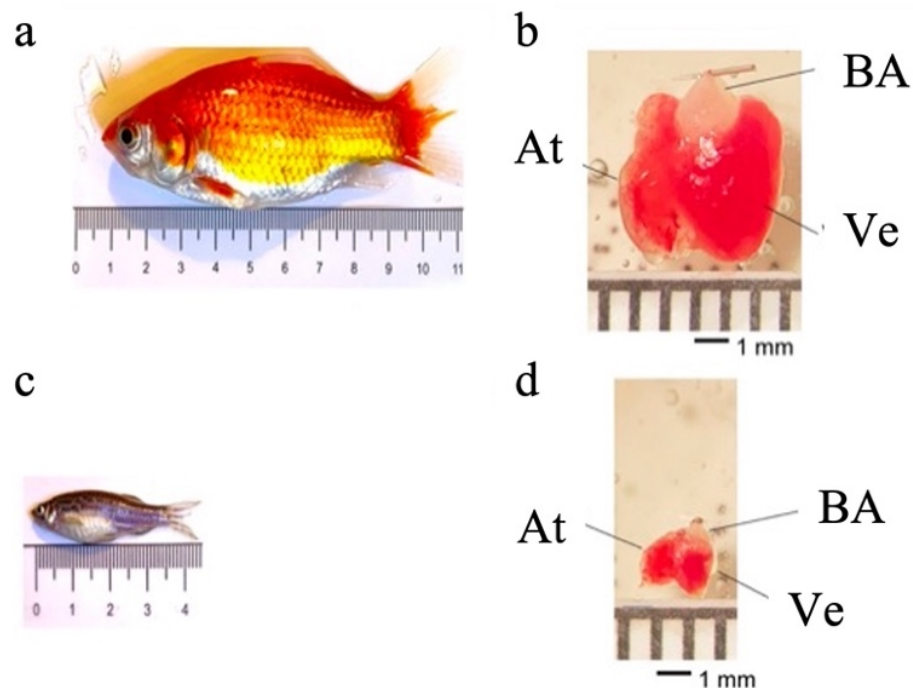
Figure 3.1: Adult goldfish measuring roughly 9.4 mm (a) and zebrafish measuring 3.7 mm (c) pictured for scale. Adult goldfish hearts (b) are significantly larger when compared to adult zebrafish hearts (d). Structural components including the ventricle (Ve), the atrium (At), and the bulbus arteriosus (BA) are labelled in the goldfish and zebrafish heart.

Another physiological advantage of the goldfish heart is that, at room temperature (23°C), the ventricular APs (**Figures 3.2a, b**) and Ca^{2+} transients exhibit significantly longer durations (**Figures 3.2a, c**) than those of zebrafish (**Figures 3.2d–f**). These findings make the goldfish heart a better model to be compared with other mammalian models.

Figure 3.2a shows the main characteristics of both APs and Ca^{2+} transients recorded from goldfish. The AP parameters were longer for goldfish (**Figure 3.2b**) having an APD30 of 278.4 ± 12.4 ms, APD50 of 370.4 ± 8.8 ms, and APD90 of 481.5 ± 9.5 ms (n = 25 measurements, N = 14 hearts) compared to the zebrafish (**Figure 3.2e**). Specifically, zebrafish APs were observed to have an APD30 of 51.2 ± 10.4 ms, APD50 of 83.9 ± 9.4ms, andAPD90 of136.5±9.0ms (n = 219 measurements, N = 20 hearts).

Several kinetic parameters were evaluated the Ca^{2+} transients in both goldfish (**Figure 3.2c**) and zebrafish (**Figure 3.2f**), such as the RT, FT, and HD. For goldfish, the kinetic parameters of the Ca^{2+} transients were RT = 72.4 ± 4.5 ms, FT = 266.9 ± 7.9 ms, and finally HD = 402.1 ± 4.4 ms (n = 40 measurements). Interestingly, the kinetic parameters for the Ca^{2+} transients were faster in zebrafish hearts (RT = 13.3 ± 2.9 ms, FT = 153.7 ± 18.0 ms, and HD = 99.1 ± 2.7 ms; n = 11 measurements).
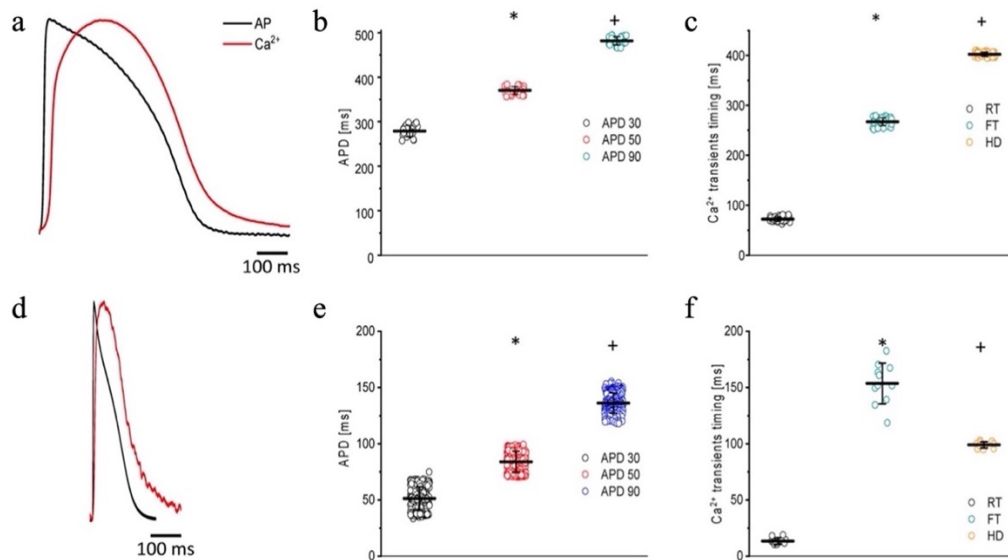
Figure 3.2: Main characteristics of both APs and Ca^{2+} transients recorded at 23°C in goldfish hearts (N=14 hearts) (a) and zebrafish hearts (N=20 hearts) (d). The kinetic parameters for goldfish intact hearts, including rise time (72.4 ± 4.5 ms), fall time (266.9 ± 7.9 ms), and half duration (402.1 ± 4.4 ms), were established (c) as well as the AP durations at 30% (278.4 ± 12.4 ms), 50% (370.4 ± 8.8 ms), and 90% (481.5 ± 9.0 ms) repolarization (b). The kinetic parameters for zebrafish intact hearts, including rise time (13.3 ± 2.9 ms), fall time (153.7 ± 18.0ms), and half duration (99.1 ± 2.7ms), were established (f), as well as the AP durations at 30% (51.2 ± 10.4 ms), 50% (83.9 ± 9.4 ms), and 90% (136.2.5 ± 9.0 ms) repolarization (e). The symbols *

and $^+$ differentiate between measurements that are statistically significant compared to the control values (p-value <0.01).

3.2 Role of the L-type Ca^{2+} currents in excitability and Ca^{2+} transients

In most vertebrates, the main pathway for Ca^{2+} influx is through the L-Type Ca^{2+} channel. In the experiments presented in **Figure 3.3**, we address the contribution of the L-type Ca^{2+} current to the ventricular AP kinetics and the amplitude of the Ca^{2+} transients. **Figure 3.3a** illustrates the effect of partially blocking the L-type Ca^{2+} current with 10 μM nifedipine on the goldfish epicardial AP. All the parameters that define the duration of the AP decreased after the heart was perfused with nifedipine. **Figure 3.3b** shows perfusion with nifedipine resulted in a significant reduction in the APDs. Particularly, APD30 was reduced from 278.4 ± 12.4 ms to 210.31 ± 12.8 ms, APD50 was reduced from 370.3 ± 8.8 ms to 283.6 ± 8.0 ms, and APD90 was reduced from 481.5 ± 9.5 ms to 389.5 ± 16.9 ms (n = 25 measurements, N = 4 hearts). These results indicate that the L-type Ca^{2+} channel is partially responsible for the duration of the AP phase 2 (plateau phase).

Nifedipine also had a significant effect on the amplitude and the kinetics of intracellular Ca^{2+} transients. Perfusion of the goldfish hearts with 10 μM nifedipine reduced the amplitude of the Ca^{2+} transient by 40% (**Figures 3.3c, d**). The amplitude of the Ca^{2+} transient was reduced from 0.84 ± 0.06 (n = 84 measurements) to 0.49 ± 0.04 (n = 106 measurements, N = 4 hearts). To compare the kinetics of the Ca^{2+} transients before and after nifedipine perfusion, the traces were normalized to their respected maximum amplitude (**Figure 3.3e**). The perfusion with nifedipine reduced the RT of the Ca^{2+} transients (**Figure 3f**) from 72.4 ± 4.5 ms (n = 40 measurements, N = 4 hearts) to 57.7 ± 5.1 ms (n = 22 measurements, N = 4 hearts). This reduction is a factor that can define the RT and the time-to- peak of Ca^{2+} transients. Consistent with the reduction in the duration of the AP, the HD of the Ca^{2+} transient was also significantly reduced (**Figure 3.3f**). Interestingly, **Figure 3.3f** shows that nifedipine perfusion reduced the RT and HD while not modifying the FT of Ca^{2+} transients. In order to assess the kinetic changes of the Ca^{2+} transient, we normalized the Ca^{2+} transients before and after perfusions with nifedipine. The normalized Ca^{2+} transient FT values before perfusion with nifedipine was 266.9 ± 7.9 ms for the control (n = 40 measurements, N = 4 hearts) and 269.0 ± 12.9 ms for hearts perfused with nifedipine (n = 22 measurements, N = 4 hearts).
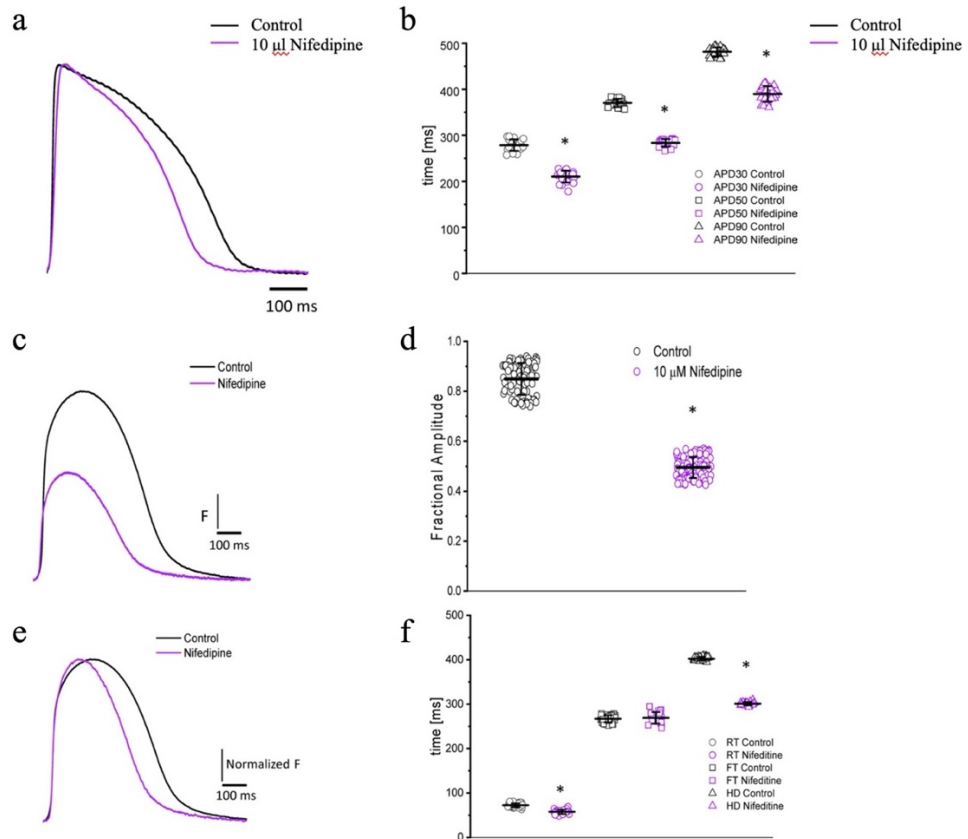
Figure 3.3: Perfusion with 10 µM nifedipine led to a significant decrease in goldfish AP duration (a) at 30% (278.4 ± 12.4 ms to 210.31 ± 12.84 ms), 50% (370.3 ± 8.8 ms to 283.6 ± 8.0 ms), and 90% (481.5 ± 9.5 ms to 389.5 ± 16.9 ms) repolarization (b). Time course of Ca^{2+} transients in the absence and presence of nifedipine (c). Perfusion with 10 µM nifedipine significantly reduced the amplitude of Ca^{2+} transient by 40% (d). The normalized goldfish Ca^{2+} transient recordings (e) show a significant change in the kinetics of this systolic event. Furthermore, both the rise time (f) and half duration (f) of the Ca^{2+} transients were significantly reduced (from 72.4 ± 4.5 ms to 57.7 ± 5.1 ms and from 402.1 ± 4.4 ms to 300.9 ± 3.7 ms, respectively). Although the fall time of the Ca^{2+} transients increased from 266.9 ± 7.9 ms to 269.0 ± 12.9 ms, this change was not significant (f). The symbol * differentiates between statistically significant measurements ($p < 0.01$, N = 4 hearts).

Nifedipine likely mediated the attenuation of the Ca^{2+} transient amplitude in one of two ways. Either nifedipine reduced the amplitude of the Ca^{2+} current entering through the L-type Ca^{2+} channels, or nifedipine reduced the duration of the AP and, as such, shortened the duration of the L-type Ca^{2+} current. To discriminate between these two hypotheses, we performed experiments in which we first perfused the heart with nifedipine and then used flash photolysis to locally inactivate it. We previously demonstrated (Ramos-Franco et al., 2016) that local photolysis of nifedipine can produce

a significant change in Ca^{2+} signaling without affecting the time course of the APs. This occurs because the intact heart presents important electrotonic behavior. When there is a change in the local Ca^{2+} current, the rest of the tissue will "voltage-clamp" the photolyzed volume and, thus, impede the change in the membrane potential. **Figure 3.4** illustrates the results of the nifedipine photolysis. **Figure 3.4a** shows the time course of the Ca^{2+} transients from a heart perfused with 10 μM nifedipine and externally paced at 1 Hz before and after the photolytic stimulus. Upon photolysis of nifedipine (after the violet arrow), there was an increase in the amplitude of goldfish epicardial Ca^{2+} transients. **Figure 3.4b** and **3.4c** shows simultaneous recordings of Ca^{2+} transients and AP upon a photolytic stimulus. Although there was a significant increase in the amplitude of the Ca^{2+} transients, there was not a measurable effect on the kinetics of the AP. **Figures 3.4e** and **3.4f** show the time course of the AP does not change before and after the photolytic stimulus (n = 20 measurements, N = 4 hearts). **Figure 3.4d** illustrates the fractional increase in the amplitude of the Ca^{2+} transients after the photolytic stimulus. The fractional amplitude of the Ca^{2+} transient increased from 0.97 ± 0.01 before the flash to 1.11 ± 0.02 after the flash (n = 22 measurements, N = 4 hearts).
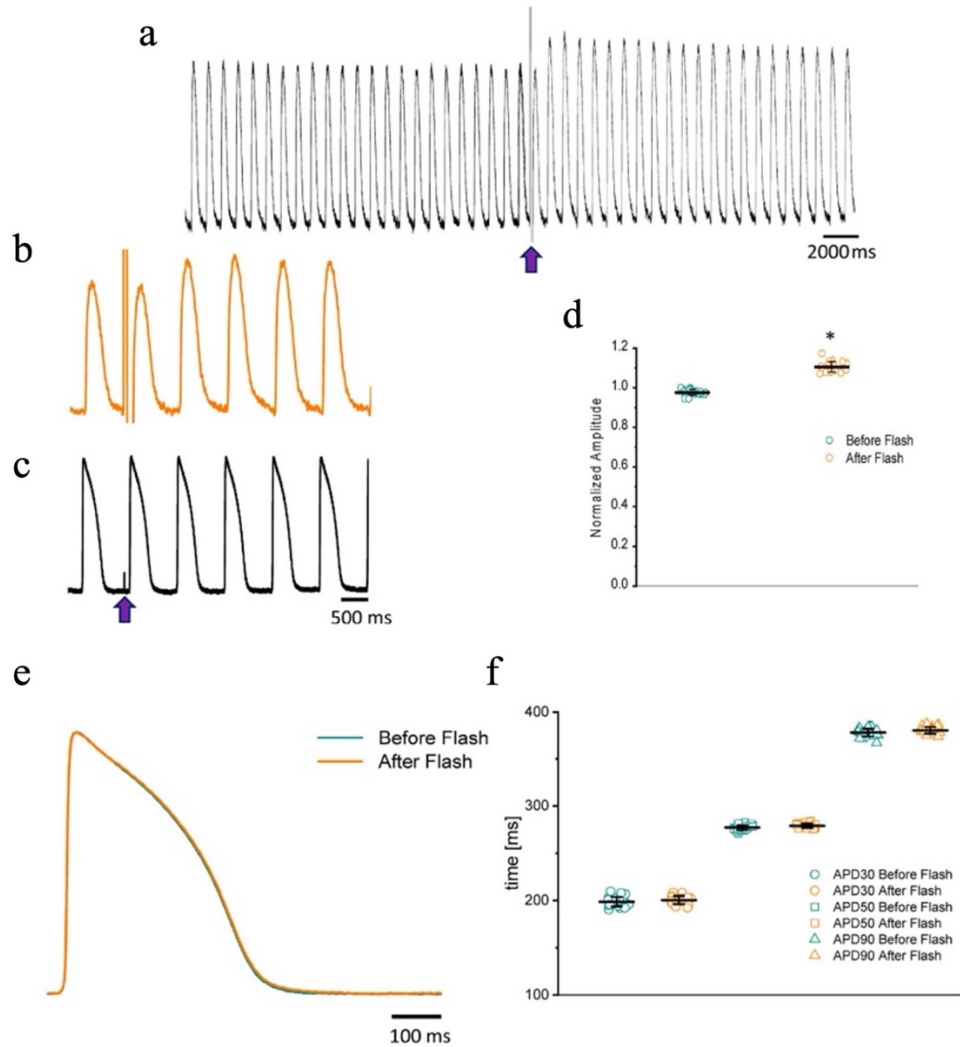
Figure 3.4: The time course of the Ca²⁺ transient recorded from goldfish hearts externally paced at 1 Hz before and after the photolytic stimulus. Simultaneous recordings of Ca²⁺ transients and AP upon introduction of a photolytic stimulus (a, b) reveal a significant increase in the amplitude of the Ca²⁺ transients without a measurable effect on the kinetics of the AP (c). The fractional amplitude of the Ca²⁺ transient increased from 0.97 ± 0.01 before the flash to 1.11 ± 0.02 after the flash (d). There was no significant change in the AP duration at 30, 50, and 90% repolarization before and after the photolytic stimulus due to the electrotonus imposed by the ventricular tissue (e, f). The symbol * differentiates between statistically significant measurements ($p < 0.01$, N = 4 hearts).

3.3 Contribution of SR Ca release to Ca^{2+} transients and the repolarization of the AP

For numerous vertebrates, including mammals and birds, the contribution of the SR Ca^{2+} release to the total change in free cytoplasmic Ca^{2+} concentration during systole plays an essential role in determining the behavior of its Ca^{2+} transients. In order to investigate this process in the goldfish heart, we performed experiments in which we abolished the Ca^{2+} release from the SR. By perfusing the heart with 10 μM Ry and 2 μM Tg, we were able to lock the ryanodine receptor (RyRs) in a subconductance state and block the SERCA pump, respectively (**Figure 3.5a**). These effects led to a depletion in the intra-SR Ca^{2+} concentration, reducing the amplitude of the Ca^{2+} transients. A summary of the results presented in **Figure 3.5b** evinces that perfusion with Ry and Tg significantly decreased the amplitude of Ca^{2+} transients (30°C) and decreased the fractional SR Ca^{2+} release from 1.0 ± 0.05 for the control condition (n = 204 measurements, N = 5 hearts) to 0.45 ± 0.01 (n = 60 measurements, N = 5 hearts), a decrease of approximately 55%. Because the Ca^{2+} transient recorded in the presence of Ry and Tg mostly represents the influx of Ca^{2+} across the plasma membrane, it is possible to calculate the gain of the Ca^{2+} induced Ca^{2+} release as:

$$\text{Gain }_{CICR} = \frac{\text{Amplitude }_{control}\text{ of }Ca^{2+}}{\text{Amplitude }_{Ry-Tg}\text{ of }Ca^{2+}}$$

The Gain_{CICR} in the goldfish heart was calculated to be 2.25 ± 0.06. Not surprisingly, mice are also a common model used to study cardiac excitability and Ca^{2+} transients' behavior, and this inspired us to compare the goldfish model to the mouse model. Similar experiments were performed in mice in order to see how the mouse model compared to the goldfish model in terms of SR Ca^{2+} release contribution. The amplitude Ca^{2+} transient dramatically decreased upon perfusion with Ry and Tg (**Figure 3.5c**), and this trend was consistent across multiple Ca^{2+} transient measurements (**Figure 3.5d**). The fractional release also decreased from 0.96 ± 0.02 for the control condition (n = 239 measurements, N = 5 hearts) to 0.06 ± 0.007 for hearts perfused with Ry and Tg (n = 626 measurements, N = 5 hearts), a decrease of 90% (**Figure 3.5d**). Finally, the Gain_{CICR} was calculated to be 16.27 ± 0.027 for the mouse heart.

Ca^{2+} released from the SR not only alters the Ca^{2+} transient, but it can also have a drastic impact on the repolarization of the AP. Experiments presented in **Figures 3.5e** and **3.5f** were designed to discern how Ca^{2+} release from the SR impacted AP repolarization. **Figure 3.5e** indicates that impairment of Ca^{2+} release from the SR, induced by Ry and Tg, prolonged the duration of the goldfish ventricular AP at 30°C. APD30 displayed an increase (**Figure 3.5f**) from 72.9 ± 2.0 ms for the control condition (n = 180 measurements, N = 5 hearts) to 102.1 ± 4.5 ms in the presence of Ry and Tg (n = 33 measurements, N = 5 hearts). Following a similar trend, perfusion with Ry and Tg prolonged APD50 (**Figure 3.5f**) from 163.2 ± 5.1 ms (n = 180 measurements, N=5hearts) to 177.9 ± 6.5ms (n=33 measurements,N=5 hearts) and APD90 (**Figure 3.5f**) from 375.5 ± 12.9 ms (n = 180 measurements) to 406.9 ± 19.5 ms (n = 33 measurements).

The prolongation of the AP duration by Ry and Tg was also observed in goldfish ventricular APs recorded at 23°C. **Figure 3.5g** shows that, although the APs are longer at this lower temperature, Ry and Tg still prolonged the AP duration at all the levels. APD30 changed (**Figure 3.5h**) from 321.5 ± 7.9 ms (n = 40 measurements) to 347.1 ± 4.9 ms (n = 40 measurements, N = 5 hearts), APD50 (**Figure 3.5h**) increased from 385.53 ± 5.0 ms (n = 40 measurements) to 409.8 ± 7.9 ms (n = 40 measurements), and APD90 (**Figure 3.5h**) increased from 424.3 ± 4.8 ms (n = 40 measurements, N = 5 hearts) to 448.8 ± 8.9 ms (n = 40 measurements, N = 5 hearts). These results suggest that Ca^{2+} dependent inactivation of the L-type Ca^{2+} channel is the most likely mechanism prolonging the AP duration in the absence of Ca^{2+} release from the SR.
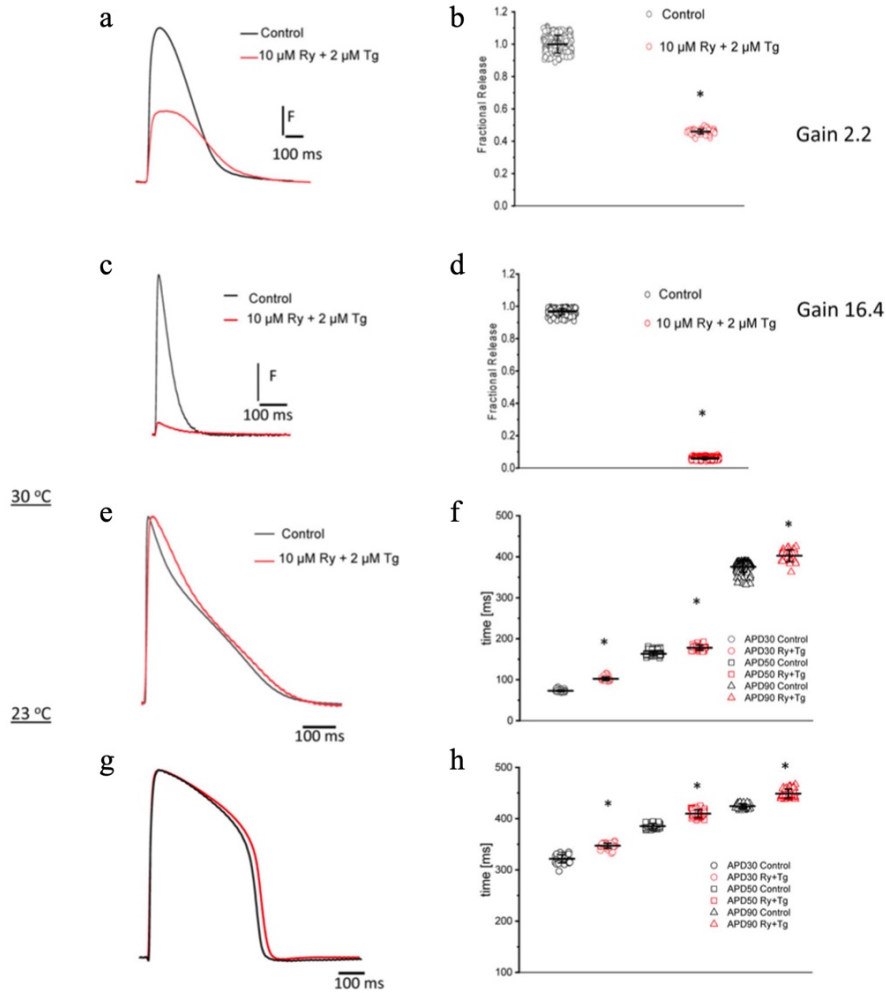
Figure 3.5: Typical Ca^{2+} transient recordings before and after perfusion of the goldfish heart with 10 μM Ry and 2 μM Tg (a). A summary of the results illustrates a statistically significant decrease in the amplitude of the Ca^{2+} transient as well as a 55% decrease in the fractional release (b; from 1.0 ± 0.05 for the control condition to 0.45 ± 0.01 for hearts perfused with Ry and Tg). Ca^{2+} transient recordings before and after perfusion of the mouse heart with 10 μM Ry and 2 μM Tg (c). Treatment with Ry and Tg in mouse hearts dramatically reduced the amplitude of Ca^{2+} transients (d). The fractional release was also reduced by approximately 90% (from 0.96 ± 0.02 for control to 0.06 ± 0.007 for hearts perfused with Ry and Tg). The calculated Gain $_{CICR}$ was 16.27 ± 0.027 for the mouse heart. Perfusion with 10 μM Ry and 2 μM Tg at 30°C impaired Ca^{2+} release from the SR (e) and prolonged the duration of the goldfish ventricular AP at 30% (f) (from 72.9 ± 2.0 ms for the control condition to 102.1 ± 4.5 ms in the presence of Ry and Tg), 50% (from 163.2 ± 5.1 ms to 177.9 ± 6.5 ms), and 90% repolarization (from 375.5 ± 12.9 ms to 406.9 ± 19.5 ms). Perfusion with 10 μM Ry and 2 μM Tg at 23°C also impaired Ca^{2+} release from the SR (g) and prolonged the duration of the action potential at 30% (h) (from 321.5 ± 7.9 ms to 347.1 ± 4.9 ms), 50% (increased from 385.53 ± 5.0 ms to 409.8 ± 7.9 ms), and 90% repolarization (from 424.3 ± 4.8 ms to 448.8 ± 8.9 ms). The symbol *

differentiates measurements that are statistically significant between the two consecutive heart rates (p < 0.01, N = 5 hearts).

3.4 Discussion

Comparison Between Goldfish Hearts and Other Vertebrates

Goldfish (Carassius auratus) are members of the same phylum (Chordata), class (Actinopterygii), order (Cypriniformes), and family (Cyprinidae) as the zebrafish (Danio rerio). Both species can also regenerate their heart following injury (Poss et al., 2002; Grivas et al., 2014; Kang et al., 2016; Mokalled et al., 2016). Though the similarities between the goldfish and the zebrafish can form an extensive list, there are a few exigent differences between the two models. The most obvious difference being that the adult goldfish (**Figures 3.1a, c**) and its heart (**Figures 3.1b**, **d**) are both significantly larger when compared to the zebrafish. It is important to note that goldfish and zebrafish ventricular myocytes do not present t-tubules, contrary to mammalian ventricular myocytes. Though this structural difference may seem significant, we do not expect the absence of t-tubules to dramatically affect the time course of Ca^{2+} transients. Indeed, numerous animal models lack a t-tubule network. For example, mammalian atrial cells have a highly reduced t-tubules network (McNutt and Fawcett, 1969; Michailova et al., 2002; Richards et al., 2011), which is compensated for by the presence of surface dyads and a Ca^{2+}-induced Ca^{2+} release and Ca^{2+} propagation within the myocytes (Hüser et al., 1996). Furthermore, ventricular myocytes in birds also lack a t-tubule network (Sheard et al., 2019), and yet they present fast Ca^{2+} transients. The important parameter critical in defining the time course of the Ca^{2+} transients is not the presence (or absence) of a t-tubule network, but the time course of the Ca^{2+} influx across the plasma membrane and the kinetics of activation of ryanodine receptors.

A noteworthy difference between the zebrafish and goldfish models is that the heart rate for goldfish (109 beats/min) (Ferreira et al., 2014) is much closer to larger mammals (i.e., canines and humans) when compared to the zebrafish heart rate (162–169 beats/min) (Lee et al., 2016). Furthermore, **Figure 3.2a** describes both the characteristics of APs and Ca^{2+} transients recorded in goldfish ventricles. The goldfish AP is significantly longer than that of zebrafish (**Figure 3.2b, e**). Interestingly, the APD90 recorded in goldfish ventricular myocytes (**Figure 3.2b**) is very similar to values recorded in the endocardial ventricular layer of dog hearts (Piktel et al., 2011) at a similar temperature (25°C). Additionally, the epicardial APs in goldfish present a waveform very similar to the one recorded at the dog endocardial layer, in that the goldfish epicardial APs do not present a "spike and dome" behavior when compared to epicardial AP recorded from dogs (Litovsky and Antzelevitch, 1990; Antzelevitch et al., 1991; Lukas and Antzelevitch, 1993; Yan and Antzelevitch, 1996). Finally, the goldfish APD90 is very similar to the human QT segment at the same temperature (Bjørnstad et al., 1994).

The kinetic parameters (i.e., RT, FT, and HD) for goldfish Ca^{2+} transients (**Figures 3.2a, c**) are much slower, not only when compared to the zebrafish (**Figures 3.2d, f**), but also when compared to rodents, such as rats (Zoghbi et al., 2000, 2004) and mice (Escobar et al., 2006, 2012; Ferreiro et al., 2012). Interestingly, the goldfish Ca^{2+} transients present similar kinetic characteristics within canine hearts both in isolated myocytes (A. E. Belevych et al., 2011) and at the intact heart level (Laurita et al., 2003).

41

Role of the L-type Ca²⁺ Channels in Excitability and Ca²⁺ Transients of the Goldfish Heart

In most vertebrate species, the influx of Ca^{2+} through the L-type Ca^{2+} channel is critical in defining the time course of APs and is the main mechanism triggering ventricular Ca^{2+} release. Results presented in **Figure 3.3** and **Figure 3.4** depict the role of L-type Ca^{2+} currents in goldfish excitability and its ability to activate the excitation–contraction coupling process.

Previous studies conducted on fish hearts show how nifedipine perfusion can block L-type Ca^{2+} currents (Maylie and Morad, 1995) and reduce the duration of the AP (Nemtsas et al., 2010); this is nearly identical to what has been previously observed in mammals (Sugiura and Joyner, 1992; Baláti et al., 1998; Ferreiro et al., 2012; Ramos-Franco et al., 2016). Not surprisingly, the same pattern was also observed in goldfish hearts (**Figures 3.3a, d**), suggesting there is an influx of Ca^{2+} through L-type Ca^{2+} channels that occurs during the plateau phase of the ventricular AP. One consequence of a decreased Ca^{2+} influx during the plateau phase of the AP is a reduction in the amplitude of the Ca^{2+} transients. Upon perfusion of the goldfish heart with nifedipine, we observed an attenuation of the Ca^{2+} transient during systole as well as a change in the kinetic behavior of the Ca^{2+} transients (**Figures 3.3c-f**). It has been previously reported that nifedipine reduces the amplitude of Ca^{2+} transients in some fish models (Xie et al., 2008; Bovo et al., 2013; van Opbergen et al., 2018a); however, there is no evidence of Ca^{2+} transient shortening. This is interesting because several mammalian models exhibit a shortening in the HD of the Ca^{2+} transients in response to nifedipine (Escobar et al., 2004; Ramos-Franco et al., 2016).

The amplitude of the Ca^{2+} transient can decrease as a result of a smaller L-type Ca^{2+} current amplitude. Additionally, a reduction in the amplitude of the Ca^{2+} transient can be induced by shortening the AP. This induces a shortening of the L-type Ca^{2+} current and brings fewer Ca^{2+} ions into the ventricular myocyte. In goldfish, we observed a nifedipine-driven change in the amplitude of the Ca^{2+} transient that was independent of the AP duration (**Figure 3.4**). In **Figure 3.4**, we demonstrate photolytic inhibition of a fraction of nifedipine blocking the L-type Ca^{2+} channels produced an increase in the amplitude of the Ca^{2+} transient (**Figures 3.4a–d**) without a change in the kinetic properties of the AP (**Figures 3.4e, f**). This is analogous to what our group previously observed in experiments conducted in mouse hearts (Ramos-Franco et al., 2016).

Role of Intracellular Ca²⁺ Release on Excitability and Ca²⁺ Transients

Depending on the vertebrate species, the Ca^{2+} released from the SR can play either a major or minor role in contributing to the systolic Ca^{2+} during the cardiac cycle. The role of the Ca^{2+} release from the SR ranges dramatically and can be made evident when comparing frogs, in which Ca^{2+} release from the SR is not present (Anderson et al., 1989), to mice, in which most of the Ca^{2+} increase during diastole depends on Ca^{2+} released from this intracellular store (Ferreiro et al., 2012; Kornyeyev et al., 2012; Ramos-Franco et al., 2016). **Figures 3.5a, b** show that, in goldfish hearts, there is a

significant contribution from the SR to the myoplasmic systolic Ca^{2+}; however, this contribution is less than the one observed in smaller mammals such as mice (**Figures 3.5c, d**). This was especially impressive because previous experiments performed in fish-isolated myocytes only showed a very small contribution of the SR (Shiels and White, 2005; Bovo et al., 2013) to the free systolic Ca^{2+}. Furthermore, the lower contribution of the SR Ca^{2+} release of goldfish hearts in comparison with the mouse is encouraging because larger mammalian models, such as dogs, also present a lower SR Ca^{2+} contribution ($\sim$40%) (Belevych et al., 2007).

Interestingly, the inhibition of Ca^{2+} release from the SR promoted by the perfusion of the goldfish hearts with Ry and Tg also modified the repolarization of ventricular AP. **Figures 3.5e, f** illustrate that, in the presence of Ry and Tg, the APs are longer at both $30°C$ and $23°C$ (**Figures 3.5g, h**). Increased Ca^{2+}-dependent inactivation of L-type Ca^{2+} channels shortens the action potentials when Ca^{2+} release is larger but reduced Ca^{2+}-dependent inactivation prolongs the action potential if the Ca^{2+} release from the sarcoplasmic reticulum is impaired. Interestingly, this effect is contrary to what we observe in mice hearts. Upon coronary perfusion of mice hearts with Ry and Tg, the minuscule amount of Ca^{2+} released from the SR is unable to activate the NCX in the forward mode and, thus, shortens the AP duration. On the other hand, the NCX can also prolong the AP for a larger Ca^{2+} release while in the forward mode by activating an inward Na^+ current (Ferreiro et al., 2012; Ramos-Franco et al., 2016). This is because the NCX in the forward mode removes one Ca^{2+} ion from the cytosol to produce an influx of three Na^+ ions from the extracellular space to the cytosol. Thus, a larger increase in the intracellular Ca^{2+} concentration results in a larger Ca^{2+} extrusion from the cytosol. This large extrusion, consequently, increases Na^+ influx from the extracellular space into the cytosol. The net influx of a positive charge from the Na^+ ions induces a depolarization of the membrane potential, prolonging the duration of the AP. Interestingly, the same AP prolongation behavior observed in goldfish hearts in response to Ry and Tg has been previously observed in dog hearts, in which BAPTA-mediated attenuation of Ca^{2+} release prolonged the AP (Horváth et al., 2016). Although the prolongation of the AP is due to the effect of SR Ca^{2+} release on Ca^{2+}-dependent inactivation, changes in the time course of the action potential also change the delay-rectifying and inward-rectifying K^+ current. Furthermore, prolongation of the AP also leads to an inactivation of the Na^+ current, preventing alteration of Na^+ currents in a major way.

Chapter 4: Intrinsic sympathetic NS activity and effect of AP and intracellular Ca^{2+} dynamics

4.1 How does the sympathetic drive regulate heart rate of the Langendorff fish heart?

      In order to elicit a sympathetic response and assess the β-adrenergic regulation of the goldfish heart, we first perfused the heart with 100 nM isoproterenol. Goldfish ventricular chronotropic properties were examined via AP recordings and spontaneous heart rate recordings (**Figure 4.1**). Perfusion of the goldfish intact heart with 100 nM isoproterenol altered the AP morphology (**Figure 4.1a**) and had a positive chronotropic effect, significantly increasing the heart rate by 46% (**Figures 4.1b, c**; from 0.87 ± 0.01 Hz to 1.27 ± 0.02 Hz).
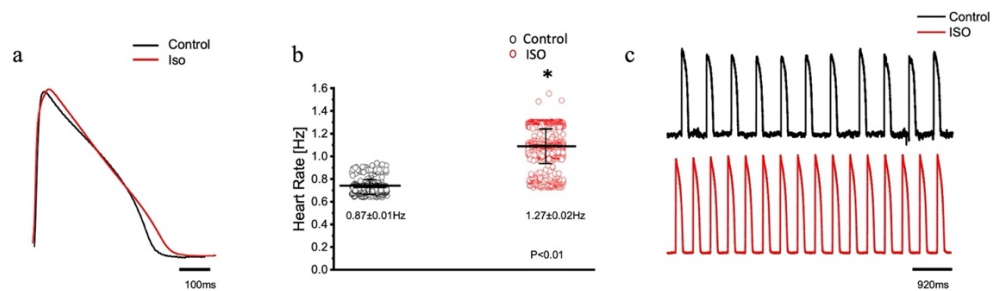
Figure 4.1: Goldfish ventricular action potential and spontaneous heart rate recordings before (black) and after perfusion with 100 nM isoproterenol (red). Perfusion of the goldfish intact heart with 100 nM isoproterenol altered the action potential morphology (a) and had a positive chronotropic effect, significantly increasing the heart rate (b; from 0.87 ± 0.01 Hz to 1.27 ± 0.02 Hz, p<0.01, n=160 for the control, n=263 for ISO, N=4). The positive chronotropic effect following isoproterenol perfusion is also reflected in spontaneous AP recordings from the left ventricle (c). An asterisk denotes a significant difference between the two distributions. The data are presented as multiple measurements (n; dot cloud) recorded for different measurements (n) on different hearts (N) with the mean ± SEM (solid lines).

4.2 How does a sympathetic NS agonist alter AP morphology and Ca^{2+} dynamics in the Goldfish ventricle?

      Interestingly, all kinetic parameters of the AP significantly changed following isoproterenol perfusion; APD30 increased from 228.10 ± 14.40 ms to 237.90 ± 11.80 ms (**Figure 4.2a**), APD50 decreased from 353.90 ± 30.40 ms to 300.30 ± 20.00 ms (**Figure 4.2b**), and APD90 increased from 455.40 ± 20.10 ms to 468.70 ± 27.00 ms (**Figure 4.2c**).
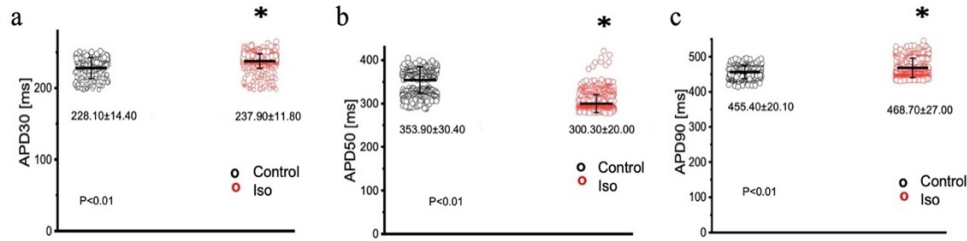
Figure 4.2: Kinetic parameters of the Goldfish ventricular action potential before (black) and after (red) perfusion with 100 nM isoproterenol. Following isoproterenol perfusion, APD30s significantly increased from 228.10 ± 14.40 ms to 237.90 ± 11.80 ms (p<0.01, n=113 for the control, n=113 for ISO, N=4) (a), APD50 decreased from 353.90 ± 30.40 ms to 300.30 ± 20.00 ms (p<0.01, n=143 for the control, n=316 for ISO, N=4) (b), and APD90 significantly increased from 455.40 ± 20.10 ms to 468.70 ± 27.00 ms (p<0.01, n=95 for the control, n=256 for ISO, N=4) (c). An asterisk denotes a significant difference between the two distributions. The data are presented as multiple measurements (n; dot cloud) recorded for different measurements (n) on different hearts (N) with the mean ± SEM (solid lines).

In many vertebrate species, stimulation of either autonomic nervous system branch will not only alter cardiac excitability, but also cardiac contractility. In order to assess if eliciting a sympathetic response altered the inotropic and/or the lusitropic properties of the goldfish ventricle, experiments were performed in which the amplitude and kinetics of the Ca^{2+} transient were examined in the presence and absence of 100 nM isoproterenol (**Figure 4.3**). Stimulation of β-adrenergic receptors altered the morphology of the Ca^{2+} transient (**Figure 4.3a**) and significantly increased the normalized amplitude of the Ca^{2+} transient (**Figure 4.3b**; from 1.00 ± 0.07 to 1.10 ± 0.04).
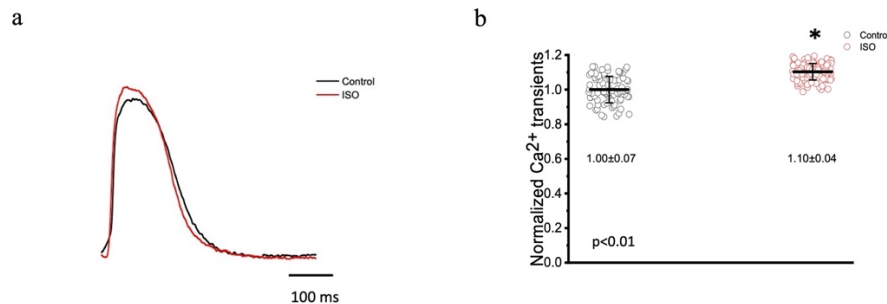
Figure 4.3: Goldfish ventricular Ca^{2+} transient recording and normalized amplitude in the absence (black) and presence (red) of 100 nM isoproterenol. Stimulation of ß-adrenergic receptors altered the morphology of the Ca^{2+} transient (a) and significantly increased the normalized amplitude of the Ca^{2+} transient from 1.00 ± 0.07 to 1.10 ± 0.04 (p<0.01, n=65 for the control, n=67 for ISO, N=8) (b). An asterisk denotes a significant difference between the two distributions. The data are presented as multiple measurements (n; dot cloud) recorded for different measurements (n) on different hearts (N) with the mean ± SEM (solid lines).

4.3 How do sympathetic NS agonists alter Ca^{2+} transient kinetics?

To detect if isoproterenol significantly altered the kinetics of the Ca^{2+} transient, the three following parameters of the Ca^{2+} transient were assessed (**Figure 4.4**): rise time (RT), fall time (FT), and half duration (HD). A significant change in any aforementioned kinetic parameter is a reflection of a significant corresponding change in myocardial Ca^{2+} handling dynamics. Perfusion with isoproterenol significantly increased the velocity of every Ca^{2+} transient kinetic parameter in the goldfish heart (Figures **Figures 4.4a, b, c**; RT: from 27.98 ± 4.60 ms to 22.47 ± 3.50 ms, FT: from 150.08 ± 22.80 ms to 135.88 ± 20.30 ms, and HD: from 148.60 ± 8.10 ms to 134.87 ± 5.20 ms, respectively), implying perfusion with isoproterenol increased the rate of relaxation of the goldfish myocardium during diastole, resulting in a positive lusitropic effect (**Figure 4.4b**). The presence of a β-adrenergic drive suggests the presence of a parasympathetic one, as they are the two antagonistic branches of the autonomic nervous system.
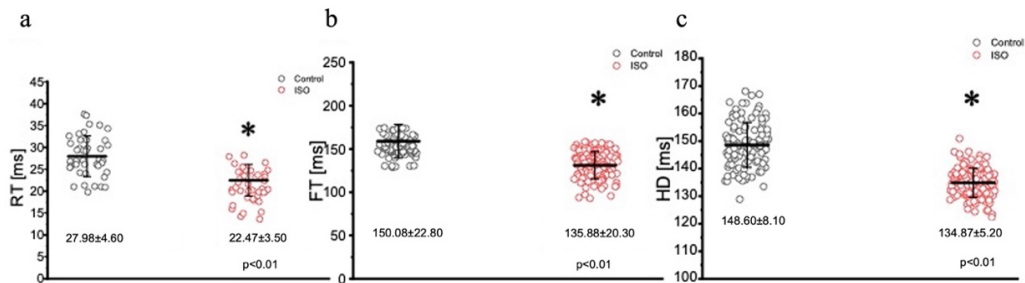
Figure 4.4: Kinetic parameters of the goldfish ventricular Ca^{2+} transients before (black) and after (red) perfusion with 100 nM isoproterenol. Perfusion of the goldfish heart with 100 nM isoproterenol significantly decreased the rise time (RT) of the Ca^{2+} transient from 27.98 ± 4.60 ms to 22.47 ± 3.50 ms (p<0.01, n=65 for the control, n=96 for ISO, N=8) (a), decreased the fall time (FT) of the Ca^{2+} transient from 150.08 ± 22.80 ms to 135.88 ± 20.30 ms (p<0.01, n=76 for the control, n=76 for ISO, N=8) (b), and significantly decreased the half duration (HD) of the Ca^{2+} transient from 148.60 ± 8.10 ms to 134.87 ± 5.20 ms (p<0.01, n=64 for the control, n=72 for ISO, N=8) (c). An asterisk denotes a significant difference between the two distributions. The data are presented as multiple measurements (n; dot cloud) recorded for different measurements (n) on different hearts (N) with the mean ± SEM (solid lines).

4.4 How does a sympathetic NS agonist alter the ECG morphology and kinetics?

The effects of catecholamines on whole heart electrical activity were assessed through transmural electrocardiogram recordings (**Fig. 4.5**). The 3 main components of the goldfish electrocardiogram are presented in **Fig. 4.5a** and consist of the QRS complex (ventricular depolarization), J wave (likely due to a voltage gradient due to the presence

of a prominent AP notch in the epicardium but not the endocardium), and T wave (ventricular repolarization). Application of isoproterenol altered the morphology of the goldfish electrocardiogram (**Figure 4.5a**) and increased the heart rate (**Figures 4.5b, c**; from 1.10 ± 0.40 Hz to 3.10 ± 0.70 Hz).
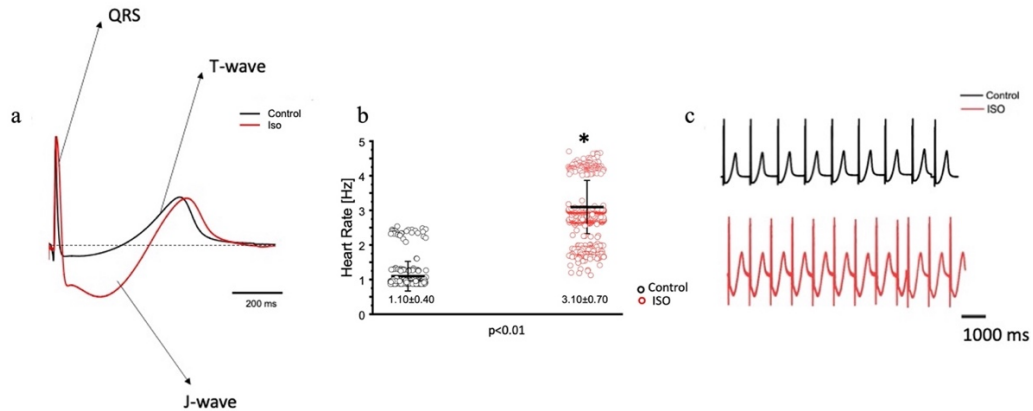
Figure 4.5: Goldfish ventricular electrocardiogram recordings before (black) and after (red) perfusion with 100 nM isoproterenol. The 3 main components of the goldfish electrocardiogram are presented: QRS complex, J wave, and T wave. Application of isoproterenol altered the morphology of the goldfish electrocardiogram (a) and increased the spontaneous heart rate from 1.10 ± 0.40 Hz to 3.10 ± 0.70 Hz ($p<0.01$, n=180 for the control, n=412 for ISO, N=6) (b). Electrocardiogram recordings before and after isoproterenol perfusion reflect an increased heart rate in response to isoproterenol (c). An asterisk denotes a significant difference between the two distributions. The data are presented as multiple measurements (n; dot cloud) recorded for different measurements (n) on different hearts (N) with the mean $\pm$ SEM (solid lines).

Furthermore, application of isoproterenol also significantly altered the duration of the QRS wave, T wave, and J wave (**Fig. 4.6**). The QRS complex significantly decreased from 22.70 ± 1.30 ms to 17.30 ± 2.80 ms (**Fig. 4.6a**), the T wave significantly increased from 164.70 ± 53.20 ms to 292.10 ± 58.10 ms (**Fig. 4.6b**), and the J wave significantly increased from 126.10 ± 42.30 ms to 333.10 ± 105.30 ms (**Fig. 4.6c**).
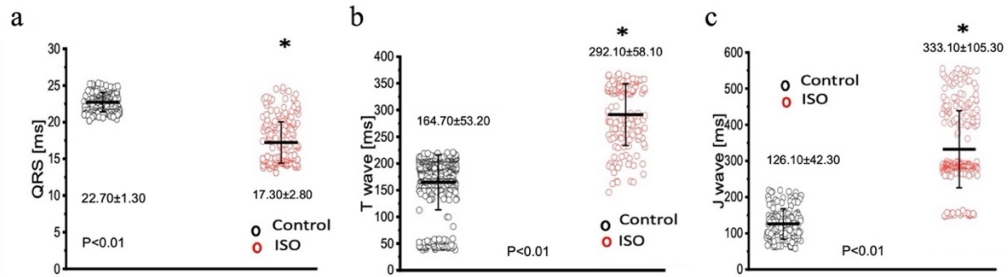
Figure 4.6: Perfusion with 100 nM isoproterenol significantly altered the time course of all three components in the goldfish electrocardiogram. The duration of the QRS complex significantly decreased from 22.70 ± 1.30 ms to 17.30 ± 2.80 ms (p<0.01, n=80 for the control, n=121 for ISO, N=6) (a), the T wave significantly increased from 164.70 ± 53.20 ms to 292.10 ± 58.10 ms (p<0.01, n=110 for the control, n=120 for ISO, N=6) (b), and the J wave significantly increased from 126.10 ± 42.30 ms to 333.10 ± 105.30 ms (p<0.01, n=74 for the control, n=118 for ISO, N=6) (c). An asterisk denotes a significant difference between the two distributions. The data are presented as multiple measurements (n; dot cloud) recorded for different measurements (n) on different hearts (N) with the mean ± SEM (solid lines).

4.5 Discussion

In most vertebrate hearts, both excitability and contractility are tightly regulated by the autonomic nervous system. Though there is a significant amount of research regarding the sympathetic and parasympathetic regulation of many vertebrate species, there is little known about how autonomic regulation impacts the electrical and mechanical function of fish hearts specifically. To our knowledge, it is not clear how autonomically driven AP kinetics impact contractility in the intact fish heart, which has become an increasingly popular model used to understand human cardiac physiology and pathophysiology. In this study, we investigated how stimulation of either autonomic branch regulated the time course of APs and electrocardiograms, and how these electrical changes correlated with changes in left ventricular Ca^{2+} transient measurements at the whole heart level. Our results indicate the presence of a fully developed dual control from both the adrenergic and cholinergic nerves in the goldfish heart, highly resembling the pattern found in other vertebrate models.

β-adrenergic stimulation increased cardiac excitability and contractility

It is well established that stimulation of β-adrenergic receptors will have a positive chronotropic, dromotropic, inotropic, and lusitropic effect in any vertebrate species exhibiting full autonomic regulation. In the fish model, the autonomous rhythm of the heart is determined by the pacemaker region located near the atrial chamber, identified over 100 years ago (Keith and Mackenzie, 1910). Pacemaker APs are categorized by a gradual and slow diastolic depolarization (Phase 4), toward the threshold voltage of the AP upstroke (Phase 0) (Harper et al. 1995; Haverinen and Vornanen, 2007; Saito, 1973; Tessadori et al. 2012). There are three main mechanisms by which an organism can modulate its heart rate, all of which end with an altered slope of the diastolic depolarization during diastole. This slope, set by the sinoatrial node, can be modified positively (by the sympathetic nervous system) or negatively (by the parasympathetic nervous system) by shifting the maximum diastolic potential, or decreasing the rate of depolarization, or (positively or negatively) shifting the membrane potential threshold; all of which could either increase or decrease the time required for the membrane potential to reach the threshold and fire an AP. In the goldfish model, administration of isoproterenol altered ventricular AP morphology and had a positive chronotropic effect (**Figures 4.1a-c**). Remarkably, previous studies have observed isoproterenol to induce strikingly similar AP morphological changes in canine endocardial myocytes and guinea pig cardiomyocytes (O'Hara and Rudy, 2012; Szentandrássy et al. 2012; Sala et al. 2018).

The changes in the AP morphology can be better observed in **Figure 4.2**, where the kinetics of the ventricular AP are presented following adrenergic stimulation with isoproterenol. Perfusion with isoproterenol lead to a significant increase in APD30 and APD90 (**Figures 4.2a**, **c**, respectively) and a significant decrease in APD50 (**Figure 4.2b**). Interestingly, canine endocardial myocytes treated with isoproterenol exhibit lengthening of APD90 (Szentandrássy et al. 2012; Sala et al. 2018), similar to what we observed for the goldfish. Unlike mammals, many fish species lack the slow component

of the delay rectifier current (I_{Ks}), the main current system mediating repolarization effects of adrenergic stimulation on cardiac AP duration (Vornanen, 2017). The absence of this repolarizing current could explain the counterintuitive prolongation of APD30 and APD90 in the presence of an adrenergic stimulus. However, the role of I_{Ks} in response to adrenergic stimulation is not yet elucidated in the goldfish heart, and further studies are necessary to corroborate this hypothesis.

Epicardial Ca^{2+} transient recordings from the goldfish ventricle show that the administration of isoproterenol altered the morphology of the Ca^{2+} transient, and significantly increased the normalized amplitude of the Ca^{2+} transient (**Figures 4.3a, b**), a trend also observed in guinea pigs (Katra et al. 2004). The positive chronotropic effect (**Figures 4.1c** and **Figure 4.5c**) in response to β-adrenergic stimulation could be explained by the alterations present in the Ca^{2+} transient dynamics followed by isoproterenol perfusion. A significant increase in the Ca^{2+} transient amplitude following adrenergic stimulation (**Figure 4.3b**) suggests isoproterenol increased the Ca^{2+} current, likely through the LTCC (Bazmi and Escobar, 2020). As previously discussed, β-adrenergic stimulation activates a cascade of events that phosphorylate numerous Ca^{2+} handling proteins, including pln on serine 16 and threonine 17. Phosphorylation of pln removes its inhibitory effect on the cardiac sarcoplasmic endoplasmic reticulum ATPase, thus increasing Ca^{2+} load into the sarcoplasmic reticulum. An increased Ca^{2+} transient amplitude increases the influx of positive charges into the myocardium and reduces the AP threshold; both of which increase the conduction velocity of the AP, resulting in a positive dromotropic effect. Furthermore, an increased Ca^{2+} current will increase the amount of Ca^{2+} in the sarcoplasmic reticulum and ultimately increase Ca^{2+} induced Ca^{2+} release. This would then increase the strength of contraction, resulting in the positive inotropic effect observed in **Figure 4.3**. To our knowledge, a positive inotropic effect in response to adrenergic stimulation has yet to be observed in the ventricle of any other fish species (Abramochkin and Vornanen, 2017; Molina et al. 2007; Vornanen and Tuomennoro, 1999; Vornanen et al. 2010). However, it is likely previous studies did not observe positive dromotropic effects considering many of them performed similar experiments on isolated cardiomyocytes, and not at the intact heart level. Looking at changes in the kinetic properties of the goldfish heart, it is likely isoproterenol also had a positive lusitropic effect. Although all three kinetic parameters of the goldfish Ca^{2+} transient decreased following isoproterenol perfusion (**Figures 4.4a, b, c**), the lusitropic effect can be best observed in **Figure 4.4b**, as the fall time of the Ca^{2+} transient significantly decreased, suggesting isoproterenol increased the rate of myocardial relaxation during diastole.

Transmural electrocardiograms were recorded in the presence and absence of isoproterenol (**Figure 4.5**) to examine its effect on whole heart electrical activity. Indeed, isoproterenol perfusion not only altered the morphology of the electrocardiogram (**Figure 4.5a**) but also reaffirmed the positive chronotropic effect (**Figures 4.5b, c**) of isoproterenol presented in **Figure 4.1**. The positive chronotropic effect could be due to an increased slope of diastolic depolarization, as many other mammals exhibit the same pattern in response to adrenergic stimulation (Randall et al. 2020).

Isoproterenol's significant effect on whole heart excitability (**Figure 4.6**) not only reaffirms the presence of a positive chronotropic effect, but also suggests the instigation of a positive dromotropic effect. Because the QRS complex represents ventricular depolarization, its duration indirectly measures intraventricular impulse conduction. Thus, the positive dromotropic effect induced by isoproterenol can best be observed in F**igure 4.6a**, where administration of the catecholamine significantly reduced the duration of the QRS complex and increased the rate of intraventricular impulse conduction. Furthermore, isoproterenol significantly increased the duration of the T wave, and significantly prolonged the duration of the J wave (**Figures 4.6b, c**). An increased J wave duration is consistent with the prolongation of the APD30 in the presence of 100 nM of isoproterenol (**Figure 4.2a**). These modifications observed in the electrocardiogram further solidify the hypothesis that goldfish exhibit sympathetic regulation, as perfusion with a catecholamine significantly modified cardiac excitability. The cardiac AP alters the mechanical function of vertebrate hearts by increasing intracellular free Ca^{2+} concentration, ultimately inducing cardiac contractions (Coraboeuf, 1978; Randall et al. 2020). In the goldfish heart, Ca^{2+} influx through the L-type Ca^{2+} channels is the most likely trigger of Ca^{2+} release from the sarcoplasmic reticulum (Bazmi and Escobar, 2020), which ultimately augments cardiac contractile properties. Therefore, modifications in Ca^{2+} handling dynamics are essential for understanding how cardiac excitability alters cardiac contractility.

Chapter 5:

Intrinsic parasympathetic NS activity and effect of AP and intracellular Ca^{2+} dynamics

5.1 How does the parasympathetic drive regulate heart rate of the Langendorff fish heart?

The parasympathetic nervous system, on the other hand, is thought to be the dominant branch of the autonomic nervous system. To elicit a parasympathetic response and induce a cholinergic response, 5 μM carbamylcholine was administered to the goldfish intact heart. As before, the chronotropic properties of the heart were assessed via AP and spontaneous heart rate recordings. Not surprisingly, the administration of carbamylcholine altered the AP morphology (**Figure 5.1a**) and had a negative chronotropic effect, reducing the heart rate by 92.2% (**Figure 5.1b, c**; from 0.98 ± 0.05 Hz to 0.13 ± 0.08 Hz).
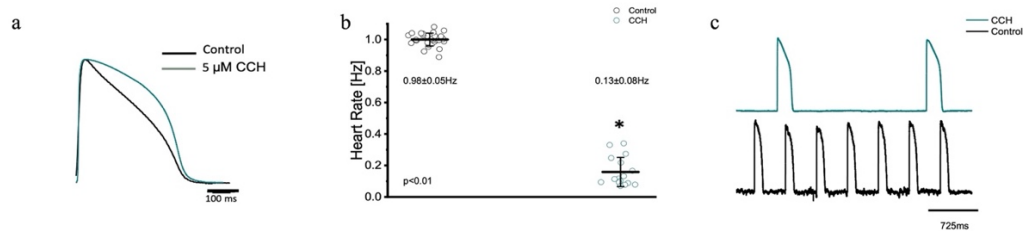
Figure 5.1 Goldfish ventricular action potential and spontaneous heart rate recordings before (black) and after (green) perfusion with 5 μM carbamylcholine. Administration of carbamylcholine altered the AP morphology (a) and had a negative chronotropic effect, reducing the heart rate from 0.98 ± 0.05 Hz to 0.13 ± 0.08 Hz (p<0.01, n=29 for the control, n=16 for CCH, N=4) (b). The negative chronotropic effect following carbamylcholine perfusion is also reflected in spontaneous AP recordings from the left ventricle (c). An asterisk denotes a significant difference between the two distributions. The data are presented as multiple measurements (n; dot cloud) recorded for different measurements (n) on different hearts (N) with the mean ± SEM (solid lines).

5.2 How does a parasympathetic NS agonist alter AP and Ca^{2+} dynamics in the Goldfish ventricle?

Not surprisingly, carbamylcholine administration significantly altered all three kinetic parameters of the AP (**Figure 5.2a, b, c**; APD30 increased from 235.90 ± 12.10 ms to 295.30 ± 11.50 ms, APD50 decreased from 388.10 ± 23.90 ms to 651.40 ± 49.50 ms, and APD90 increased from 446.70 ± 14.60 ms to 833.60 ± 30.00 ms, respectively).
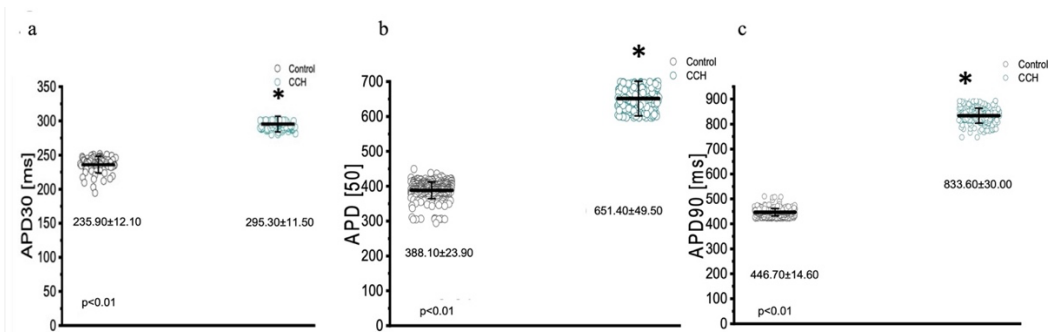
Figure 5.2: Kinetic parameters of the goldfish ventricular action potential before (black) and after (green) perfusion with 5 μM carbamylcholine. APD30 significantly increased from 235.90 ± 12.10 ms to 295.30 ± 11.50 ms (p<0.01, n=60 for the control, n=49 for CCH, N=4) (a), APD50 significantly increased from 388.10 ± 23.90 ms to 651.40 ± 49.50 ms (p<0.01, n=60 for the control, n=59 for CCH. N=4) (b), and APD90 significantly increased from 446.70 ± 14.60 ms to 833.60 ± 30.00 ms (p<0.01, n=16 for the control, n=84 for CCH, N=4) (c). An asterisk denotes a significant difference between the two distributions. The data are presented as multiple measurements (n; dot cloud) recorded for different measurements (n) on different hearts (N) with the mean ± SEM (solid lines).

In many vertebrate species, stimulation of either autonomic nervous system branch will not only alter cardiac excitability, but also cardiac contractility. To assess if stimulation of either autonomic nervous system branch altered the inotropic and/or the lusitropic properties of the goldfish ventricle, experiments were performed in which the amplitude and kinetics of the Ca^{2+} transient were examined in the presence and absence of a cholinergic agonist.

To assess cholinergic regulation of contractility specifically, Ca^{2+} transients were recorded from the epicardial wall of the goldfish ventricle in the presence and absence of 5 μM carbamylcholine (**Figure 5.3**). Administration of carbamylcholine had a negative inotropic effect, as the amplitude of the Ca^{2+} transient (**Figure 5.3a**) decreased in the presence of carbamylcholine. This negative inotropic effect is also presented in **Figure 5.3b**, where the normalized amplitude of the Ca^{2+} transient significantly decreased from 1.00 ± 0.10 to 0.49 ± 0.03 following cholinergic stimulation.
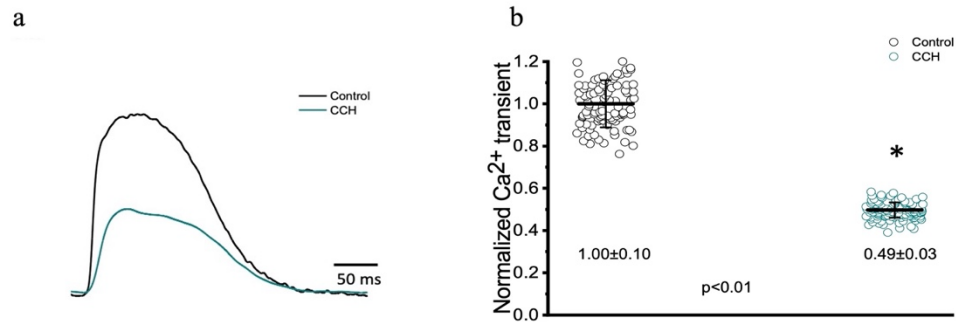
Figure 5.3: Goldfish ventricular Ca²⁺ transient recording and normalized amplitude in the absence (black) and presence (green) of 5 μM carbamylcholine. Perfusion with carbamylcholine altered the morphology of the Ca²⁺ transient (a) and significantly decreased the normalized amplitude of the Ca²⁺ from 1.00 ± 0.10 to 0.49 ± 0.03 (p<0.01, n=108 for the control, n=143 for CCH, N=8) (b). An asterisk denotes a significant difference between the two distributions. The data are presented as multiple measurements (n; dot cloud) recorded for different measurements (n) on different hearts (N) with the mean ± SEM (solid lines).

5.3 How does a parasympathetic NS agonist alter Ca²⁺ transient kinetics?

      The three kinetic properties of the Ca²⁺ transient, the rise time (RT), fall time (FT), and half duration (HD) were also evaluated to better understand how stimulation of the cholinergic pathway affected Ca²⁺ handling kinetics in the goldfish myocardium (**Fig. 5.4**). Although administration of 5 μM carbamylcholine did not significantly increase the rise time of the Ca²⁺ transient (**Figure 5.4a**; 30.20 ± 5.40 ms to 31.20 ± 3.20 ms), it did significantly increase the half duration of the Ca²⁺ transient (**Figure 5.4c**; from 151.80 ± 2.30 ms to 160.30 ± 4.00 ms). This effect can be due to the longer APs induced via cholinergic stimulation. Interestingly we were unable to observe a significant difference in the relaxation time (**Figure 5.4b**; from 161.50 ± 15.10 ms to 150.70 ± 12.10 ms) of the Ca²⁺ transient. This suggests carbamylcholine application did not significantly modify the lusitropic property of the goldfish myocardium in these experiments; however, a significant change in the half duration of the Ca²⁺ transient does indicate the presence of an intrinsic parasympathetic tone in the goldfish isolated heart, capable of modifying Ca²⁺ transient kinetics.
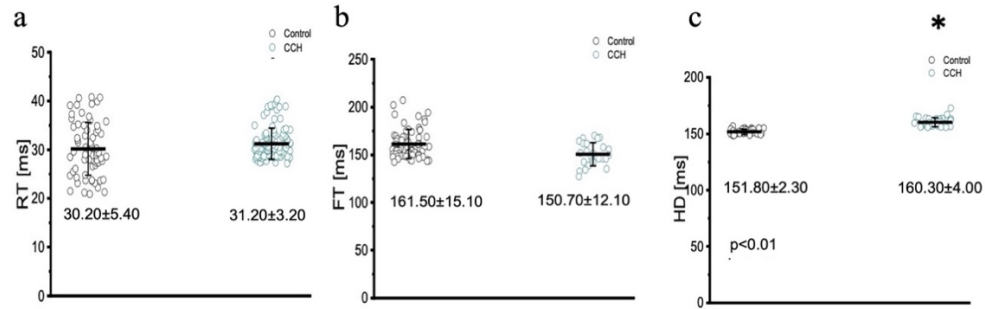
Figure 5.4: The three kinetic properties of the Ca^{2+} transient, the rise time (RT), fall time (FT), and half duration (HD) before (black) and after (green) perfusion with 5 µM carbamylcholine. Administration of 5 µM carbamylcholine did not significantly increase the rise time of the Ca^{2+} transient from 30.20 ± 5.40 ms to 31.20 ± 3.20 ms ($p > 0.01$, n=69 for the control, n=85 for CCH, N=8) (a) or decrease the fall time (FT) from 161.50 ± 15.10 ms to 150.70 ± 12.10 ms ($p > 0.01$, n=59 for the control, n=27 for CCH, N=8) (b). However, the half duration of the Ca^{2+} transient significantly increased from 151.80 ± 2.30 ms to 160.30 ± 4.00 ms ($p < 0.01$, n=29 for the control, n=31 for CCH, N=8) (c). An asterisk denotes a significant difference between the two distributions. The data are presented as multiple measurements (n; dot cloud) recorded for different measurements (n) on different hearts (N) with the mean ± SEM (solid lines).

5.4 How does a parasympathetic NS agonist alter the ECG morphology and kinetics?

To further assess how cholinergic stimulation altered whole heart electrical activity in the goldfish model, transmural electrocardiograms were recorded in the presence and absence of 5 µM carbamylcholine (**Figure 5.5**). The morphology of the goldfish electrocardiogram changed dramatically in response to cholinergic stimulation (**Figure 5.5a**), and significantly decreased the spontaneous heart rate (**Figure 5.5b, c**; from 1.00 ± 0.04 Hz to 0.15 ± 0.09 Hz).
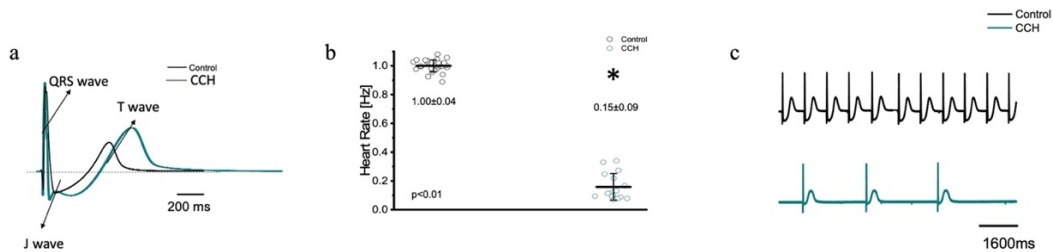
Figure 5.5: Transmural ventricular electrocardiogram recordings in the absence (black) and presence (green) of 5 μM carbamylcholine. The 3 main components of the goldfish electrocardiogram are presented: QRS complex, J wave, and T wave (A). Carbamylcholine administration significantly altered the kinetic parameters of all the electrocardiographic signals. Administration of carbamylcholine significantly decreased heart rate from 1.00 ± 0.04 Hz to 0.15 ± 0.09 Hz (p<0.01, n=29 for the control, n=16 for CCH, N=6) (B). Electrocardiogram recordings before and after carbamylcholine perfusion reflect a decreased heart rate in response to carbamylcholine (C). An asterisk denotes a significant difference between the two distributions. The data are presented as multiple measurements (n; dot cloud) recorded for different measurements (n) on different hearts (N) with the mean ± SEM (solid lines).

Cholinergic stimulation significantly altered the duration of the QRS complex, the T wave, and the J wave (**Figure 5.6**). The QRS complex significantly decreased from: 33.20 ± 2.40 ms to 31.90 ± 1.80 ms (**Figure 5.6a**), the T wave significantly increased from 370.20 ± 3.70 ms to 379.70 ± 14.40 ms (**Figure 5.6b**), and the J wave significantly increased from 169.20 ± 30.20 ms to 326.60 ± 23.30 ms (**Figure 5.6c**). The increased J wave duration is likely reflective of the decreased heart rate observed in Figures 5.1c and 5.5c.
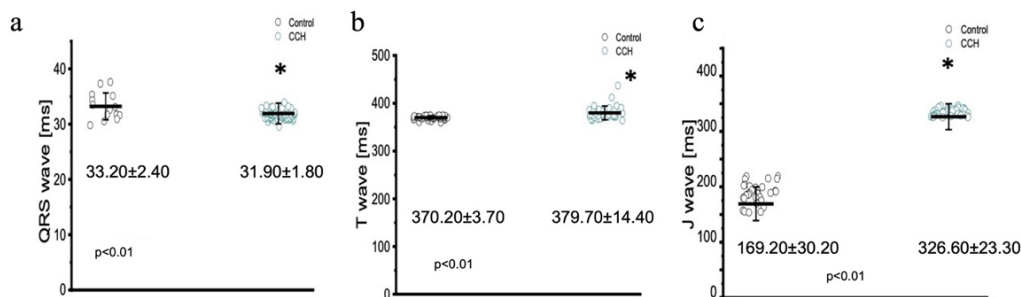
Figure 5.6: Perfusion with 5 μM carbamylcholine significantly altered the time course of all three components in the goldfish electrocardiogram. The duration of the QRS significantly decreased from 33.20 ± 2.40 ms to 31.90 ± 1.80 ms (p<0.01, n=15 for the control, n=59 for CCH, N=6) (a), the T wave increased from 370.20 ± 3.70 ms to 379.70 ± 14.40 ms (p<0.01, n=31 for the control, n=36 for CCH. N=6) (b), and the J wave showed a significant increase from 169.20 ± 30.20 ms to 326.60 ± 23.30 ms (p<0.01, n=32 for the control, n=31 for CCH. N=6) (c). An asterisk denotes a significant difference between the two distributions. The data are presented as multiple measurements (n; dot cloud) recorded for different measurements (n) on different hearts (N) with the mean ± SEM (solid lines).

5.5 Discussion

Muscarinic Stimulation Decreased Cardiac Excitability and Contractility

As previously mentioned, an organism with an adrenergic drive could potentially also have a cholinergic drive, as they are the two antagonistic branches of the autonomic nervous system. Cholinergic control, however, is stronger than adrenergic control and has a negative chronotropic, dromotropic, inotropic, and lusitropic effect (Axelsson et al. 1987; Farrell, 1984; Urbá-Holmgren et al. 1977; Laurent et al. 1983; Randall et al. 1968). In the goldfish model, perfusing the heart with 5 µM carbamylcholine prolonged the AP (**Figure 5.1a**) and had a negative chronotropic effect (**Figures 5.1b, c**). The strong negative chronotropic effect induced by cholinergic stimulation could be mediated by an ACh activated potassium current (I_{KAch}); a major current found in fish atrial myocytes responsible for the repolarization of the membrane potential (Abramochkin and Vornanen, 2017; Molina et al. 2007; Vornanen et al. 2010).

Furthermore, the activation of a muscarinic receptor will produce inhibition of the adenylyl cyclase reducing the levels of cAMP, preventing PKA mediated phosphorylation. It is important to note, however, the levels of cAMP are finely regulated by PDEs, which contribute to the lowered cAMP concentrations. Nevertheless, lowered PKA levels result in a reduction in key phosphorylation sites, which ultimately decrease the slope of the diastolic depolarization, and decrease heart rate. Furthermore, administration of carbamylcholine induced prolongation of two kinetic parameters of the AP duration (**Figures 5.2a, c**). Considering previous research has shown the presence of Ca^{2+} dependent inactivation of the L-type Ca^{2+} channel in goldfish ventricular myocytes (Bazmi and Escobar, 2020), it is likely a decreased sarcolemmal Ca^{2+} influx mediated by carbamylcholine (**Figure 5.3b**) decelerated inactivation and prolonged the duration of the action potential.

A reduction in the Ca^{2+} current amplitude (**Figure 5.3b**) is likely to have reduced the slope of the diastolic depolarization, and as such, induced a negative chronotropic effect. As mentioned before, there are numerous mechanisms by which this slope may change. During cholinergic stimulation, PDEs and inhibition of adenylyl cyclase reduce cAMP levels, which not only lowers the activation of PKA, but also reduces stimulation of HCN channels. The current produced by these channels, I_f, typically increases the slope of the diastolic depolarization. However, in the presence of a cholinergic agonist, stimulation of I_f decreases, thus reducing the slope of the diastolic depolarization and ultimately reducing heart rate. Interestingly, HCN4 pacemaker channels have only been identified in the pacemaker region of the goldfish and zebrafish (Newton et al. 2014; Tessadori et al. 2012). Another possible mechanism by which muscarinic receptor stimulation induced a negative chronotropic response could be activation (I_{KAch}), although the contribution of this current is still poorly elucidated in fish ventricular myocytes (Abramochkin and Vornanen, 2017; Molina et al. 2007; Vornanen et al. 2010). Activation of I_{KACh} would induce hyperpolarization of the maximum diastolic potential, decreasing the heart rate. A decreased Ca^{2+} current and activation of I_{KACh} also lead to a negative dromotropic effect as a decreased Ca^{2+} current will decrease the influx of

positive charges, increase the threshold of the AP, and decrease the mean diastolic potential, all of which reduce AP conduction velocity and induce a negative dromotropic effect.

Modifications presented in the kinetic properties of the goldfish heart following carbamylcholine perfusion (**Figure 5.4**) suggest stimulation of the muscarinic receptor induced a minor negative lusitropic effect. While the half duration of the Ca^{2+} transient significantly increased in response to carbamylcholine perfusion (**Figure 5.4c**), the rise time and fall time were not significantly altered (**Figures 5.4a, b**). These results are interesting because the effect of carbamylcholine is in the opposite direction of what happens in mouse hearts and is very similar to larger mammals (Aguilar-Sanchez et al. 2019).

In order to determine how the stimulation of a cholinergic response modulated whole heart electrical activity, electrocardiograms were recorded in the presence and absence of carbamylcholine (**Figure 5.5**). Perfusion with carbamylcholine altered electrocardiogram morphology (**Figures 5.5a**) and reaffirmed the negative chronotropic effect (**Figures 5.5b, c**) presented in **Figure 5.1b**. Modification of whole heart excitability in response to muscarinic stimulation is presented in **Figure 5.6**. Interestingly, the duration of the QRS complex decreased in response to carbamylcholine administration, suggesting a slight positive dromotropic response, something typically observed in tachycardia. Currently, little is known about the depolarizing ventricular currents in the goldfish, which could provide further insight as to why cholinergic stimulation would reduce the duration of the QRS complex. Carbamylcholine perfusion also significantly increased the T and J wave durations (**Figures 5.6a-c**); however, the increased J wave was expected as there was a corresponding increase in APD30 (**Figure 5.2a**).

The negative chronotropic effect induced by stimulation of the muscarinic receptors could also be explained by modifications of the Ca^{2+} transient. Administration of 5 µM carbamylcholine modified Ca^{2+} transient morphology and significantly decreased the amplitude of the Ca^{2+} transient, suggesting stimulation of muscarinic receptors may have had a negative inotropic effect (**Figures 5.3a, 5.3b**). This is particularly interesting because previous studies conducted in isolated cardiac myocytes suggest muscarinic stimulation produced minor changes in cardiac chronotropic and inotropic properties in the fish heart (Fritsche and Nilsson, 1990; Laurent et al. 1983; Steele et al. 2009). This discrepancy, however, could be explained by the fact that other experiments were conducted in isolated myocytes, while our experiments were performed in the intact heart. As the heart is an electrically coupled organ, isolation of cardiac myocytes disrupts this electrical coupling, which may alter cardiac contractile properties.

Chapter 6:

The effect of increasing the heart rate and temperature on AP morphology and intracellular [Ca^{2+}] dynamics

6.1 How do ventricular electrical properties respond to an increasing heart rate?

Like with other vertebrates, the fish heart needs to increase its heart rate to cope with environmental and stress conditions. For example, a fish escaping from a predator needs to increase the rate of skeletal muscle action potentials and contractions (Rome et al., 1993) in order to escape the predator. Here, we carried out experiments in goldfish to evaluate how an increased heart rate could modify the APs and Ca^{2+} transients (**Figure 6.1**). **Figure 6.1a** illustrates the time courses of APs as a function of the heart rate. It is important to note that as the heart rate increased, the duration of the APs got shorter. **Figure 6.1b-d** reveal how the APD30, APD50, and APD90 changed as a function of the heart rate, respectively (N = 6 hearts). A summary of the results is presented in **Table 3.1**.

Heart rate	1.2 Hz n = 87 N = 5	1.5 Hz n = 125 N = 5	1.7 Hz n = 122 N = 5	2.0 Hz n = 191 N = 5	2.2 Hz n = 184 N = 5
APD					
APD$_{30}$ (ms)	164.3 ± 9.9	152.6 ± 6.3	128.6 ± 4.7	125.3 ± 3.7	126.5 ± 2.7
APD$_{50}$ (ms)	244.1 ± 11.5	227.0 ± 6.4	205.3 ± 3.6	200.1 ± 3.4	201.6 ± 1.9
APD$_{90}$ (ms)	356.6 ± 5.2	329.0 ± 6.5	309.3 ± 2.3	300.5 ± 4.9	300.3 ± 2.0

Table 3.1 kinetic parameters of the AP as function of the heart rate

6.2 Does an increased heart rate modify the kinetics of the Ca^{2+} transients?

Ca^{2+} transients from the goldfish heart also present a strong heart-rate dependency. **Figure 6.1e** shows how the amplitude of the Ca^{2+} transients decreased as a function of the heart rate (**Figure 6.1f**). The traces of Ca^{2+} transients shown in **Figure 6.1e** were normalized by their maximum amplitude (**Figure 6.1g**) to gain a clearer understanding of how a change in heart rate affected Ca^{2+} transient kinetics. The Ca^{2+} transients exhibited a strong change in kinetic behavior. Specifically, as the heart rate increased, all the kinetic parameters became shorter. **Figures 6.1h-6.1j** all depict how the amplitude, RT, FT, and HD of the Ca^{2+} transients became smaller as a function of the heart rate, respectively. An outline of the results is shown in **Table 3.2**.

Heart rate	1.2 Hz n = 107 N = 5	1.5 Hz n = 150 N = 5	1.7 Hz n = 165 N = 5	2.0 Hz n = 200 N = 5	2.2 Hz n = 217 N = 5
Times					
Fractional amplitude	0.82 ± 0.01	0.67 ± 0.02	0.58 ± 0.02	0.45 ± 0.01	0.38 ± 0.01
Rise time (ms)	19.1 ± 1.2	16.5 ± 0.4	16.2 ± 0.4	15.8 ± 0.4	16.0 ± 0.5
Fall time (ms)	271.0 ± 11.1	222.9 ± 4.5	214.7 ± 4.7	201.9 ± 5.2	198.3 ± 5.1
Half duration (ms)	308.0 ± 4.8	231.2 ± 3.1	213.6 ± 2.8	186.9 ± 1.9	181.9 ± 2.2

Table 3.2 kinetic parameters of the Ca^{2+} transient as function of the heart rate
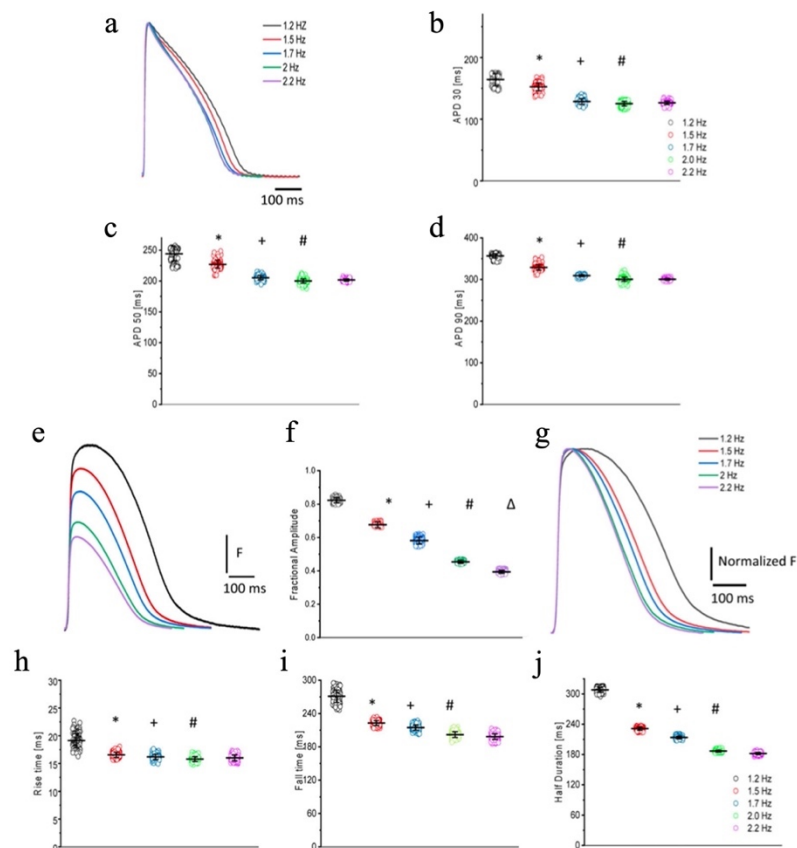
Figure 6.1: Time courses of APs and Ca^{2+} transients in goldfish hearts as a function of the heart rate (a). As the heart rate increased, the duration of the APs at 30% (b), 50% (c), and 90% (d) repolarization decreased (see Table 3.1). The amplitude of the Ca^{2+} transients decreased (e) in a step staircase manner as a function of the heart rate (f). There was a strong change in the kinetic behavior, which is better observed after normalization of the Ca^{2+} transient amplitude (g). There was a reduction in the rise time (h), fall time (i), and the half duration (j) of the Ca^{2+} transients as a function of heart rate (see Table 3.2). The symbols *, $^+$, #, and Δ differentiate measurements that are statistically significant between the two consecutive heart rates (p < 0.01, N = 6 hearts).

6.3 What is the temperature dependency of the ventricular AP?

Because fish are poikilotherm vertebrates, we decided to assess how temperature could modify both the kinetics of APs and Ca^{2+} transients. Not surprisingly, an increase in the temperature produced a shortening of the AP duration at 30, 50, and 90% repolarization, opposite that observed in mice (Ferreiro et al., 2012). **Figure 6.2a** illustrates how increasing the temperature from 23.5°C to 28.5°C affected the AP. Specifically, when the temperature was increased by 5°C, the APD30 (**Figure 6.2b**)

shortened from 212.4 ± 12.3 ms to 164.3 ± 9.9 ms, the APD50 (**Figure 6.2b**) shortened from 320.1 ± 9.5 ms to 244.1 ± 11.5 ms, and the APD90 (**Figure 6.2b**) shortened from 443.5 ± 10.2 ms to 356.6 ± 5.25 ms (n = 87 measurements, N = 9 hearts). To evaluate the thermodynamics of the AP in greater detail, we decided to calculate the first derivative to obtain the rates of depolarization and repolarization of the AP recordings at both experimental temperatures.

$$R = \frac{dV_m(t)}{d_t}$$

These rates were then used to calculate the Q_{10}.

$$Q_{10} = \left(\frac{R_2}{R_1}\right)^{\left(\frac{10}{T_2 - T_1}\right)}$$

where R_2 is the rate at temperature 2, R_1 is the rate at temperature 1, T_2 is temperature 2, and T_1 is temperature 1. The calculated Q_{10} for the depolarization of the AP was 1.09 and 1.56 for the repolarization of the AP.

6.4 What is the temperature dependency of the intracellular Ca^{2+} Transients?

  Usually, Ca^{2+} transients have a larger temperature dependency than excitability (Kornyeyev et al., 2010; Ferreiro et al., 2012). One reason behind this increase is the temperature dependent process of hydrolyzing ATP to pump Ca^{2+} back into the SR. To better examine this process in the goldfish, we evaluated the temperature dependency of the Ca^{2+} transients.

  Figure 6.2e exemplifies the effect of raising the goldfish heart temperature by 5°C. Upon this increase in temperature, the Ca^{2+} transients were not only smaller (**Figure 6.2c, d**), they were also faster (**Figure 6.2e, f**). The amplitude of the Ca^{2+} transients decreased from 0.82 ± 0.01 (n = 107 measurements) to 0.33 ± 0.01 (n = 107 measurements, N = 9 hearts). The differences in the kinetics can be better observed in **Figure 6.2g**, where the Ca^{2+} transient traces were normalized. Interestingly, the Ca^{2+} transients illustrated in **Figure 6.2e** display a smaller amplitude. However, this can be explained by the shortened AP durations at higher temperatures. Indeed, that is what we observed here. The RT (**Figure 6.2f**) decreased from 25.0 ± 0.6 ms at 23.5°C to 19.25 ± 1.47 ms at 28.5°C (n = 110 measurements at 23°C and n = 119 measurements at 28.5°C). The FT (**Figure 6.2f**) was reduced from 334.1 ± 6.5 ms at 23.5°C to 271.0 ± 11.1 ms at 28.5°C. Finally, the HD of Ca^{2+} transients (**Figure 6.2f**) diminished from 382.6 ± 2.9 ms at 23.5°C to 308.0 ± 4.8 ms at 28.5°C (n = 110 measurements at 23°C and n = 120 measurements at 28.5°C, N = 9 hearts). Once again, to have a better thermodynamic picture of the effect of temperature on Ca^{2+} transients we calculated Q_{10}.

For these experiments, we first calculated the time constant for activation (τ_{on}) and the time constant for the relaxation (τ_{off}) of the Ca^{2+} transients.

τ_{on} and τ_{off} were calculated as

$$\tau_{on} = \frac{RT}{2.2} \qquad \text{and} \qquad \tau_{off} = \frac{FT}{2.2}$$

And the rates R_{on} and R_{off} were calculated as

$$R_{on} = \frac{1}{\tau_{on}} \qquad \text{and} \qquad R_{off} = \frac{1}{\tau_{off}}$$

Then, the Q_{10} calculated for the Ca^{2+} transient activation was 1.68 and the relaxation of the Ca^{2+} transient was Q_{10} was 1.52.
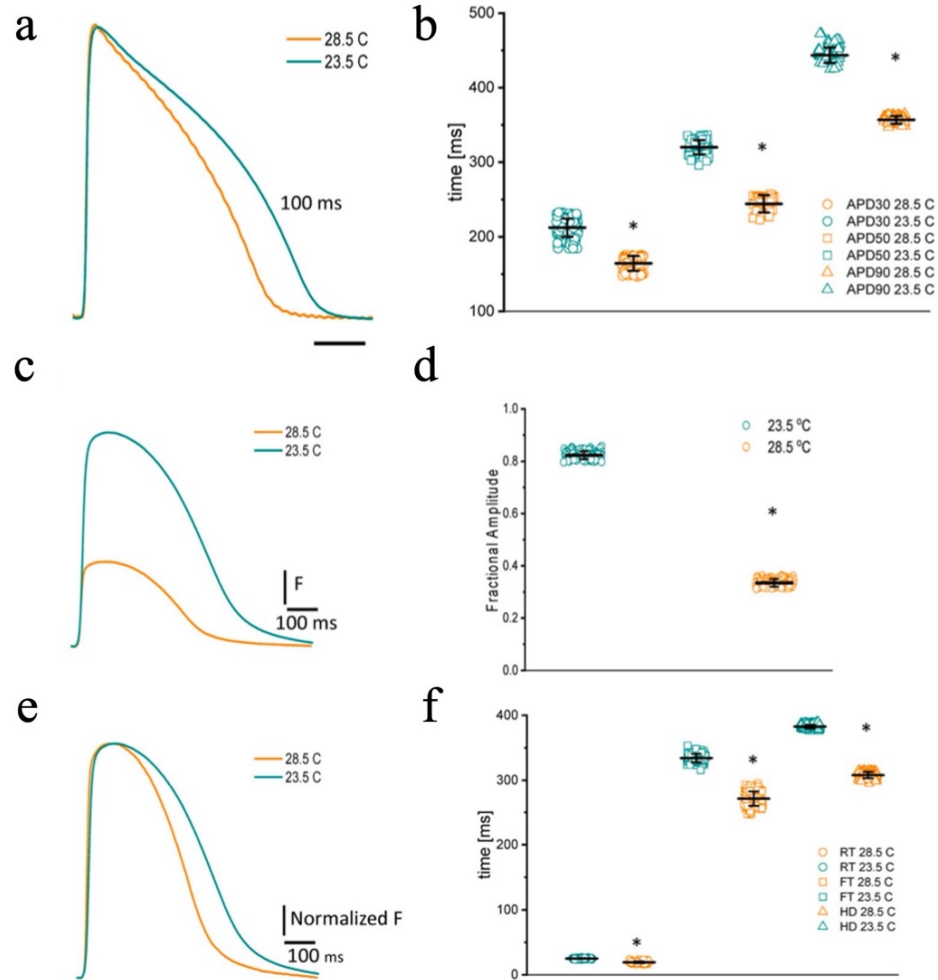
Figure 6.2: Effects of increasing the temperature from 23.5 to 28.5°C on AP and Ca²⁺ transients from goldfish hearts (a). The increased temperature shortened the AP duration at 30% (b) (from 212.4 ± 12.3 ms to 164.3 ± 9.9 ms), 50% (from 320.1 ± 9.5 ms to 244.1 ± 11.5 ms), and 90% repolarization (from 443.5 ± 10.2 ms to 356.6 ± 5.25 ms). The increase in temperature also leads to shorter and smaller Ca²⁺ transients (c). The effect of temperature on the amplitude of the Ca²⁺ transients is illustrated in panel (d). Moreover, the Ca²⁺ transient traces were normalized to better observe the changes in their kinetics (e). The global increase in temperature of the heart reduced the rise time (f) (from 25.0 ± 0.6 ms at 23.5°C to 19.25 ± 1.47 ms at 28.5°C), fall time (from 334.1 ± 6.5 ms at 23.5°C to 271.0 ± 11.1 ms at 28.5°C), and half duration (from 382.6 ± 2.9 ms at 23.5°C to 308.0 ± 4.8 ms at 28.5°C) of Ca²⁺ transients. The symbol * differentiates between statistically significant measurements ($p < 0.01$, N = 9 hearts).

6.5 Discussion

Heart Rate Dependency of APs and Ca²⁺ Transients

The AP duration of goldfish hearts changes significantly in response to a change in heart rate, suggesting AP duration to be frequency dependent (**Figures 6.1a–d**). The profile of decrease of the AP duration at the three levels (i.e., APD30, APD50, and APD90), shows a similar profile to those previously observed for mammals (Litovsky and Antzelevitch, 1989; Lukas and Antzelevitch, 1993; Ferreiro et al., 2012) and other fish models (Lin et al., 2014, 2015; Rayani et al., 2018)

Another important outcome of the heart rate dependency in goldfish hearts is the effect on the Ca^{2+} transient amplitude (**Figure 6.1e**). Specifically, the appearance of a negative staircase behavior emerges in response to an increased heart rate (**Figure 6.1f**). All the kinetic parameters, the RT, FT, and HD of the Ca^{2+} transients became faster (**Figures 6.1g–j**), as was observed in other fish models (Lin et al., 2015; Rayani et al., 2018). In terms of the negative staircase behavior of Ca^{2+} transients, there are reports for other fish models related to a decrease in the amplitude of Ca^{2+} transients (Lin et al., 2015) and in developed pressure (Haustein et al., 2015). Interestingly, although mice display a significant negative staircase profile in the amplitude of the Ca^{2+} transients (Kornyeyev et al., 2012), larger mammals present a positive staircase profile in their mechanical response (Langer, 1967; Kodama et al., 1981; Opitz, 1980; Bouchard and Bose, 1989; Hattori et al., 1991). The discrepancy in the staircase behavior observed between larger mammals and goldfish could imply that goldfish not only have a faster Ca^{2+} reloading rate of the SR, but also have a more prominent Ca^{2+} -dependent inactivation of L-type Ca^{2+} channels.

Temperature Dependency of APs and Ca²⁺ Transients

Fish cannot systemically regulate their body temperature; thus, the temperature of the water has a large influence on the physiological behavior of the animal's cardiac function (Ferreira et al., 2014; Vornanen, 2016). We illustrate this idea in **Figure 6.2**, in which both the time course of the AP and Ca^{2+} transients of goldfish hearts display a significant temperature dependency. Interestingly, the depolarization of the AP has a much lower temperature dependency (Q10) than the repolarization (**Figures 6.2a, b**). The depolarization of an AP is mainly dependent on the activation of voltage-dependent Na^+ channels, thus expounding the observed thermodynamic behavior. The repolarization, on the other hand, can include multiple events that can be regulated by the Ca^{2+} released from the SR. Some mechanisms regulating the repolarization of the AP include the activation of the NCX in its forward mode and/or the Ca^{2+}-dependent inactivation of the L-type Ca^{2+} channel. The reduction in the AP duration as a function of the temperature increase has been reported by other authors in other fish models (Lin et al., 2014; Vornanen, 2016; Badr et al., 2018; Rayani et al., 2018). However, there was no information about the Ca^{2+} transients' amplitude and its temperature dependency in fish models.

Remarkably, the amplitude (**Figures 6.2c, d**), activation (**Figures 6.2e, f**), relaxation (**Figure 6.2f**), and HD (**Figure 6.2f**) of goldfish ventricular Ca^{2+} transients also present a significant temperature dependency (**Figures 6.2c, e**). Interestingly, raising the temperature by only 5°C significantly reduced the amplitude of the Ca^{2+} transient (**Figures 6.2c, d**). Moreover, the decrease in the Ca^{2+} transient amplitude can be due to the shortening of the AP at higher temperatures. If the AP is shorter, then the duration of the L-type Ca^{2+} current is also shorter and less Ca^{2+} is brought into the cell. A very similar temperature dependency has been reported in other species (Edman et al., 1974; Mattiazzi and Nilsson, 1976), in which the mechanical activity and the force–velocity relationship were measured in rabbit papillary muscle. The authors conclude that the observed decrease in contractility cannot be solely related to a decrease in the duration of Ca^{2+} release, but may also be related to an increase in the rate of Ca^{2+} sequestration by the SR.

The temperature dependency of the activation and relaxation of the Ca^{2+} transients presents several interesting features. The RT and the activation time constant of the Ca^{2+} transient have a larger temperature dependency (Q10) than the FT and the relaxation time constant. This thermodynamic behavior can be attributed to the highly cooperative process of Ca^{2+} release from the SR, which depends on the intra-SR Ca^{2+} content (Kornyeyev et al., 2010). Furthermore, as the Ca^{2+} content depends on the activity of the SERCA pump, and this pump needs to hydrolyze ATP to reload the SR, it is expected that this process will have a substantial temperature dependency. On the other hand, the relaxation of the Ca^{2+} transient depends on multiple factors, such as the binding of Ca^{2+} to intracellular Ca^{2+} buffers, which usually has a weak temperature dependency. Altogether, it is logical to expect that relaxation will have a smaller temperature dependency than the activation of the Ca^{2+} transients (Genge et al., 2016; Rayani et al., 2018).

Disadvantages and Limitations

The only animal model with a heart capable of perfectly replicating the mechanical intricacies that constitute the human heart, is another human. For decades, scientists have attempted to identify and establish animal models with which pathogenesis of human disease at a cellular and molecular level could be understood; however, due to the unique limitations in each vertebrate model, our knowledge of the human cardiac physiology remains limited. The goldfish model is no different.

Perhaps the most obvious limitation of the goldfish model is its two chambered heart. This fundamental morphological difference makes most classically used vertebrate models such as the dog, mouse, guinea pig, or rabbit far superior in the furtherments of crucial surgical therapeutic interventions. Furthermore, the fish cardiac myocytes are significantly smaller in size compared to mammals, and do not possess T-tubules. Although it does have smaller invaginations, caveolae, this invagination does not function identical to the mammalian model.

Another limitation presented in this thesis arises from the inherent disadvantage of using the fluorescent indicator, Rhod-2AM. It should be noted that although there are methods in which other fluorescent dyes can be calibrated, there is no established method of calibration for Rhod-2AM. The Ca^{2+} transient kinetics are associated with the fluorescent properties of the dye, and if a different dye were to be used, the Ca2+ transients would have a slightly different morphology, based on the dissociation properties of the dye. Furthermore, Rhod-2AM also acts as a Ca^{2+} buffer once inside the cytosol, altering the true kinetics of intracellular Ca^{2+} handling.

Finally, another limitation of this thesis corresponds to the chapters where the role of the autonomic nervous system is assessed. All experiments presented in this thesis were done at the intact heart level, where the hearts where physically extracted from the animal. Once an animal's heart is taken out of its body, it is likely they lose an intrinsic level of parasympathetic regulation offered by the vagus nerve interacting with the heart. Once lost, there is no way to accurately assess all mechanisms of autonomic regulation of a heart. However, as mentioned, our studies were done at the intact heart level and not at the cellular level. This minimized the electrical uncoupling of electrically, mechanically, and metabolically coupled processes and diminished the insult that would have been received if the cardiac cells are separated from the heart and studied independently.

Conclusions

The results presented here demonstrate how the duration and kinetics of the goldfish epicardial AP are compatible with endocardial APs of larger mammals such as humans or dogs. This is exemplified by our data showing how the influx of Ca^{2+} through L- type Ca^{2+} channels in goldfish not only defined the AP duration, but was also a key trigger in inducing Ca^{2+} release from the SR. Furthermore, we found that goldfish hearts had a similar AP temperature (Antzelevitch et al. 1991; Gurabi et al. 2014) and heart rate dependency (Burashnikov and Antzelevitch 1998; Krishnan and Antzelevitch 1991) when compared to larger mammals.

Remarkably, goldfish exhibited a negative staircase behavior in response to a change in heart rate, opposite to that of larger mammals (Opitz 1980; Hattori, Toyama, and Kodama 1991; Langer 1967; Bouchard and Bose 1989; Kodama et al. 1981; Vila Petroff, Palomeque, and Mattiazzi 2003; Palomeque, Vila Petroff, and Mattiazzi 2004). An important component of Ca^{2+} transients during systole comes from the Ca^{2+} released from the SR. Interestingly, the fraction of Ca^{2+} released from the SR, which contributes to the amplitude of the Ca^{2+} transient, is similar between goldfish and larger mammals (A. Belevych et al. 2007). Previous studies have shown how impaired Ca^{2+} release from the SR will lengthen the duration of the AP (Verduyn et al. 1995; Horackova 1986). This decrease in the AP duration could imply that a Ca^{2+} dependent inactivation of the L-type Ca^{2+} channels may have an important role in controlling how much Ca^{2+} is getting into the ventricular myocytes (Bazmi and Escobar 2019).

Interestingly, our results indicate that stimulation of the goldfish autonomic nervous system by commonly used agonists resulted in a corresponding change in cardiac dromotropism, chronotropism, ionotropism, and lusitropism in a similar manner observed in humans.

In conclusion, the data obtained from our experiments allow us to propose the goldfish heart as an excellent model for performing physiological experiments at the intact heart level. Moreover, its shared similarities with larger mammals opens a new avenue for goldfish hearts to be used as a model to study human physiology and pathology.

References

Abramochkin, D. V., and Vornanen, M. (2017). Seasonal changes of cholinergic response in the atrium of Arctic navaga cod (Eleginus navaga). *Journal of Comparative Physiology B*, *187*(2), 329–338. https://doi.org/10.1007/s00360-016-1032-y

Aguilar-Sanchez, Y., Fainstein, D., Mejia-Alvarez, R., and Escobar, A. L. (2017a). Local Field Fluorescence Microscopy: Imaging Cellular Signals in Intact Hearts. *Journal of Visualized Experiments*, *121*, 55202. https://doi.org/10.3791/55202

Aguilar-Sanchez, Y., Fainstein, D., Mejia-Alvarez, R., and Escobar, A. L. (2017b). Local Field Fluorescence Microscopy: Imaging Cellular Signals in Intact Hearts. *Journal of Visualized Experiments*, *121*, 55202. https://doi.org/10.3791/55202

Aguilar-Sanchez, Y., Rodriguez de Yurre, A., Argenziano, M., Escobar, A. L., and Ramos-Franco, J. (2019a). Transmural Autonomic Regulation of Cardiac Contractility at the Intact Heart Level. *Frontiers in Physiology*, *10*, 773. https://doi.org/10.3389/fphys.2019.00773

Anderson, M. E., Fox, I. J., Swayze, C. R., and Donaldson, S. K. (1989). Frog ventricle: Participation of SR in excitation-contraction coupling. *American Journal of Physiology-Heart and Circulatory Physiology*, *256*(5), H1432–H1439. https://doi.org/10.1152/ajpheart.1989.256.5.H1432

Antzelevitch, C., Sicouri, S., Litovsky, S. H., Lukas, A., Krishnan, S. C., Di Diego, J. M., Gintant, G. A., and Liu, D. W. (1991). Heterogeneity within the ventricular wall. Electrophysiology and pharmacology of epicardial, endocardial, and M cells. *Circulation Research*, *69*(6), 1427–1449. https://doi.org/10.1161/01.RES.69.6.1427

Axelsson, M., Ehrenström, F., and Nilsson, S. (1987). Cholinergic and adrenergic influence on the teleost heart in vivo. *Experimental Biology*, *46*(4), 179–186.

Badr, A., Abu-Amra, E.-S., El-Sayed, M. F., and Vornanen, M. (2018). Electrical excitability of roach (*Rutilus rutilus*) ventricular myocytes: Effects of extracellular K^+, temperature, and pacing frequency. *American Journal of Physiology-Regulatory, Integrative and Comparative Physiology*, *315*(2), R303–R311. https://doi.org/10.1152/ajpregu.00436.2017

Baláti, Varró, and Papp. (1998). Comparison of the cellular electrophysiological characteristics of canine left ventricular epicardium, M cells, endocardium and Purkinje fibres. *Acta Physiologica Scandinavica*, *164*(2), 181–190. https://doi.org/10.1046/j.1365-201X.1998.00416.x

Bazmi, M., and Escobar, A. L. (2019). How Ca2+ influx is attenuated in the heart during a "fight or flight" response. *Journal of General Physiology*, *151*(6), 722–726. https://doi.org/10.1085/jgp.201912338

Bazmi, M., and Escobar, A. L. (2020). Excitation–Contraction Coupling in the Goldfish (Carassius auratus) Intact Heart. *Frontiers in Physiology*, *11*, 1103. https://doi.org/10.3389/fphys.2020.01103

Belevych, A. E., Terentyev, D., Terentyeva, R., Nishijima, Y., Sridhar, A., Hamlin, R. L., Carnes, C. A., and Györke, S. (2011). The relationship between arrhythmogenesis and impaired contractility in heart failure: Role of altered ryanodine receptor function. *Cardiovascular Research*, *90*(3), 493–502. https://doi.org/10.1093/cvr/cvr025

Belevych, A., Kubalova, Z., Terentyev, D., Hamlin, R. L., Carnes, C. A., and Györke, S. (2007). Enhanced Ryanodine Receptor-Mediated Calcium Leak Determines Reduced Sarcoplasmic Reticulum Calcium Content in Chronic Canine Heart Failure. *Biophysical Journal*, *93*(11), 4083–4092. https://doi.org/10.1529/biophysj.107.114546

Bers, D. M. (2002). Cardiac excitation–contraction coupling. Nature, 415(6868), 198-205. https://doi.org/10.1038/415198a

Bjørnstad, H., Mortensen, E., Sager, G., and Refsum, H. (1994). Effect of bretylium tosylate on ventricular fibrillation threshold during hypothermia in dogs. *The American Journal of Emergency Medicine*, *12*(4), 407–412. https://doi.org/10.1016/0735-6757(94)90049-3

Bouchard, R. A., and Bose, D. (1989). Analysis of the interval-force relationship in rat and canine ventricular myocardium. *American Journal of Physiology-Heart and Circulatory Physiology*, *257*(6), H2036–H2047. https://doi.org/10.1152/ajpheart.1989.257.6.H2036

Bovo, E., Dvornikov, A. V., Mazurek, S. R., de Tombe, P. P., and Zima, A. V. (2013). Mechanisms of Ca2+ handling in zebrafish ventricular myocytes. *Pflügers Archiv - European Journal of Physiology*, *465*(12), 1775–1784. https://doi.org/10.1007/s00424-013-1312-2

Brum, G., Osterrieder, W., and Trautwein, W. (1984). Beta-adrenergic increase in the calcium conductance of cardiac myocytes studied with the patch clamp. *Pflugers Archiv: European Journal of Physiology*, *401*(2), 111–118. https://doi.org/10.1007/BF00583870

Burashnikov, A., and Antzelevitch, C. (1998). Acceleration-Induced Action Potential Prolongation and Early Afterdepolarizations. *Journal of Cardiovascular Electrophysiology*, *9*(9), 934–948. https://doi.org/10.1111/j.1540-8167.1998.tb00134.x

Chablais, F., and Jaźwińska, A. (2012). The regenerative capacity of the zebrafish heart is dependent on TGFβ signaling. *Development*, *139*(11), 1921–1930. https://doi.org/10.1242/dev.078543

Chen, J., Zhu, J. X., Wilson, I., and Cameron, J. S. (2005). Cardioprotective effects of KATP channel activation during hypoxia in goldfish *Carassius auratus*. *Journal of Experimental Biology*, *208*(14), 2765–2772. https://doi.org/10.1242/jeb.01704

Chi, N. C., Bussen, M., Brand-Arzamendi, K., Ding, C., Olgin, J. E., Shaw, R. M., Martin, G. R., and Stainier, D. Y. R. (2010). Cardiac conduction is required to preserve cardiac chamber morphology. *Proceedings of the National Academy of Sciences*, *107*(33), 14662–14667. https://doi.org/10.1073/pnas.0909432107

Chin, D., and Means, A. R. (2000). Calmodulin: A prototypical calcium sensor. *Trends in Cell Biology*, *10*(8), 322–328. https://doi.org/10.1016/S0962-8924(00)01800-6

Chopra, S. S., Stroud, D. M., Watanabe, H., Bennett, J. S., Burns, C. G., Wells, K. S., Yang, T., Zhong, T. P., and Roden, D. M. (2010). Voltage-Gated Sodium Channels Are Required for Heart Development in Zebrafish. *Circulation Research*, *106*(8), 1342–1350. https://doi.org/10.1161/CIRCRESAHA.109.213132

Cohn, J. N. (1989). Sympathetic nervous system activity and the heart. *American Journal of Hypertension*, *2*(12 Pt 2), 353S-356S.

Collins, J. H., Kranias, E. G., Reeves, A. S., Bilezikjian, L. M., and Schwartz, A. (1981). Isolation of phospholamban and a second proteolipid component from canine cardiac sarcoplasmic reticulum. *Biochemical and Biophysical Research Communications*, *99*(3), 796–803. https://doi.org/10.1016/0006-291X(81)91235-3

Coraboeuf, E. (1978). Ionic basis of electrical activity in cardiac tissues. *American Journal of Physiology-Heart and Circulatory Physiology*, *234*(2), H101–H116. https://doi.org/10.1152/ajpheart.1978.234.2.H101

Cota, G., Nicola Siri, L., and Stefani, E. (1984). Calcium channel inactivation in frog (Rana pipiens and Rana moctezuma) skeletal muscle fibres. *The Journal of Physiology*, *354*(1), 99–108. https://doi.org/10.1113/jphysiol.1984.sp015365

Cotter, P. A., and Rodnick, K. J. (2006). Differential effects of anesthetics on electrical properties of the rainbow trout (Oncorhynchus mykiss) heart. *Comparative Biochemistry and Physiology Part A: Molecular and Integrative Physiology*, *145*(2), 158–165. https://doi.org/10.1016/j.cbpa.2006.06.001

Curran, J., Brown, K. H., Santiago, D. J., Pogwizd, S., Bers, D. M., and Shannon, T. R. (2010). Spontaneous Ca waves in ventricular myocytes from failing hearts depend on Ca2+-calmodulin-dependent protein kinase II. *Journal of Molecular and Cellular Cardiology*, *49*(1), 25–32. https://doi.org/10.1016/j.yjmcc.2010.03.013

Ding, Z., Peng, J., Liang, Y., Yang, C., Jiang, G., Ren, J., and Zou, Y. (2017). Evolution of Vertebrate Ryanodine Receptors Family in Relation to Functional Divergence and Conservation. *International Heart Journal*, *58*(6), 969–977. https://doi.org/10.1536/ihj.16-558

Edman, K. A. P., Mattiazzil, A., and Nilsson, E. (1974). The Influence of Temperature on the Force-Velocity Relationship in Rabbit Papillary Muscle. *Acta Physiologica Scandinavica*, *90*(4), 750–756. https://doi.org/10.1111/j.1748-1716.1974.tb05643.x

Escobar, A. L., Fernández-Gómez, R., Peter, J.-C., Mobini, R., Hoebeke, J., and Mijares, A. (2006a). IgGs and Mabs against the β2-adrenoreceptor block A-V conduction in mouse hearts: A possible role in the pathogenesis of ventricular arrhythmias. *Journal of Molecular and Cellular Cardiology*, *40*(6), 829–837. https://doi.org/10.1016/j.yjmcc.2006.03.430

Escobar, A. L., Fernández-Gómez, R., Peter, J.-C., Mobini, R., Hoebeke, J., and Mijares, A. (2006b). IgGs and Mabs against the β2-adrenoreceptor block A-V conduction in mouse hearts: A possible role in the pathogenesis of ventricular arrhythmias. *Journal of Molecular and Cellular Cardiology*, *40*(6), 829–837. https://doi.org/10.1016/j.yjmcc.2006.03.430

Escobar, A. L., Perez, C. G., Reyes, M. E., Lucero, S. G., Kornyeyev, D., Mejía-Alvarez, R., and Ramos-Franco, J. (2012). Role of inositol 1,4,5-trisphosphate in the regulation of ventricular Ca2+ signaling in intact mouse heart. *Journal of Molecular and Cellular Cardiology*, *53*(6), 768–779. https://doi.org/10.1016/j.yjmcc.2012.08.019

Escobar, A. L., Ribeiro-Costa, R., Villalba-Galea, C., Zoghbi, M. E., Pérez, C. G., and Mejía-Alvarez, R. (2004a). Developmental changes of intracellular Ca^{2+} transients in beating rat hearts. *American Journal of Physiology-Heart and Circulatory Physiology*, *286*(3), H971–H978. https://doi.org/10.1152/ajpheart.00308.2003

Escobar, A. L., Ribeiro-Costa, R., Villalba-Galea, C., Zoghbi, M. E., Pérez, C. G., and Mejía-Alvarez, R. (2004b). Developmental changes of intracellular Ca^{2+} transients in beating rat hearts. *American Journal of Physiology-Heart and Circulatory Physiology*, *286*(3), H971–H978. https://doi.org/10.1152/ajpheart.00308.2003

Evans, D. B. (1986). Modulation of cAMP: Mechanism for positive inotropic action. *Journal of Cardiovascular Pharmacology*, *8 Suppl 9*, S22-29.

Farrell, A. P. (1984). A review of cardiac performance in the teleost heart: Intrinsic and humoral regulation. *Canadian Journal of Zoology*, *62*(4), 523–536. https://doi.org/10.1139/z84-079

Ferreira, E. O., Anttila, K., and Farrell, A. P. (2014). Thermal Optima and Tolerance in the Eurythermic Goldfish (*Carassius auratus*): Relationships between Whole-Animal Aerobic Capacity and Maximum Heart Rate. *Physiological and Biochemical Zoology*, *87*(5), 599–611. https://doi.org/10.1086/677317

Ferreira, G., Yi, J., Ríos, E., and Shirokov, R. (1997). Ion-dependent Inactivation of Barium Current through L-type Calcium Channels. *Journal of General Physiology*, *109*(4), 449–461. https://doi.org/10.1085/jgp.109.4.449

Ferreira, G., Ríos, E., and Reyes, N. (2003). Two Components of Voltage-Dependent Inactivation in Cav1.2 Channels Revealed by Its Gating Currents. *Biophysical Journal*, *84*(6), 3662–3678. https://doi.org/10.1016/S0006-3495(03)75096-6

Ferreiro, M., Petrosky, A. D., and Escobar, A. L. (2012a). Intracellular Ca $^{2+}$ release underlies the development of phase 2 in mouse ventricular action potentials. *American Journal of Physiology-Heart and Circulatory Physiology*, *302*(5), H1160–H1172. https://doi.org/10.1152/ajpheart.00524.2011

Ferreiro, M., Petrosky, A. D., and Escobar, A. L. (2012b). Intracellular Ca $^{2+}$ release underlies the development of phase 2 in mouse ventricular action potentials. *American Journal of Physiology-Heart and Circulatory Physiology*, *302*(5), H1160–H1172. https://doi.org/10.1152/ajpheart.00524.2011

Fritsche, R., and Nilsson, S. (1990). Autonomic nervous control of blood pressure and heart rate during hypoxia in the cod, Gadus morhua. *Journal of Comparative Physiology B*, *160*(3), 287–292. https://doi.org/10.1007/BF00302594

Gamperl, A. K., Gillis, T. E., Farrell, A. P., and Brauner, C. J. (Eds.). (2017). *The cardiovascular system: Morphology, control and function* (First edition). Elsevier, Academic Press.

Garofalo, F., Imbrogno, S., Tota, B., and Amelio, D. (2012). Morpho-functional characterization of the goldfish (Carassius auratus L.) heart. *Comparative Biochemistry and Physiology Part A: Molecular and Integrative Physiology*, *163*(2), 215–222. https://doi.org/10.1016/j.cbpa.2012.05.206

Genge, C. E., Lin, E., Lee, L., Sheng, X., Rayani, K., Gunawan, M., Stevens, C. M., Li, A. Y., Talab, S. S., Claydon, T. W., Hove-Madsen, L., and Tibbits, G. F. (2016). The Zebrafish Heart as a Model of Mammalian Cardiac Function. In B. Nilius, P. de Tombe, T. Gudermann, R. Jahn, R. Lill, and O. H. Petersen (Eds.), *Reviews of Physiology, Biochemistry and Pharmacology, Vol. 171* (Vol. 171, pp. 99–136). SpTyrode International Publishing. https://doi.org/10.1007/112_2016_5

Grivas, J., Haag, M., Johnson, A., Manalo, T., Roell, J., Das, T. L., Brown, E., Burns, A. R., and Lafontant, P. J. (2014). Cardiac repair and regenerative potential in the goldfish (Carassius auratus) heart. *Comparative Biochemistry and Physiology Part C: Toxicology and Pharmacology*, *163*, 14–23. https://doi.org/10.1016/j.cbpc.2014.02.002

Gurabi, Z., Koncz, I., Patocskai, B., Nesterenko, V. V., and Antzelevitch, C. (2014). Cellular Mechanism Underlying Hypothermia-Induced Ventricular Tachycardia/Ventricular Fibrillation in the Setting of Early Repolarization and the Protective Effect of Quinidine, Cilostazol, and Milrinone. *Circulation: Arrhythmia and Electrophysiology*, *7*(1), 134–142. https://doi.org/10.1161/CIRCEP.113.000919

Harper, A. A., Newton, I. P., and P. W. Watt. (1995). (1995). The effect of temperature on spontaneous action potential discharge of the isolated sinus venosus from winter and summer plaice (Pleuronectes platessa). *The Journal of Experimental Biology*, *198*(Pt 1), 137–140.

Hattori, Y., Toyama, J., and Kodama, I. (1991). Cytosolic calcium staircase in ventricular myocytes isolated from guinea pigs and rats. *Cardiovascular Research*, *25*(8), 622–629. https://doi.org/10.1093/cvr/25.8.622

Haustein, M., Hannes, T., Trieschmann, J., Verhaegh, R., Köster, A., Hescheler, J., Brockmeier, K., Adelmann, R., and Khalil, M. (2015). Excitation-Contraction Coupling in Zebrafish Ventricular Myocardium Is Regulated by Trans-Sarcolemmal Ca2+ Influx and Sarcoplasmic Reticulum Ca2+ Release. *PLOS ONE*, *10*(5), e0125654. https://doi.org/10.1371/journal.pone.0125654

Haverinen, J., and Vornanen, M. (2007). Temperature acclimation modifies sinoatrial pacemaker mechanism of the rainbow trout heart. *American Journal of Physiology-Regulatory, Integrative and Comparative Physiology*, *292*(2), R1023–R1032. https://doi.org/10.1152/ajpregu.00432.2006

Hayes, J. S., and Mayer, S. E. (1981). Regulation of guinea pig heart phosphorylase kinase by cAMP, protein kinase, and calcium. *American Journal of Physiology-Endocrinology and Metabolism*, *240*(3), E340–E349. https://doi.org/10.1152/ajpendo.1981.240.3.E340

Henning, R. J. (1992). Vagal stimulation during muscarinic and β-adrenergic blockade increases atrial contractility and heart rate. *Journal of the Autonomic Nervous System*, *40*(2), 121–129. https://doi.org/10.1016/0165-1838(92)90023-A

Hildebrandt, J. D., Sekura, R. D., Codina, J., Iyengar, R., Manclark, C. R., and Birnbaumer, L. (1983). Stimulation and inhibition of adenylyl cyclases mediated by distinct regulatory proteins. *Nature*, *302*(5910), 706–709. https://doi.org/10.1038/302706a0

Horackova, M. (1986). Excitation–contraction coupling in isolated adult ventricular myocytes from the rat, dog, and rabbit: Effects of various inotropic interventions in the presence of ryanodine. *Canadian Journal of Physiology and Pharmacology*, *64*(12), 1473–1483. https://doi.org/10.1139/y86-249

Horváth, B., Váczi, K., Hegyi, B., Gönczi, M., Dienes, B., Kistamás, K., Bányász, T., Magyar, J., Baczkó, I., Varró, A., Seprényi, G., Csernoch, L., Nánási, P. P., and Szentandrássy, N. (2016). Sarcolemmal Ca 2+ -entry through L-type Ca 2+ channels controls the profile of Ca 2+ -activated Cl − current in canine ventricular myocytes. *Journal of Molecular and Cellular Cardiology*, *97*, 125–139. https://doi.org/10.1016/j.yjmcc.2016.05.006

Huttner, I. G., Trivedi, G., Jacoby, A., Mann, S. A., Vandenberg, J. I., and Fatkin, D. (2013). A transgenic zebrafish model of a human cardiac sodium channel mutation exhibits

bradycardia, conduction-system abnormalities and early death. *Journal of Molecular and Cellular Cardiology*, *61*, 123–132. https://doi.org/10.1016/j.yjmcc.2013.06.005

Kang, J., Hu, J., Karra, R., Dickson, A. L., Tornini, V. A., Nachtrab, G., Gemberling, M., Goldman, J. A., Black, B. L., and Poss, K. D. (2016). Modulation of tissue repair by regeneration enhancer elements. *Nature*, *532*(7598), 201–206. https://doi.org/10.1038/nature17644

Kass, R. S., and Sanguinetti, M. C. (1984). Inactivation of calcium channel current in the calf cardiac Purkinje fiber. Evidence for voltage- and calcium-mediated mechanisms. *Journal of General Physiology*, *84*(5), 705–726. https://doi.org/10.1085/jgp.84.5.705

Katra, R. P., Pruvot, E., and Laurita, K. R. (2004). Intracellular calcium handling heterogeneities in intact guinea pig hearts. *American Journal of Physiology-Heart and Circulatory Physiology*, *286*(2), H648–H656. https://doi.org/10.1152/ajpheart.00374.2003

Katra, R. P., and Laurita, K. R. (2005). Cellular mechanism of calcium-mediated triggered activity in the heart. *Circulation Research*, *96*(5), 535–542. https://doi.org/10.1161/01.RES.0000159387.00749.3c

Katz, A. M. (1967). Regulation of Cardiac Muscle Contractility. *Journal of General Physiology*, *50*(6), 185–196. https://doi.org/10.1085/jgp.50.6.185

Keith, A. (1910). RECENT RESEARCHES ON THE ANATOMY OF THE HEART. *The Lancet*, *175*(4506), 101–103. https://doi.org/10.1016/S0140-6736(01)74711-3

Ko, C. Y., Liu, M. B., Song, Z., Qu, Z., and Weiss, J. N. (2017). Multiscale Determinants of Delayed Afterdepolarization Amplitude in Cardiac Tissue. *Biophysical Journal*, *112*(9), 1949–1961. https://doi.org/10.1016/j.bpj.2017.03.006

Kodama, I., Shibata, S., Toyama, J., and Yamada, K. (1981). Electromechanical Effects of Anthopleurin-A (AP-A) on Rabbit Ventricular Muscle: Influence of Driving Frequency, Calcium Antagonists, Tetrodotoxin, Lidocaine and Ryanodine. *British Journal of Pharmacology*, *74*(1), 29–37. https://doi.org/10.1111/j.1476-5381.1981.tb09952.x

Kon, T., Omori, Y., Fukuta, K., Wada, H., Watanabe, M., Chen, Z., Iwasaki, M., Mishina, T., Matsuzaki, S. S., Yoshihara, D., Arakawa, J., Kawakami, K., Toyoda, A., Burgess, S. M., Noguchi, H., and Furukawa, T. (2020). The Genetic Basis of Morphological Diversity in Domesticated Goldfish. *Current Biology*, *30*(12), 2260-2274.e6. https://doi.org/10.1016/j.cub.2020.04.034

Konantz, J., and Antos, C. L. (2014). Reverse Genetic Morpholino Approach Using Cardiac Ventricular Injection to Transfect Multiple Difficult-to-target Tissues in the Zebrafish Larva. *Journal of Visualized Experiments*, *88*, 51595. https://doi.org/10.3791/51595

Kornyeyev, D., Petrosky, A. D., Zepeda, B., Ferreiro, M., Knollmann, B., and Escobar, A. L. (2012). Calsequestrin 2 deletion shortens the refractoriness of Ca2+ release and reduces rate-dependent Ca2+-alternans in intact mouse hearts. *Journal of Molecular and Cellular Cardiology*, *52*(1), 21–31. https://doi.org/10.1016/j.yjmcc.2011.09.020

Kornyeyev, D., Reyes, M., and Escobar, A. L. (2010a). Luminal Ca $^{2+}$ content regulates intracellular Ca $^{2+}$ release in subepicardial myocytes of intact beating mouse hearts: Effect of exogenous buffers. *American Journal of Physiology-Heart and Circulatory Physiology*, *298*(6), H2138–H2153. https://doi.org/10.1152/ajpheart.00885.2009

Kornyeyev, D., Reyes, M., and Escobar, A. L. (2010b). Luminal Ca $^{2+}$ content regulates intracellular Ca $^{2+}$ release in subepicardial myocytes of intact beating mouse hearts: Effect of exogenous buffers. *American Journal of Physiology-Heart and Circulatory Physiology*, *298*(6), H2138–H2153. https://doi.org/10.1152/ajpheart.00885.2009

Krebs, E. G. (1972). Protein kinases. *Current Topics in Cellular Regulation*, *5*, 99–133.

Krishnan, S. C., and Antzelevitch, C. (1991). Sodium channel block produces opposite electrophysiological effects in canine ventricular epicardium and endocardium. *Circulation Research*, *69*(2), 277–291. https://doi.org/10.1161/01.RES.69.2.277

Lacampagne, A., Caputo, C., and Argibay, J. (1996). Effect of ryanodine on cardiac calcium current and calcium channel gating current. *Biophysical Journal*, *70*(1), 370–375. https://doi.org/10.1016/S0006-3495(96)79580-2

Langer, G. A. (1967). Sodium Exchange in Dog Ventricular Muscle. *Journal of General Physiology*, *50*(5), 1221–1239. https://doi.org/10.1085/jgp.50.5.1221

Laurent, P., Holmgren, S., and Nilsson, S. (1983). Nervous and humoral control of the fish heart: Structure and function. *Comparative Biochemistry and Physiology Part A: Physiology*, *76*(3), 525–542. https://doi.org/10.1016/0300-9629(83)90455-3

Laurita, K. R., Katra, R., Wible, B., Wan, X., and Koo, M. H. (2003). Transmural Heterogeneity of Calcium Handling in Canine. *Circulation Research*, *92*(6), 668–675. https://doi.org/10.1161/01.RES.0000062468.25308.27

Lee, K. S., Marban, E., and Tsien, R. W. (1985). Inactivation of calcium channels in mammalian heart cells: Joint dependence on membrane potential and intracellular calcium. *The Journal of Physiology*, *364*(1), 395–411. https://doi.org/10.1113/jphysiol.1985.sp015752

Lee, L., Genge, C. E., Cua, M., Sheng, X., Rayani, K., Beg, M. F., Sarunic, M. V., and Tibbits, G. F. (2016). Functional Assessment of Cardiac Responses of Adult Zebrafish (Danio rerio) to Acute and Chronic Temperature Change Using High-Resolution Echocardiography. *PLOS ONE*, *11*(1), e0145163. https://doi.org/10.1371/journal.pone.0145163

Lee, W. C., and Shideman, F. E. (1959). Role of Myocardial Catecholamines in Cardiac Contractility. *Science*, *129*(3354), 967–968. https://doi.org/10.1126/science.129.3354.967

Leo, S., Gattuso, A., Mazza, R., Filice, M., Cerra, M. C., and Imbrogno, S. (2019). Cardiac influence of the β3-adrenoceptor in the goldfish (*Carassius auratus*): A protective role under hypoxia? *Journal of Experimental Biology*, jeb.211334. https://doi.org/10.1242/jeb.211334

Lin, E., Craig, C., Lamothe, M., Sarunic, M. V., Beg, M. F., and Tibbits, G. F. (2015). Construction and use of a zebrafish heart voltage and calcium optical mapping system, with integrated electrocardiogram and programmable electrical stimulation. *American Journal of Physiology-Regulatory, Integrative and Comparative Physiology*, *308*(9), R755–R768. https://doi.org/10.1152/ajpregu.00001.2015

Lin, E., Ribeiro, A., Ding, W., Hove-Madsen, L., Sarunic, M. V., Beg, M. F., and Tibbits, G. F. (2014). Optical mapping of the electrical activity of isolated adult zebrafish hearts: Acute effects of temperature. *American Journal of Physiology-Regulatory, Integrative and Comparative Physiology*, *306*(11), R823–R836. https://doi.org/10.1152/ajpregu.00002.2014

Lindemann, J. P., and Watanabe, A. M. (1985). Muscarinic cholinergic inhibition of beta-adrenergic stimulation of phospholamban phosphorylation and Ca2+ transport in guinea pig ventricles. *The Journal of Biological Chemistry*, *260*(24), 13122–13129.

Lipp, P., Mechmann, S., and Pott, L. (1987). Effects of calcium release from sarcoplasmic reticulum on membrane currents in guinea pig atrial cardioballs. *Pflûgers Archiv European Journal of Physiology*, *410*(1–2), 121–131. https://doi.org/10.1007/BF00581904

Litovsky, S. H., and Antzelevitch, C. (1989). Rate dependence of action potential duration and refractoriness in canine ventricular endocardium differs from that of epicardium: Role of the transient outward current. *Journal of the American College of Cardiology*, *14*(4), 1053–1066. https://doi.org/10.1016/0735-1097(89)90490-7

Litovsky, S. H., and Antzelevitch, C. (1990). Differences in the electrophysiological response of canine ventricular subendocardium and subepicardium to acetylcholine and isoproterenol. A direct effect of acetylcholine in ventricular myocardium. *Circulation Research*, *67*(3), 615–627. https://doi.org/10.1161/01.RES.67.3.615

López Alarcón, M. M., Rodríguez de Yurre, A., Felice, J. I., Medei, E., and Escobar, A. L. (2019a). Phase 1 repolarization rate defines Ca2+ dynamics and contractility on intact mouse hearts. *Journal of General Physiology*, *151*(6), 771–785. https://doi.org/10.1085/jgp.201812269

López Alarcón, M. M., Rodríguez de Yurre, A., Felice, J. I., Medei, E., and Escobar, A. L. (2019b). Phase 1 repolarization rate defines Ca2+ dynamics and contractility on intact mouse hearts. *Journal of General Physiology*, *151*(6), 771–785. https://doi.org/10.1085/jgp.201812269

Lukas, A., and Antzelevitch, C. (1993). Differences in the electrophysiological response of canine ventricular epicardium and endocardium to ischemia. Role of the transient outward current. *Circulation*, *88*(6), 2903–2915. https://doi.org/10.1161/01.CIR.88.6.2903

Málaga-Trillo, E., Laessing, U., Lang, D. M., Meyer, A., and Stuermer, C. A. O. (2002). Evolution of Duplicated reggie Genes in Zebrafish and Goldfish. *Journal of Molecular Evolution*, *54*(2), 235–245. https://doi.org/10.1007/s00239-001-0005-1

Marks, A. R. (2013). Calcium cycling proteins and heart failure: Mechanisms and therapeutics. *Journal of Clinical Investigation*, *123*(1), 46–52. https://doi.org/10.1172/JCI62834

Mattiazzi, A., Argenziano, M., Aguilar-Sanchez, Y., Mazzocchi, G., and Escobar, A. L. (2015). Ca2+ Sparks and Ca2+ waves are the subcellular events underlying Ca2+ overload during ischemia and reperfusion in perfused intact hearts. *Journal of Molecular and Cellular Cardiology*, *79*, 69–78. https://doi.org/10.1016/j.yjmcc.2014.10.011

Mattiazzi, A. R., and Nilsson, E. (1976). The Influence of Temperature on the Time Course of the Mechanical Activity in Rabbit Papillary Muscle. *Acta Physiologica Scandinavica*, *97*(3), 310–318. https://doi.org/10.1111/j.1748-1716.1976.tb10268.x

Maylie, J., and Morad, M. (1995). Evaluation of T- and L-type Ca2+ currents in shark ventricular myocytes. *American Journal of Physiology-Heart and Circulatory Physiology*, *269*(5), H1695–H1703. https://doi.org/10.1152/ajpheart.1995.269.5.H1695

Mejía-Alvarez, R., Manno, C., Villalba-Galea, C. A., del Valle Fernández, L., Costa, R., Fill, M., Gharbi, T., and Escobar, A. L. (2003a). Pulsed local-field fluorescence microscopy: A new approach for measuring cellular signals in the beating heart. *Pflügers Archiv - European Journal of Physiology*, *445*(6), 747–758. https://doi.org/10.1007/s00424-002-0963-1

Mersereau, E. J., Poitra, S. L., Espinoza, A., Crossley, D. A., and Darland, T. (2015). The effects of cocaine on heart rate and electrocardiogram in zebrafish (Danio rerio). *Comparative Biochemistry and Physiology Part C: Toxicology and Pharmacology*, *172–173*, 1–6. https://doi.org/10.1016/j.cbpc.2015.03.007

Mokalled, M. H., Patra, C., Dickson, A. L., Endo, T., Stainier, D. Y. R., and Poss, K. D. (2016). Injury-induced *ctgfa* directs glial bridging and spinal cord regeneration in zebrafish. *Science*, *354*(6312), 630–634. https://doi.org/10.1126/science.aaf2679

Molina, C. E., Gesser, H., Llach, A., Tort, L., and Hove-Madsen, L. (2007). Modulation of membrane potential by an acetylcholine-activated potassium current in trout atrial myocytes. *American Journal of Physiology-Regulatory, Integrative and Comparative Physiology*, *292*(1), R388–R395. https://doi.org/10.1152/ajpregu.00499.2005

Nakamura, T., Lozano, P. R., Ikeda, Y., Iwanaga, Y., Hinek, A., Minamisawa, S., Cheng, C.-F., Kobuke, K., Dalton, N., Takada, Y., Tashiro, K., Ross Jr, J., Honjo, T., and Chien, K. R. (2002). Fibulin-5/DANCE is essential for elastogenesis in vivo. *Nature*, *415*(6868), 171–175. https://doi.org/10.1038/415171a

Nakayama, T., Kurachi, Y., Noma, A., & Irisawa, H. (1984). Action potential and membrane currents of single pacemaker cells of the rabbit heart. Pflügers Archiv, 402(3), 248-257.

Nemtsas, P., Wettwer, E., Christ, T., Weidinger, G., and Ravens, U. (2010). Adult zebrafish heart as a model for human heart? An electrophysiological study. *Journal of Molecular and Cellular Cardiology*, *48*(1), 161–171. https://doi.org/10.1016/j.yjmcc.2009.08.034

Newton, C. M., Stoyek, M. R., Croll, R. P., and Smith, F. M. (2014). Regional innervation of the heart in the goldfish, *Carassius auratus*: A confocal microscopy study: Innervation of the goldfish heart. *Journal of Comparative Neurology*, *522*(2), 456–478. https://doi.org/10.1002/cne.23421

Novak, A. E., Taylor, A. D., Pineda, R. H., Lasda, E. L., Wright, M. A., and Ribera, A. B. (2006). Embryonic and larval expression of zebrafish voltage-gated sodium channel α-subunit genes. *Developmental Dynamics*, *235*(7), 1962–1973. https://doi.org/10.1002/dvdy.20811

O'Hara, T., and Rudy, Y. (2012). Quantitative comparison of cardiac ventricular myocyte electrophysiology and response to drugs in human and nonhuman species. *American Journal of Physiology-Heart and Circulatory Physiology*, *302*(5), H1023–H1030. https://doi.org/10.1152/ajpheart.00785.2011

Osterrieder, W., Brum, G., Hescheler, J., Trautwein, W., Flockerzi, V., and Hofmann, F. (1982). Injection of subunits of cyclic AMP-dependent protein kinase into cardiac myocytes modulates Ca2+ current. *Nature*, *298*(5874), 576–578. https://doi.org/10.1038/298576a0

Palomeque, J., Vila Petroff, M. G., and Mattiazzi, A. (2004). Pacing Staircase Phenomenon in the Heart: From Bodwitch to the XXI Century. *Heart, Lung and Circulation*, *13*(4), 410–420. https://doi.org/10.1016/j.hlc.2004.08.006

Peterson, B. Z., DeMaria, C. D., and Yue, D. T. (1999). Calmodulin Is the Ca2+ Sensor for Ca2+-Dependent Inactivation of L-Type Calcium Channels. *Neuron*, *22*(3), 549–558. https://doi.org/10.1016/S0896-6273(00)80709-6

Peterson, B. Z., Lee, J. S., Mulle, J. G., Wang, Y., de Leon, M., and Yue, D. T. (2000). Critical Determinants of Ca2+-Dependent Inactivation within an EF-Hand Motif of L-Type Ca2+ Channels. *Biophysical Journal*, *78*(4), 1906–1920. https://doi.org/10.1016/S0006-3495(00)76739-7

Petroff, M. G. V., Palomeque, J., and Mattiazzi, A. R. (2003). Na$^+$-Ca^{2+} Exchange Function Underlying Contraction Frequency Inotropy in the Cat Myocardium. *The Journal of Physiology*, *550*(3), 801–817. https://doi.org/10.1113/jphysiol.2003.044321

Piktel, J. S., Jeyaraj, D., Said, T. H., Rosenbaum, D. S., and Wilson, L. D. (2011). Enhanced Dispersion of Repolarization Explains Increased Arrhythmogenesis in Severe Versus Therapeutic Hypothermia. *Circulation: Arrhythmia and Electrophysiology*, *4*(1), 79–86. https://doi.org/10.1161/CIRCEP.110.958355

Pitt, G. S., Zühlke, R. D., Hudmon, A., Schulman, H., Reuter, H., and Tsien, R. W. (2001). Molecular Basis of Calmodulin Tethering and Ca2+-dependent Inactivation of L-type Ca2+ Channels. *Journal of Biological Chemistry*, *276*(33), 30794–30802. https://doi.org/10.1074/jbc.M104959200

Poss, K. D., Wilson, L. G., and Keating, M. T. (2002). Heart Regeneration in Zebrafish. *Science*, *298*(5601), 2188–2190. https://doi.org/10.1126/science.1077857

Qin, N., Olcese, R., Bransby, M., Lin, T., and Birnbaumer, L. (1999). Ca2+-induced inhibition of the cardiac Ca2+ channel depends on calmodulin. *Proceedings of the National Academy of Sciences*, *96*(5), 2435–2438. https://doi.org/10.1073/pnas.96.5.2435

Ramachandran, K. V., Hennessey, J. A., Barnett, A. S., Yin, X., Stadt, H. A., Foster, E., Shah, R. A., Yazawa, M., Dolmetsch, R. E., Kirby, M. L., and Pitt, G. S. (2013). Calcium influx through L-type CaV1.2 Ca2+ channels regulates mandibular development. *Journal of Clinical Investigation*, *123*(4), 1638–1646. https://doi.org/10.1172/JCI66903

Ramos-Franco, J., Aguilar-Sanchez, Y., and Escobar, A. L. (2016). Intact Heart Loose Patch Photolysis Reveals Ionic Current Kinetics During Ventricular Action Potentials. *Circulation Research*, *118*(2), 203–215. https://doi.org/10.1161/CIRCRESAHA.115.307399

Randall, W. C., Randall, D. C., and Ardell, J. L. (2020). Autonomic Regulation of Myocardial Contractility. In I. H. Zucker and J. P. Gilmore (Eds.), *Reflex Control of the Circulation* (1st Edition, pp. 67–103). Taylor and Francis. https://doi.org/10.1201/9780367813338

Randall, W., Wechsler, J., Pace, J., and Szentivanyi, M. (1968). Alterations in myocardial contractility during stimulation of the cardiac nerves. *American Journal of Physiology-Legacy Content*, *214*(5), 1205–1212. https://doi.org/10.1152/ajplegacy.1968.214.5.1205

Ravens, U. (2018). Ionic basis of cardiac electrophysiology in zebrafish compared to human hearts. *Progress in Biophysics and Molecular Biology*, *138*, 38–44. https://doi.org/10.1016/j.pbiomolbio.2018.06.008

Rayani, K., Lin, E., Craig, C., Lamothe, M., Shafaattalab, S., Gunawan, M., Li, A. Y., Hove-Madsen, L., and Tibbits, G. F. (2018). Zebrafish as a model of mammalian cardiac function: Optically mapping the interplay of temperature and rate on voltage and calcium dynamics. *Progress in Biophysics and Molecular Biology*, *138*, 69–90. https://doi.org/10.1016/j.pbiomolbio.2018.07.006

Rome, L. C., Swank, D., and Corda, D. (1993). How Fish Power Swimming. *Science*, *261*(5119), 340–343. https://doi.org/10.1126/science.8332898

Saito, T. (1973). Effects of vagal stimulation on the pacemaker action potentials of carp heart. *Comparative Biochemistry and Physiology Part A: Physiology*, *44*(1), 191–199. https://doi.org/10.1016/0300-9629(73)90381-2

Sala, L., Hegyi, B., Bartolucci, C., Altomare, C., Rocchetti, M., Váczi, K., Mostacciuolo, G., Szentandrássy, N., Severi, S., Pál Nánási, P., and Zaza, A. (2018). Action potential contour contributes to species differences in repolarization response to β-adrenergic stimulation. *EP Europace*, *20*(9), 1543–1552. https://doi.org/10.1093/europace/eux236

Sandblom, E., and Axelsson, M. (2011). Autonomic control of circulation in fish: A comparative view. *Autonomic Neuroscience*, *165*(1), 127–139. https://doi.org/10.1016/j.autneu.2011.08.006

Serbanovic-Canic, J., de Luca, A., Warboys, C., Ferreira, P. F., Luong, L. A., Hsiao, S., Gauci, I., Mahmoud, M., Feng, S., Souilhol, C., Bowden, N., Ashton, J.-P., Walczak, H., Firmin, D., Krams, R., Mason, J. C., Haskard, D. O., Sherwin, S., Ridger, V., … Evans, P. C. (2017). Zebrafish Model for Functional Screening of Flow-Responsive Genes. *Arteriosclerosis, Thrombosis, and Vascular Biology*, *37*(1), 130–143. https://doi.org/10.1161/ATVBAHA.116.308502

Shiels, H. A., and White, E. (2005). Temporal and spatial properties of cellular Ca^{2+} flux in trout ventricular myocytes. *American Journal of Physiology-Regulatory, Integrative and Comparative Physiology*, *288*(6), R1756–R1766. https://doi.org/10.1152/ajpregu.00510.2004

Steele, S. L., Lo, K. H. A., Li, V. W. T., Cheng, S. H., Ekker, M., and Perry, S. F. (2009). Loss of M_2 muscarinic receptor function inhibits development of hypoxic bradycardia and alters cardiac β-adrenergic sensitivity in larval zebrafish (*Danio rerio*). *American Journal of Physiology-Regulatory, Integrative and Comparative Physiology*, *297*(2), R412–R420. https://doi.org/10.1152/ajpregu.00036.2009

Sugiura, H., and Joyner, R. W. (1992). Action potential conduction between guinea pig ventricular cells can be modulated by calcium current. *American Journal of Physiology-*

Heart and Circulatory Physiology, *263*(5), H1591–H1604. https://doi.org/10.1152/ajpheart.1992.263.5.H1591

Suko, J., Maurer-Fogy, I., Plank, B., Bertel, O., Wyskovsky, W., Hohenegger, M., and Hellmann, G. (1993). Phosphorylation of serine 2843 in ryanodine receptor-calcium release channel of skeletal muscle by cAMP-, cGMP- and CaM-dependent protein kinase. *Biochimica et Biophysica Acta (BBA) - Molecular Cell Research*, *1175*(2), 193–206. https://doi.org/10.1016/0167-4889(93)90023-I

Szentandrássy, N., Farkas, V., Bárándi, L., Hegyi, B., Ruzsnavszky, F., Horváth, B., Bányász, T., Magyar, J., Márton, I., and Nánási, P. (2012). Role of action potential configuration and the contribution of Ca $^{2+}$ and K $^{+}$ currents to isoprenaline-induced changes in canine ventricular cells: Isoprenaline in canine heart. *British Journal of Pharmacology*, *167*(3), 599–611. https://doi.org/10.1111/j.1476-5381.2012.02015.x

Tessadori, F., van Weerd, J. H., Burkhard, S. B., Verkerk, A. O., de Pater, E., Boukens, B. J., Vink, A., Christoffels, V. M., and Bakkers, J. (2012). Identification and Functional Characterization of Cardiac Pacemaker Cells in Zebrafish. *PLoS ONE*, *7*(10), e47644. https://doi.org/10.1371/journal.pone.0047644

Tillotson, D. (1979). Inactivation of Ca conductance dependent on entry of Ca ions in molluscan neurons. *Proceedings of the National Academy of Sciences*, *76*(3), 1497–1500. https://doi.org/10.1073/pnas.76.3.1497

Tsai, C.-T., Wu, C.-K., Chiang, F.-T., Tseng, C.-D., Lee, J.-K., Yu, C.-C., Wang, Y.-C., Lai, L.-P., Lin, J.-L., and Hwang, J.-J. (2011). In-vitro recording of adult zebrafish heart electrocardiogram—A platform for pharmacological testing. *Clinica Chimica Acta; International Journal of Clinical Chemistry*, *412*(21–22), 1963–1967. https://doi.org/10.1016/j.cca.2011.07.002

Urbá-Holmgren, R., González, R. M., and Holmgren, B. (1977). Is yawning a cholinergic response? *Nature*, *267*(5608), 261–262. https://doi.org/10.1038/267261a0

Valdivia, H. H., Kaplan, J. H., Ellis-Davies, G. C., and Lederer, W. J. (1995). Rapid adaptation of cardiac ryanodine receptors: Modulation by Mg2+ and phosphorylation. *Science (New York, N.Y.)*, *267*(5206), 1997–2000. https://doi.org/10.1126/science.7701323

Valverde, C. A., Kornyeyev, D., Ferreiro, M., Petrosky, A. D., Mattiazzi, A., and Escobar, A. L. (2010). Transient Ca2+ depletion of the sarcoplasmic reticulum at the onset of reperfusion. *Cardiovascular Research*, *85*(4), 671–680. https://doi.org/10.1093/cvr/cvp371

Valverde, C. A., Mundiña-Weilenmann, C., Reyes, M., Kranias, E. G., Escobar, A. L., and Mattiazzi, A. (2006). Phospholamban phosphorylation sites enhance the recovery of intracellular Ca2+ after perfusion arrest in isolated, perfused mouse heart.

Cardiovascular Research, *70*(2), 335–345.
https://doi.org/10.1016/j.cardiores.2006.01.018

van Opbergen, C. J. M., Koopman, C. D., Kok, B. J. M., Knöpfel, T., Renninger, S. L., Orger, M. B., Vos, M. A., van Veen, T. A. B., Bakkers, J., and de Boer, T. P. (2018). Optogenetic sensors in the zebrafish heart: A novel in vivo electrophysiological tool to study cardiac arrhythmogenesis. *Theranostics*, *8*(17), 4750–4764. https://doi.org/10.7150/thno.26108

van Opbergen, C. J. M., van der Voorn, S. M., Vos, M. A., de Boer, T. P., and van Veen, T. A. B. (2018). Cardiac Ca2+ signalling in zebrafish: Translation of findings to man. *Progress in Biophysics and Molecular Biology*, *138*, 45–58. https://doi.org/10.1016/j.pbiomolbio.2018.05.002

Verduyn, S. C., Vos, M. A., Gorgels, A. P., Zande, J., Leunissen, J. D. M., and Wellens, H. J. (1995). The Effect of Flunarizine and Ryanodine on Acquired Torsades de Pointes Arrhythmias in the Intact Canine Heart. *Journal of Cardiovascular Electrophysiology*, *6*(3), 189–200. https://doi.org/10.1111/j.1540-8167.1995.tb00770.x

Vornanen, M. (2016). The temperature dependence of electrical excitability in fish hearts. *Journal of Experimental Biology*, *219*(13), 1941–1952. https://doi.org/10.1242/jeb.128439

Vornanen, M. (2017). Electrical Excitability of the Fish Heart and Its Autonomic Regulation. In A. K. Gamperl, T. E. Gillis, A. P. Farrell, and C. J. Brauner (Eds.), *Fish Physiology* (Vol. 36, pp. 99–153). Elsevier. https://doi.org/10.1016/bs.fp.2017.04.002

Vornanen, M., Hälinen, M., and Haverinen, J. (2010). Sinoatrial tissue of crucian carp heart has only negative contractile responses to autonomic agonists. *BMC Physiology*, *10*, 10. https://doi.org/10.1186/1472-6793-10-10

Vornanen, M., Shiels, H. A., and Farrell, A. P. (2002). Plasticity of excitation–contraction coupling in fish cardiac myocytes. *Comparative Biochemistry and Physiology Part A: Molecular and Integrative Physiology*, *132*(4), 827–846. https://doi.org/10.1016/S1095-6433(02)00051-X

Vornanen, M., and Tuomennoro, J. (1999). Effects of acute anoxia on heart function in crucian carp: Importance of cholinergic and purinergic control. *The American Journal of Physiology*, *277*(2), R465-475. https://doi.org/10.1152/ajpregu.1999.277.2.R465

Watanabe, A. M., and Lindemann, J. P. (1984). Mechanisms of Adrenergic and Cholinergic Regulation of Myocardial Contractility. In N. Sperelakis (Ed.), *Physiology and Pathophysiology of the Heart* (Vol. 34, pp. 377–404). SpTyrode US. https://doi.org/10.1007/978-1-4757-1171-4_17

Weilenmann, C. M., Vittone, L., Cingolani, G., and Mattiazzi, A. (1987). Dissociation between contraction and relaxation: The possible role of phospholamban phosphorylation. *Basic Research in Cardiology*, *82*(6), 507–516. https://doi.org/10.1007/BF01907220

Xie, Y., Ottolia, M., John, S. A., Chen, J.-N., and Philipson, K. D. (2008). Conformational changes of a Ca^{2+}-binding domain of the Na^{+}/Ca^{2+} exchanger monitored by FRET in transgenic zebrafish heart. *American Journal of Physiology-Cell Physiology*, *295*(2), C388–C393. https://doi.org/10.1152/ajpcell.00178.2008

Xing, N., Ji, L., Song, J., Ma, J., Li, S., Ren, Z., Xu, F., and Zhu, J. (2017). Cadmium stress assessment based on the electrocardiogram characteristics of zebra fish (Danio rerio): QRS complex could play an important role. *Aquatic Toxicology (Amsterdam, Netherlands)*, *191*, 236–244. https://doi.org/10.1016/j.aquatox.2017.08.015

Yamauchi, A. (1980). Fine structure of the fish heart. In *Comparative Anatomy and Development* (pp. 119–148). Academic Press.

Yan, G.-X., and Antzelevitch, C. (1996). Cellular Basis for the Electrocardiographic J Wave. *Circulation*, *93*(2), 372–379. https://doi.org/10.1161/01.CIR.93.2.372

Yin, F., Liu, W., Chai, J., Lu, B., Murphy, R. W., and Luo, J. (2018). CRISPR/Cas9 Application for Gene Copy Fate Survey of Polyploid Vertebrates. *Frontiers in Genetics*, *9*, 260. https://doi.org/10.3389/fgene.2018.00260

Zhang, J.-F., Ellinor, P. T., Aldrich, R. W., and Tsien, R. W. (1994). Molecular determinants of voltage-dependent inactivation in calcium channels. *Nature*, *372*(6501), 97–100. https://doi.org/10.1038/372097a0

Zhang, H., Dvornikov, A. V., Huttner, I. G., Ma, X., Santiago, C. F., Fatkin, D., and Xu, X. (2018). A Langendorff-like system to quantify cardiac pump function in adult zebrafish. *Disease Models and Mechanisms*, dmm.034819. https://doi.org/10.1242/dmm.034819

Zhang, J., Chen, B., Zhong, X., Mi, T., Guo, A., Zhou, Q., Tan, Z., Wu, G., Chen, A. W., Fill, M., Song, L.-S., and Chen, S. R. W. (2014). The cardiac ryanodine receptor luminal Ca2+ sensor governs Ca2+ waves, ventricular tachyarrhythmias and cardiac hypertrophy in calsequestrin-null mice. *Biochemical Journal*, *461*(1), 99–106. https://doi.org/10.1042/BJ20140126

Zoghbi, M. E., Bolaños, P., Villalba-Galea, C., Marcano, A., Hernández, E., Fill, M., and Escobar, A. L. (2000). Spatial Ca2+ Distribution in Contracting Skeletal and Cardiac Muscle Cells. *Biophysical Journal*, *78*(1), 164–173. https://doi.org/10.1016/S0006-3495(00)76582-9

Zoghbi, M. E., Copello, J. A., Villalba-Galea, C. A., Vélez, P., Diaz Sylvester, P. L., Bolaños, P., Marcano, A., Fill, M., and Escobar, A. L. (2004). Differential Ca2+ and Sr2+ regulation of intracellular divalent cations release in ventricular myocytes. *Cell Calcium*, *36*(2), 119–134. https://doi.org/10.1016/j.ceca.2004.01.023

Zucker, I. H., and Gilmore, J. P. (2020). *Reflex Control of the Circulation* (I. H. Zucker and J. P. Gilmore, Eds.; 1st ed.). CRC Press. https://doi.org/10.1201/9780367813338

Zühlke, R. D., Pitt, G. S., Deisseroth, K., Tsien, R. W., and Reuter, H. (1999). Calmodulin supports both inactivation and facilitation of L-type calcium channels. *Nature*, *399*(6732), 159–162. https://doi.org/10.1038/20200